1   **Mass spectrometry strategies to unveil modified aminophospholipids of biological interest**

2

3   Simone Colombo[1], Pedro Domingues[1,] and M. Rosário Domingues[1,2*]

4   [1]Mass Spectrometry Centre, Department of Chemistry & QOPNA, University of Aveiro, Campus

5   Universitário de Santiago, 3810-193 Aveiro, Portugal

6   [2]Department of Chemistry & CESAM, University of Aveiro, Campus Universitário de Santiago,

7   3810-193 Aveiro, Portugal

8

9

10   Running title: Mass spectrometry of modified aminophospholipids

11

12

13

14

15   Address reprint requests to: M. Rosário M. Domingues, Lipidomic laboratory, [1]Mass Spectrometry

16   Centre, Departamento de Química, Universidade de Aveiro, Campus Universitário de Santiago,

17   3810-193 Aveiro (PORTUGAL)

18   E-mail: mrd@ua.pt

19   Phone: +351 234 370698

20   Fax: +351 234 370084

Abstract

The biological functions of modified aminophospholipids (APL) have become a topic of interest during the last two decades, and distinct roles have been found for these biomolecules in both physiological and pathological contexts. Modifications of APL include oxidation, glycation, and adduction to electrophilic aldehydes, altogether contributing to a high structural variability of modified APL. An outstanding technique used in this challenging field is mass spectrometry (MS). MS has been widely used to unveil modified APL of biological interest, mainly when associated with soft ionization methods (electrospray and matrix-assisted laser desorption ionization) and coupled with separation techniques as liquid chromatography. This review summarizes the biological roles and the chemical mechanisms underlying APL modifications and comprehensively reviews the current MS-based knowledge that has been gathered until now for their analysis. The interpretation of the MS data obtained by *in vitro*-identification studies is explained in detail. The perspective of an analytical detection of modified APL in clinical samples is explored, highlighting the fundamental role of MS in unveiling APL modifications and their relevance in pathophysiology.

40

Table of Contents

64

65 **IV. Conclusions**

66 **V. Abbreviations**

67 **VI. Acknowledgments**

68 **VII. References**

69

70

71

72 **I. Introduction**

73   Phosphatidylethanolamine (PE) and phosphatidylserine (PS) are the two classes of

74 glycerophospholipids named aminophospholipids (APL), as they bear a free amine in the polar head

75 group. In mammalian cells, PE and PS are mainly confined to the inner leaflet of the membrane

76 (Schick, Kurica, and Chacko 1976; Higgins and Evans 1978) where they are responsible for both

77 structural and signaling roles. They allow membranes to be fluid as well as impermeable to water and

78 solutes, mediate communication among cells and provide a membrane anchor for signaling

79 macromolecules (Vance and Tasseva 2013). PE is the second most abundant phospholipid class in

80 cell membranes of mammalian organisms, making up 20% of the whole phospholipid profile, while

81 PS is present in a minor amount, constituting 2-10% of all phospholipids (Vance 2008). The

82 biological functions of APL are considerably dependent on their location in the outer or in the inner

83 leaflet on the membrane. Upon physiological conditions, PE and PS are mainly confined to the inner

84 leaflet, maintained by specific flippases, which show a higher selectivity for PS (Daleke 2003), and

85 scramblases (Bevers, Comfurius, and Zwaal 1983; Connor and Schroit 1990; Schroit and Zwaal 1991;

86 Connor et al. 1992; Daleke and Lyles 2000). This specific location is crucial for PS signaling events.

87 Externalized PS is a known activator of the blood-clotting cascade (Higgins and Evans 1978; Bevers,

88 Comfurius, and Zwaal 1983; Connor and Schroit 1990; Connor et al. 1992; Daleke and Lyles 2000;

89 Daleke 2003) and a hallmark of cells facing apoptosis (Fadok et al. 2001; Zwaal, Comfurius, and

Bevers 2005; Balasubramanian, Mirnikjoo, and Schroit 2007; Segawa et al. 2014). In mammalian cells, PE is involved in the modulation of the cell membrane curvature (Cullis and De Kruijff 1978; Verkleij et al. 1984). The presence of PE in the double layer was also associated with the regulation of contractile ring disassembly during cytokinesis of mammalian cells (Emoto and Umeda 2000) and the arrangement of Golgi membrane fusion in early-divided mitotic cells (Pécheur et al. 2002). Furthermore, PE can modify several proteins in mammalian cells, acting as a donor of ethanolamine moiety (Menon and Stevens 1992; Signorell et al. 2008). Table 1 provides an overview of current knowledge on the functions and roles of PE and PS in mammalian cells.

APL are prone to be modified by oxidation (Domingues et al. 2009; Simões et al. 2010; Maciel et al. 2011; Melo, Santos, et al. 2013), glycation (Simões et al. 2010; Maciel, da Silva, et al. 2013; Melo, Silva, et al. 2013; Annibal et al. 2016), and reactive molecules such as electrophilic aldehydes (Bernoud-Hubac et al. 2004; Bacot et al. 2007). These changes in native APL may occur under physiological and pathological conditions through non-enzymatic reactions with reactive oxygen species (ROS), glucose, and other carbonyl compounds, or through enzyme-catalyzed reactions, generating a vast number of differently modified derivatives which display several biological functions. Oxidized PS (ox-PS) is externalized in cell membranes as an important "eat me" marker of apoptosis, and several studies highlighted it as a more potent signal for activated macrophages when compared to native PS (Kagan et al. 2002; Koty et al. 2002; Fabisiak et al. 2005; Greenberg et al. 2006). In addition to its interaction with macrophages, ox-PS mediates other biological functions that controversially relate it to the modulation of the immune system, from the inhibition of peripheral T-cells proliferation in human blood (Seyerl et al. 2008) to the induction of cytokine production in monocytes and dendritic cells (Silva et al. 2012). Also, PE oxidized by ROS (ox-PE) was found to be an active component of oxidized low-density lipoproteins (ox-LDL), that mediates the binding between platelets and annexin (Zieseniss et al. 2001). Furthermore, several biological roles have been investigated for ox-PE generated by lipoxygenase (LOX) in activated human or murine blood cells (Thomas et al. 2010; Zhao et al. 2011; Hammond et al. 2012). More recently, Kagan *et al.* (Kagan et

al. 2016) reported the central role of PE oxidation products with modifications in arachidonic acid and adrenic acid chains in the mediation of ferroptosis, a controlled cell death process. Moreover, PE and PS can react with glucose or electrophilic aldehydes and form adducts, which biological functions are far from being understood. The formation of glycated species and advanced glycation end products (AGE) of PE were reported in LDL incubated with glucose (Ravandi, Kuksis, and Shaikh 2000). Glycated PE (gly-PE) was also detected in red blood cells from both healthy and diabetic subjects (Ravandi et al. 1996; Lertsiri, Shiraishi, and Miyazawa 1998; Fountain et al. 1999; Nakagawa 2005). Interestingly, Simões *et al.* (Simões et al. 2013b; Simões et al. 2013a) reported that glycated PE species are inducers of a pro-inflammatory phenotype in several populations of human peripheral immune cells. Conversely, only one study reported the occurrence of a PS AGE in red blood cells from healthy subjects (Fountain et al. 1999). This study provided evidence that glycation of PS is also likely to occur *in vivo*, despite the authors could not detect an increase in the concentration of the same product in plasma samples from diabetic subjects (Fountain et al. 1999) . Aldehyde-modified APL (al-PE and al-PS) were also highlighted as a family of bioactive molecules. Al-PE pyrrole adducts present in LDL from normolipidemic volunteers were found to enhance the viability of macrophages (Riazy et al. 2011). Guo *et al.* (Guo et al. 2011) treated human umbilical vein endothelial cells (HUVEC) with al-PE and observed an increase in the expression of monocyte adhesion molecules, leading to endothelial dysfunction and inflammation. A comprehensive view of the biological activities modified APL is reported in Table 2, which consists of a summary of the functions that have been so far investigated for each group of derivatives. Moreover, Table 2 merges the studies reporting the occurrence of modified APL in models of inflammatory diseases and clinical samples from inflammation-related pathologies, including diabetes, atherosclerosis, Alzheimer's disease (AD) and cystic fibrosis.

Even though the biological relevance of modified APL is evident, a link between the structural changes in APL, the biological function of the modified derivatives and their occurrence as biomarkers of diseases has not been identified yet. To this end, it is necessary to be able to predict

142 and to understand the type of modifications that can occur *in vivo* upon pathophysiological conditions.

143 In parallel, it is of fundamental importance to develop analytical strategies aimed to characterize the

144 structural complexity of modified APL and detect these biomolecules in biological samples. In the

145 following section, the chemistry of APL modifications will be reviewed, sorting the chemical

146 reactions that can induce their modification. The remaining sections of this review will

147 comprehensively examine the information that mass spectrometry (MS-)based approaches have

148 provided for the analysis of modified APL, *in vitro* and biological samples, over the last two decades.

149 The description of the structural modifications that can occur is accompanied by detailed explanations

150 of the MS and MS/MS data that have been acquired for identification, structural characterization,

151 detection and quantification of modified APL.

152

153 **II. Chemistry of APLs Modifications**

154

155 APL can undergo several modifications, which overall lead to a variety of products of

156 biological relevance. Figure 1 proposes a schematic representation of the modifications that have

157 been described so far for APL. The chemical reactions leading to modified APL can be categorized

158 as follows:

159 A. Oxidation of the fatty acyl chains (Khaselev and Murphy 1999; Gugiu et al. 2006; Maskrey

160 et al. 2007; Tyurin et al. 2008; Tyurina et al. 2008; Domingues et al. 2009; Tyurin et al. 2009; Simões

161 et al. 2010; Thomas et al. 2010; Tyurina et al. 2010; Lloyd T. Morgan et al. 2010; Tyurina, Tyurin,

162 et al. 2011; Tyurina, Kisin, et al. 2011; Clark et al. 2011; Hammond et al. 2012; Melo, Santos, et al.

163 2013; Melo, Silva, et al. 2013; Maciel, Faria, et al. 2013; Simões et al. 2013a);

164 B. Oxidation of the polar head (Carr, van den Berg, and Winterbourn 1998; Richter et al.

165 2008; Simões et al. 2010; Üllen et al. 2010; Maciel et al. 2011; Melo, Santos, et al. 2013; Maciel et

166 al. 2014);

167   C. Adduction of glucose to the polar head with or without further oxidation of the adduct

168   (glycation and glyco-oxidation) (Ravandi, Kuksis, and Myher 1995; Ravandi et al. 1996; Requena et

169   al. 1997; Lertsiri, Shiraishi, and Miyazawa 1998; Pamplona et al. 1998; Fountain et al. 1999;

170   Breitling-Utzmann et al. 2001; Nakagawa 2005; Shoji et al. 2010; Simões et al. 2010; Sookwong et

171   al. 2011; Maciel, Faria, et al. 2013; Maciel, da Silva, et al. 2013; Annibal et al. 2016);

172   D. Adduction of aldehydes to the polar head (Bhuyan et al. 1986; Guichardant et al. 1998;

173   Bacot 2003; Amarnath et al. 2004; Tsuji et al. 2003; Zamora and Hidalgo 2003; Bernoud-Hubac et

174   al. 2004; Stadelmann-Ingrand, Pontcharraud, and Fauconneau 2004; Hisaka et al. 2010; Bacot et al.

175   2007).

176

177   *A. Oxidation of the fatty acyl chains*

178

179   Oxidation of the fatty acyl chains esterified to APL has been correlated with radical-mediated

180   or enzyme-catalyzed oxidation reactions. Radical-mediated oxidation of fatty acyl chains usually

181   relies on ROS as initial effectors of the modification pathway. ROS are generated *in vivo* by different

182   sources, such as the mitochondrial electron-transport chain and NAD(P)H oxidases, and participate

183   in the physiological metabolism of mammalian cells (Dröge 2002; Murphy 2009). Under oxidative

184   stress, the equilibrium between cellular detoxification and generation of ROS is lost in favor of an

185   excess of oxidants species. Thus, high concentrations of ROS mediate a randomly extensive oxidative

186   damage to biomolecules, including lipids (reviewed by Dröge) (Dröge 2002). Oxidative stress can

187   also be induced *in vitro* or *ex vivo* through a set of chemical, physical and enzymatic systems able to

188   mimic the biological occurrence of the oxidation reaction. These biomimetic systems are used for the

189   characterization of the oxidized APL *in vitro* and *ex vivo*, which is necessary for structure-biological

190   activity studies and facilitates the development of targeted methods for the detection and the

191   quantification of these molecules *in vivo*. A list of biomimetic systems that have been used so far for

192   APL oxidation is reported in Table 3. The most common biomimetic systems are reported in Figure

193 2 and include Fenton reaction, 2,2'-Azobis(2-amidinopropane) dihydrochloride (AAPH),

194 photosensitization and lipoxygenases (LOX).

195 Except for MPO, which catalyzes the formation of a non-radical ROS (HOCl), most of the

196 biomimetic methods grouped in Table 3 lead to the production of partially-reduced oxygen species

197 ($^•$OH, $O_2^{-•}$, $^1O_2$) and other free radicals (e.g., R-O-O$^•$ from AAPH). Free radicals mediate the

198 hydrogen abstraction and the subsequent generation of a carbon-centered radical which promptly

199 reacts with O_2, leading to the formation of one or more hydroperoxyl derivatives. These radicals are

200 particularly unstable and easily get stabilized by abstracting further (bis-)allylic hydrogen atoms from

201 surrounding lipid molecules, leading to the formation of non-radical fatty acyl hydroperoxides (R-O-

202 O-H). Consequently, metal cations such as Fe^{2+} (in the case of Fenton reaction) or Cu^{2+}, catalyze the

203 decomposition of hydroperoxides into alkoxyl radicals (RO$^•$). These radicals may abstract carbon-

204 centered hydrogen from an adjacent lipid molecule and generate hydroxides (R-O-H), or further

205 degrade into other chain-propagation radicals as alkyls (R$^•$), hydroxyl-alkyls (HOR$^•$), epoxy-alkyls

206 (OR$^•$) and epoxy-peroxyls (OROO$^•$) (Reis and Spickett 2012). Esterified APL hydroperoxides can

207 also cyclize and form a 5-membered ring that cleaves, forming a subclass of products named isoketals

208 (isoLGs) (Salomon 2005; Li et al. 2009).

209 Lipid oxidation derivatives that are named long chain oxidation products contain one or

210 several oxygen atoms inserted on the fatty acyl chains, as in the case of hydroperoxy or hydroxy, keto

211 and epoxy-derivatives. However, radical intermediates as alkoxyl radicals can further degrade

212 through a β-cleavage of the C-C bond between the oxygenated carbon atom and the unsaturation in

213 vinylic position. This cleavage leads to the formation of esterified aldehydes, keto-aldehydes,

214 hydroxy-aldehydes, carboxylic acids, keto-carboxylic acids and hydroxy-carboxylic acids, named

215 short chain oxidation products (Figure 1) (Gugiu et al. 2006; Domingues et al. 2009; Maciel, Faria,

216 et al. 2013). When radical-radical reactions occur, in some cases due to antioxidant molecules, the

217 radical-based oxidation process reaches the termination phase (Wefers and Sies 1988; Tadolini et al.

218 2000).

219

B. Oxidation of the polar heads

221

Among the ROS summarized in Table 3, the ones inducing one-electron oxidation on unsaturated fatty acyl chains have also been found to mediate radical-mediated oxidation of the polar head for both PE (Melo, Santos, et al. 2013) and PS (Maciel et al. 2011; Maciel et al. 2014). The serine center in the polar head of PS has hydrogen linked to the α-carbon, which is easily abstracted under radical attack, leading to an α-alkoxyl derivative (Maciel et al. 2011). The oxidation of the α-alkoxyl further proceeds to polar head derivatives modified as terminal acetic acid, terminal acetamide, terminal hydroxy acetaldehyde and terminal hydroperoxy acetaldehyde (Maciel et al. 2011). These modifications were observed for the first time in a study in which oxidation of PS was carried out *in vitro* through the Fenton reaction (Maciel et al. 2011). Later on, the oxidation of PS polar head to terminal acetic acid was found to occur in human keratinocytes treated with AAPH (Maciel et al. 2014). Similarly, *in vitro* irradiation of PE standards with white light in the presence of cationic porphyrins as photosensitizers (photo-oxidation) led to oxidative deamination of the ethanolamine group, with the generation of the polar head modified as terminal acetaldehyde (Figure 1) (Melo, Santos, et al. 2013).

Hypohalous acids as HOCl can also modify the polar head of PE via two-electron oxidation mechanism on the free amino group. This reaction runs by the initial formation of a chloroamine and, upon HOCl excess, continues with the formation of a dichloramine, which eventually loses two moles of HCl and leads to a terminal nitrile derivative (Carr, van den Berg, and Winterbourn 1998; Richter et al. 2008; Üllen et al. 2010).

241

C. Adduction of glucose to the polar head (glycation and glyco-oxidation)

243

244   The amino group present in the polar head of APL is reactive towards electrophilic moieties

245   as carbonyl groups. In fact, several published works mentioned the reactivity of the amino groups of

246   PE and PS towards glucose and the consequent formation of glycated APL (Ravandi, Kuksis, and

247   Myher 1995; Ravandi et al. 1996; Lertsiri, Shiraishi, and Miyazawa 1998; Oak, Nakagawa, and

248   Miyazawa 2000; Nakagawa 2005; Simões et al. 2010; Sookwong et al. 2011; Maciel, da Silva, et al.

249   2013; Maciel, Faria, et al. 2013; Melo, Silva, et al. 2013; Annibal et al. 2016). APL glycation occurs

250   via reaction between the amino group of the APL polar heads and the carbonyl moiety of glucose,

251   initially leading to a Schiff-base derivative which promptly establishes an equilibrium with the

252   Amadori ketoamine (Simões et al. 2010; Annibal et al. 2016). Glycated APL can be further modified

253   if radical driven oxidation occurs during or after the glycation. Both the Schiff-base and the Amadori

254   derivatives were found to undergo oxidation on the fatty acyl chains and the glycated polar heads

255   when ROS were present, in a process that is identified as glyco-oxidation, and leads to the production

256   of AGE of APL (Simões et al. 2010; Melo, Silva, et al. 2013; Maciel, da Silva, et al. 2013; Maciel,

257   Faria, et al. 2013; Simões et al. 2013a; Annibal et al. 2016). When the radical mechanism involves

258   the polar head glycated as Schiff base, the hydrogen atom on the methylene adjacent to the imine

259   bond is abstracted, leading to peroxyl and alkoxyl radicals. These are often stabilized through

260   reduction to the carbonyl. However, if the radical reaction occurs on the Amadori derivative, the

261   oxidation mainly affects the sugar moiety through sequential backbone cleavages (Simões et al. 2010;

262   Maciel, da Silva, et al. 2013; Annibal et al. 2016) (Figure 1).

263

264   **D. Adduction of aldehydes to the polar head**

265

266   The oxidative degradation of lipids generates a variety of low-molecular-weight aldehydes

267   including hydroxy-alkenals, keto-alkenals, γ-keto-aldehydes (Frankel et al. 1977; Benedetti,

268   Comporti, and Esterbauer 1980; Lee and Blair 2000) and isoLGs (Salomon 2005) (reviewed by Reis

269   and Spickett) (Reis and Spickett 2012). These lipid-derived aldehydes contain several electrophilic

centers, which can form covalent adducts with the free amino groups in the polar heads of APL. It has been reported for isoLG a reaction rate with PE that was 4.4-fold faster than the reaction between isoLG and lysine (Amarnath et al. 2004). Bernoud-Hubac *et al.* studied the mechanism of adduction between isoLG and PE, showing that the reaction runs with an initial formation of a Schiff base, that quickly forms a stable pyrrole through a cyclization (Bernoud-Hubac et al. 2004). On the other hand, the reaction between APL and hydroxy-alkenals was found to occur mainly by Michael addition (Guichardant et al. 1998; Bacot et al. 2007), even though adducts formed by the Schiff base-pyrrole pathway were also reported for the reaction of PE with 4,5(*E*)-epoxy-2(*E*)-heptenal (Zamora and Hidalgo 2003).

More recently, Vazdar *et al.* employed ^{1}H nuclear magnetic resonance spectroscopy, Fourier-transform infrared spectroscopy and MS to study the reactivity of PE towards 4-hydroxy-2-nonenal (HNE) and 4-oxo-2-nonenal (ONE) (Vazdar et al. 2017). This study highlighted that PE-HNE adducts, both Michael and Schiff base, preferentially cyclized towards hemiacetal and pyrrole derivatives, in contrast with PE-ONE adducts that did not tend to form cyclic derivatives.

The characterization and the detection of modified APL currently rely on platforms capable of performing specific and sensitive analyzes. Gas chromatography (GC) coupled to MS (GC-MS) has been widely used to analyze oxidized fatty acyl chains of phospholipids in their non-esterified form, as well as modified polar heads from APL, but it is not suitable for direct analysis of intact modified APL (Spickett et al. 2010). Presently, tandem MS using soft ionization methods is the most used platform in the analysis of the complex network of PE and PS modified structures, both *in vitro* and in biological samples. The next section reviews and describes all the MS strategies that have so far been used in the analysis of modified APL.

III. MS-Based Strategies for the Analysis of APL Modifications

The development of soft ionization methods, such as electrospray ionization (ESI) (Yamashita and Fenn 1984) and matrix-assisted laser desorption ionization (MALDI) (Tanaka et al. 1988; Karas and Hillenkamp 1988), made the MS analysis of intact biomolecules possible, opening a new world of MS-based approaches that has strongly grown through the last 20 years. The introduction of high-resolution MS analyzers in the last decade led to several advantages in the field of lipidomics, including reduced overlap of species in the mass spectrum (due to discrimination at 1-3 ppm or even sub-ppm level) and reduced analysis time (reviewed by Ghaste, Mistrik and Shulaev) (Ghaste, Mistrik, and Shulaev 2016). The following sections will review the current state of understanding of the information that MS-based analytical strategies have provided for all the known APL modifications

A. Applications of GC-MS in the analysis of modified APL

Since APL are non-volatile compounds, their analysis by GC-MS can only be carried out after the first step of hydrolysis of the ester bonds linking the fatty acids and the polar head to the glycerol backbone. In a subsequent step, the fatty acids and the polar head released by the hydrolytic treatment are derivatized with organic acids to produce volatile esters as, for example, trifluoroacetyl, acetyl and methyl esters (van Kuijk et al. 1985; Requena et al. 1997; Fountain et al. 1999). GC-MS typically uses electron ionization (EI) as ionization technique, which is characterized by a high in-source fragmentation that frequently causes the loss of structure of the molecular ion, hindering its observation. However, even though in EI-MS the molecular ion can be absent after the ionization process, information about its structure can be provided by the comparison of its in-source fragmentation pattern with the in-source fragmentation pattern of standards, or by direct interpretation of the fragmentation patterns.

GC-MS has been used to detect AGE of APL bearing glyco-oxidative modifications on the ethanolamine or serine polar heads. The AGE of PE known as carboxymethyl-PE (CM-PE) is a

product of PE glyco-oxidation which has been quantified *in vivo* through GC-MS analysis of its hydrolysis product, carboxymethyl-ethanolamine (CM-Etn) (Requena et al. 1997; Pamplona et al. 1998). The experimental approach was based on acid hydrolysis of CM-PE that produced the free carboxymethylated polar head (CM-Etn). Subsequently, CM-Etn was derivatized as a trifluoroacetyl-methyl ester (TFAME) and quantified through GC-MS in single ion monitoring (SIM) mode (Requena et al. 1997; Pamplona et al. 1998). This methodology allowed the quantitative assessment of CM-Etn in mitochondrial membranes of several mammals (Pamplona et al. 1998) as well as in lipid extracts of red blood cell membranes of healthy and diabetic subjects (Requena et al. 1997). In another study, two glycation and glyco-oxidation products of APL, namely N-(Glucitol)PE and carboxymethyl-PS (CM-PS), were similarly detected and quantified by GC-MS. N-(Glucitol)PE and CM-PS were hydrolyzed in acid conditions as described above, with the production of the free, modified polar heads N-(Glucitol)ethanolamine (GE) and carboxymethyl-serine (CM-Ser), respectively. The modified polar heads were derivatized as N,O-acetyl methyl esters and finally analyzed by GC-MS in SIM mode (Fountain et al. 1999). In this study, the derivatized polar heads were quantified in the lipid extracts of human red blood cells from healthy and diabetic patients, showing an increased content of GE, but not CM-Ser, in the samples of the diabetic patients when compared to nondiabetic.

GC-MS has also been used to assess the reactivity of PE polar head with fatty aldehydes generated by lipid peroxidation. Bacot (Bacot 2003) studied the in vitro reactivity of the ethanolamine group of PE with 4-hydroxy-2-hexenal (HHE), HNE and 4-hydroxydodeca-(2,6)-dienal (HDDE). Adducted PE were hydrolyzed, and the resulting ethanolamine-hydroxyalkenal adducts were derivatized as pentafluorobenzyloximes trimethylsilyl esters before GC-MS analysis (Bacot 2003). In subsequent work, the same author and others detected PE-hydroxyalkenals Michael adducts in human blood platelets and retinas of streptozocin-induced diabetic rats (Bacot et al. 2007). In this study, Michael-adducted PE were subjected to basic hydrolysis, and the resulting ethanolamine-alkenals moieties were derivatized as trifluoroacetyl esters before the GC-MS analysis. In another

study, aldehyde-carbonylation products of PE with long-chain fatty aldehydes (e.g., pentadecanal, heptadecanal, heptadecenal) were observed through GC-MS analysis (Stadelmann-Ingrand, Pontcharraud, and Fauconneau 2004). These carbonylation products were observed in rat cortex homogenates that were submitted to UV light or Fe^{2+}-induced oxidation, after basic methanolysis and derivatization of the modified ethanolamine as trimethylsilyl ether (Stadelmann-Ingrand, Pontcharraud, and Fauconneau 2004). All these works show that GC-MS has undoubtedly been one of the most important analytical techniques in the analysis of lipid modification, and still plays a crucial role in classical lipidomic studies (Li et al. 2011). However, due to several disadvantages such elaborate sample preparation, fragmentation of the molecular ions in the EI source and risk of degradation for thermolabile molecules, the relevance of this method in the study of APL modification is diminishing. As consequence of these drawbacks, MS analysis of modified APL has started to be performed mainly using soft ionization methodologies (ESI, MALDI) that preserve the structure of the analyte and, in the case of ESI, can be easily coupled with liquid chromatographic separations.

B. Applications of ESI-MS and MALDI-MS in the analysis of modified APL

Under ESI-MS and MALDI-MS analysis, APL can ionize in both negative and positive ions modes, with the formation of predominant $[M-H]^-$ ions and $[M+H]^+$ ions, respectively (Pulfer and Murphy 2003). Despite PS can also be analyzed in positive ions mode as $[M+H]^+$ ions, the identification and characterization of PS by MS is preferentially made in negative ions mode, probably due to the presence of the carboxylic acid group in the polar head (Koivusalo et al. 2001; Pulfer and Murphy 2003).

When aiming to unveil APL modifications, the analysis of mass spectra generated by direct infusion MS or by liquid chromatography (LC-)MS runs of mixtures of native and modified APL is technically simple, interpretation of results is straightforward, and the first level of information

regarding the formation of new molecular structures is provided. When the ESI-MS spectra of modified APL are compared with an ESI-MS spectrum acquired in control conditions, the new ions correspondent to modified APL appearing in the former spectrum and the mass shifts can be classified into the following regions (Domingues, Reis, and Domingues 2008):

- Long chain oxidation products region, characterized by ions that result from the insertion of one or more oxygen atoms on the unsaturated fatty acyl chain and therefore show higher m/z values than the native APL. These ions are usually attributed to epoxy-, keto-, hydroxy-, hydroperoxy- and polyhydroxy-derivatives;

- Polar head oxidation products region, characterized by ions that result from deamination or decarboxylation reactions occurring in the polar heads, and therefore show lower m/z values than the native APL.

- Adducts region, characterized by ions that result from the reaction of the free nucleophilic amino group of APL with carbonyl moieties of sugars (e.g. glycation/glyco-oxidation derivatives of PE and PS) and reactive aldehydes/ketones/carboxylic acids generated in the late stages of the fatty acyl chain-shortening oxidative degradations (e.g. HHE, HNE, acrolein, malonaldehyde, hexanoic acid). Ions of these adducts usually show higher m/z values than the native APL;

- Short chain oxidation products region, characterized by ions that result from the oxidative cleavages of the unsaturated fatty acyl chains and therefore can be observed as ions with lower m/z values than the native APL. Shortened APL usually bear carbonyl species on the $sn2$ position such as aldehydes, keto-aldehydes, hydroxy-aldehydes, as well as carboxylic acids, keto-carboxylic acids, hydroxycarboxylic acids. Oxygen insertions on the fatty acyl chains, as well as products from adduction of sugars and carbonyl species, can also occur on chain-shortened oxidation products leading to other ions with m/z values lower than the native APL, although these types of oxidative modifications have been scarcely reported.

399   -   Lyso-APL region, characterized by ions that result from the hydrolysis of the ester linkage

400   between the glycerol backbone and a fatty acyl chain.

401

402   *1. Identification of long-chain and short-chain oxidation products*

403

404   The first step when identifying long-chain oxidation products of APL is the observation in the

405 mass spectra of new peaks with different mass shifts. These shifts include ions with + 16 Da in the

406 case of hydroxyl derivatives, + 32 Da in the case of hydroperoxy (or di-hydroxy) derivatives, and +

407 14 Da in the case of keto or epoxy derivatives (16-2 Da). In Figure 3 we exemplify the presence of

408 these ions for oxidized 1-palmitoyl-2-linoleoyl-*sn*-3-glycerophosphoethanolamine (ox-PLPE) and in

409 Figure 4 (Panel C) for oxidized 1-palmitoyl-2-linoleoyl-*sn*-3-glycerophosphoserine (ox-PLPS). Long

410 chain oxidation product with multiple oxidation motifs are detected by identifying mass increments

411 corresponding to combinations of 16 Da and 14 Da. This approach allows proposing several oxidative

412 modifications as hydroxy, di- or poly-hydroxy, hydroperoxy, as well as hydroxy-peroxy, keto and

413 epoxy combined with hydroxy or hydroperoxy (Tyurina et al. 2008; Tyurin et al. 2008; Tyurin et al.

414 2009; Domingues et al. 2009; Tyurina et al. 2010; Tyurina, Tyurin, et al. 2011; Tyurina, Kisin, et al.

415 2011; Maciel et al. 2011; Maciel, Faria, et al. 2013; Melo, Silva, et al. 2013; Melo, Santos, et al. 2013;

416 Ni, Milic, and Fedorova 2015). Figure 3B shows a full ESI-MS spectrum ox-PLPE acquired in

417 positive ion mode, which allowed to identify long chain oxidation products bearing 1 oxygen atom,

418 2, 3 and 4 oxygen atoms (Domingues et al. 2009). Figure 4C shows a full ESI-MS spectrum of ox-

419 PLPS acquired in negative ion mode, reporting long chain oxidation products bearing 1, 2 and 3

420 oxygen atoms (Maciel et al. 2011).

421   Short chain oxidation products esterified to an oxidatively truncated carbon chain on the *sn-2*

422 position are detected at lower *m/z* values than the unmodified APL. These species can bear either a

423 terminal aldehydic or carboxylic group, as reported by several authors (Gugiu et al. 2006; Domingues

424 et al. 2009; Simões et al. 2010; Maciel et al. 2011; Maciel, Faria, et al. 2013). These products can be

further oxidized in the shortened carbon chain with additional keto/epoxy, hydroxy and hydroperoxy moieties (Maciel et al. 2011; Maciel, Faria, et al. 2013). As for long-chain derivatives, short chain oxidation products can be analyzed by MS either in positive and negative ion mode. Oxidation products with shortened sn-2 fatty acyl chains (9 carbon atoms) were observed in the MS spectrum of ox-PLPE acquired in positive ion mode, depicted in Figure 3B (Domingues et al. 2009). The MS spectrum of ox-PLPS in negative ion mode, reported in Figure 4C, allows identifying similar short chain oxidation products described above for ox-PE, including esterified aldehydes and carboxylic acids with 9 carbon atoms (Maciel et al. 2011). The mass shifts characteristic for long and short chain oxidation of APL, that can be observed in full MS spectra, are summarized in Table 4.

2. Identification of polar head oxidation products

APL bearing an oxidative modification in the polar heads are easily detected in the MS spectra as peaks with lower *m/z* values than the unoxidized species (Maciel et al. 2011; Melo, Santos, et al. 2013). Using photosensitized oxidation and direct infusion ESI-MS in negative ion mode, Melo *et al.* (Melo, Santos, et al. 2013) identified a series of long-chain oxidation products of PE bearing also an oxidative modification in the ethanolamine (Etn) polar head, which are summarized in Table 4. These PE modified in the polar head arose from the oxidative deamination of the Etn moiety of the polar head due to photo-oxidation. Hence they appeared in the MS spectra at odd *m/z* values with a mass shift of -1 Da when compared to the respective PE. In the case of 1-palmitoyl-2-oleoyl-*sn*-3-glycerophosphoethanolamine (POPE), the authors identified the [M-H]⁻ ion at *m/z* 731 as oxidized POPE with one oxygen insertion on the oleyl chain in *sn*-2 and the Etn polar head modified as terminal acetaldehyde (mass shift from native POPE corresponding to - 1 + 16 Da) (Figure 5).

Maciel *et al.* (Maciel et al. 2011) identified several modifications in the polar head of PS species, formed during biomimetic oxidation with the Fenton reaction (Figure 4A). The oxidation products of PS with modified polar heads were fractionated by thin layer chromatography (TLC),

exploiting the difference of polarities induced by such modifications (Figure 4B). After scraping and

lipid extraction, the modified PS separated in each TLC spots were analyzed by ESI-MS in negative

ion mode (Figure 4C). The [M-H]$^-$ ions characteristic for PE and PS modified in the polar head are

summarized in Table 4 (Maciel et al. 2011).

3. Identification of glycation and glyco-oxidation products

Glycation of APL on the polar heads can be observed in the MS spectra by observing peaks

of the native APL with a mass shift of +162 Da (Simões et al. 2010; Maciel, Faria, et al. 2013; Maciel,

da Silva, et al. 2013; Melo, Silva, et al. 2013; Annibal et al. 2016). If oxidative conditions are

superimposed on glycated APL (glyco-oxidation), the radical-based oxygenation can preferentially

affect the fatty acyl chains of the APL and leave the glycated polar head intact. In this case, when the

glyco-oxidation mixture is analyzed by ESI-MS the following ions can be observed in the MS spectra

(summarized in Table 5):

(I)   Short chain oxidation products with a glucose moiety adducted to the polar head: characterized by a negative mass shift due to the chain-shortening β-cleavage, plus a mass shift of + 162 Da due to the glycation (Simões et al. 2010; Maciel, Faria, et al. 2013; Annibal et al. 2016);

(II)   Long chain oxidation products with a glucose moiety adducted to the polar head: characterized by mass shifts of different combinations of 16 Da and 16-2 Da, due to the oxygen insertions, plus a mass shift of + 162 Da due to the glycation (Simões et al. 2010; Melo, Silva, et al. 2013; Maciel, Faria, et al. 2013; Maciel, da Silva, et al. 2013);

Figure 6B shows an ESI-MS spectrum of a gly-ox-PLPE acquired in positive ion mode which

shows the several short chains and long chain oxidation products, formed after oxidation of the fatty

acyl chain (Simões et al. 2010).

If also the glycated polar head undergoes radical oxidation, the MS spectrum of a glyco-oxidized mixture can include ions characterized by peculiar mass shifts:

(I)   Mass increments higher than + 162 Da identify glyco-oxidized APL bearing a glucose moiety with oxygen insertions (e.g. 162 Da + 14 Da = 176 Da) (Simões et al. 2010; Maciel, da Silva, et al. 2013; Melo, Silva, et al. 2013; Annibal et al. 2016);

(II)   Mass increments lower than +162 Da identify glyco-oxidized APL bearing an end-product of glucose formed through oxidative cleavage (AGE) (e.g. +28 Da, +58 Da, +72 Da) (Simões et al. 2010; Maciel, da Silva, et al. 2013; Maciel, Faria, et al. 2013; Melo, Silva, et al. 2013; Annibal et al. 2016).

As examples, the characteristic [M-H]⁻ ions of POPS AGE identified by ESI-MS are depicted in Figure 7 (Maciel, da Silva, et al. 2013).

4. Identification of aldehyde-adduction products

ESI-MS has not been extensively used in the analysis of the adducts between APL and electrophilic aldehydes, except for few studies that focused on the characterization of PE adducts with iso-LGs (Bernoud-Hubac et al. 2004), HNE (Guichardant et al. 1998), and alkanals (Annibal et al. 2014). There is currently a lack of studies aimed to characterize the potential adduction of PS with aldehydes and ketones. In what concern PE adducts, Guichardant *et al.* (Guichardant et al. 1998) identified the adducts formed by the incubation of 1,2-diheptadecanoyl-*sn*-3-glycerophosphoethanolamine (DHPE) and HNE using ESI-MS in negative ion mode. The MS spectrum of the reaction products are shown in Figure 8, which clearly depicts the characteristic mass shifts of 120 Da, 138 Da, 156 Da, corresponding to cyclized Schiff base (a), Schiff base (b), and Michael adduct (c), respectively. More recently, Annibal *et al.* (Annibal et al. 2014) employed high-resolution Orbitrap MS analysis to identify modified derivatives of 1,2-dipalmitoyl-sn-3-glycerophosphoethanolamine (DPPE) arising from its incubation with hexanal and other alkanals.

The MS spectrum of the products of the reaction between DPPE and hexanal acquired in positive ion mode, shown in Figure 9A, shows new ions that have mass shifts corresponding to the sequential adductions of up to three hexanal molecules, resulting in a series of monomeric, dimeric, and trimeric covalent adducts.

Nowadays, accurate mass analysis achievable by mass spectrometers equipped with high-resolution analyzers allows a precise identification of modified APL using data from an MS scan. However, native and modified APL having the same *m/z* (isobaric species) can be generated within a reaction occurring *in vitro* or *in vivo*, and the structural features of the modified products can easily include constitutional isomers that would not be distinguished by using direct infusion MS data, and maybe even using LC separation in the case of isomers of position. Therefore, LC separation and MS/MS structural characterization are highly recommendable to confirm the identity of the modifications. The applications of LC and MS/MS in the structural characterization of modified APL will be addressed in detail in the next paragraphs of the present review.

C. Applications of LC in the MS-based analysis of modified APL

The improvements that LC-ESI-MS methods have brought to the field of lipidomics have already been acknowledged and reviewed (Li et al. 2011; Hyötyläinen and Orešič 2016; Sethi and Brietzke 2017). In fact, LC-MS has also played a key role in the analytical separation of modified APL, mainly for the following reasons:

(I) Oxidation, glycation and aldehyde-adduction reactions generate several modified APL that might have very close *m/z,* not resolved by low-resolution instruments. Also, in more complex samples, native and modified species can be isobaric. Thus, LC-MS approaches allow the separation of these complex mixtures, based on the differences in the polarities within native and modified species (e.g., separation of hydroperoxy-PE, hydroxy-PE, and native PE);

(II)   The ionization efficiency of the modified products can be decreased through ion suppression mediated by the native APL, which are often more abundant. In such case, chromatographic separation of the analyzed mixture would increase the sensitivity towards low-abundant species.

(III)   LC protocols allow the separation of constitutional isomers of modified APL.

In most of the LC-MS protocols described in the literature for the analysis of ox-PE, reversed phase high-performance LC (RP-HPLC) was the preferred separation approach, allowing to resolve phospholipids by species through the interaction of the stationary phase with the fatty acyl chains. The insertion of oxygen atoms on the fatty acyl chains increase the polarity of the molecule and, consequently, in RP-HPLC oxidized APL elute earlier than native APL. C_{18} microbore columns with an internal diameter of 2 mm or 0.5 mm have been widely used in the chromatographic separation of ox-PE (Gugiu et al. 2006; Maskrey et al. 2007; Domingues et al. 2009; Thomas et al. 2010; Zemski Berry et al. 2010; Alwena H Morgan et al. 2010; Clark et al. 2011; Hammond et al. 2012). Microbore columns operate at low flow rates (e.g., 200 µL/min), increasing the sensitivity of the analysis. However, other LC-MS protocols for ox-PE have relied on C_{18} standard analytical columns (Khaselev and Murphy 1999; Hammond et al. 2012). Ox-PS analysis by LC-MS is a less explored field, yet Maciel *et al.* (Maciel, Faria, et al. 2013) performed a reverse phase separation of a mixture of long chain, short chain and polar head oxidation products of PS using a C_5 microbore column. There are also examples of oxidative phospholipidomics studies in which the analysis of ox-PS species has been performed by normal phase HPLC (NP-HPLC) using silica microbore columns (Tyurina et al. 2010; Tyurina, Tyurin, et al. 2011).

The first LC-MS protocols for gly-PE and glycated PS (gly-PS) were proposed in the nineties and relied on NP analytical columns. Adduction of the polar head to a glucose moiety increases the polarity of the molecule, hence in NP-HPLC glycated APL elute after native APL. This approach succeeded in the separation of native APL from their glycated derivatives, both *in vitro* (Ravandi, Kuksis, and Myher 1995) and in plasma of diabetic patients (Ravandi et al. 1996). RP-HPLC-MS has

also been carried out for the analysis of gly-PE. A C_{18} medium bore column has been used to separate

Schiff bases and Amadori derivatives of PE in human erythrocytes (Breitling-Utzmann et al. 2001).

Also, C_{18} microbore columns were used in an LC-MS/MS protocol aimed to quantify PE-AGE in

human erythrocytes and blood plasma (CE-PE and CM-PE) (Shoji et al. 2010). More recently, C_5

microbore columns have been used in LC-MS/MS protocols aimed to the *in vitro* characterization

and structural elucidation of glyco-oxidized PE (gly-ox-PE) (Simões et al. 2010) and PS (gly-ox-PS)

(Maciel, Faria, et al. 2013; Maciel, da Silva, et al. 2013). An overview of the LC columns that have

so far been coupled to MS in the analysis of modified APL is reported in Table 6.

D. Applications of MS/MS in the structural characterization of modified APL

Modified APL can be identified in an MS analysis, preferably using high accuracy

measurements and interpretation of the new ions appearing at characteristic mass shifts, as described

earlier. Besides this, the modifications identified in MS scans should be confirmed by characterizing

the new motifs of the modified APL. Such structural characterization can be achieved by MS/MS

analysis, as we will describe in the following paragraphs. The characteristic fingerprints and the

interpretation of the fragmentation patterns depend on the nature of the modification. Hence, the

MS/MS strategies proposed until now for the characterization of modified APL will be addressed,

organized by type of modification.

1. Structural characterization of long-chain and short-chain oxidation products

Long and short chain oxidation products can be characterized by the analysis of MS/MS

spectra obtained either in positive or negative ion modes. While for native and modified PE both

approaches have been used, in the case of PS the most suitable approach is the analysis of the

deprotonated molecular ions [M-H]$^-$. MS/MS analysis of long chain and short chain oxidation

products performed in the negative ion mode shows two significant families of typical fragment ions:

    (I)   carboxylate anions of the fatty acids esterified to *sn*-1 (R_1COO^-) and *sn*-2 (R_2COO^-)

            positions;

    (II)   ions arising the neutral losses of unmodified saturated *sn1* acyl chains (R_1=C=O, ketene, and

            R_1COOH, carboxylic acid) and modified unsaturated *sn2* acyl chains (R_2'=C=O, ketene, and

            R_2'COOH, carboxylic acid).

        MS/MS spectra of PE acquired in negative ion mode are usually characterized by a higher

relative abundance (RA) of R_1COO^- anions compared to R_2COO^- anions. The opposite behavior (RA

R_2COO^- > RA R_1COO^-) is commonly observed for negative ion mode MS/MS spectra of PS (Pulfer

and Murphy 2003). However, this behavior depends on the mass spectrometer and should always be

confirmed using well-known standards. The MS/MS spectra of the [M-H]$^-$ molecular ion of oxidized

APL allows the observation of the carboxylate anions of modified unsaturated FA which are usually

characterized by the mass increments due to the insertion of n oxygen atoms (n x 16 Da, n x 16-2

Da). Complementarily, the observation of the lyso-APL product ions (due to the neutral loss of the

fatty acids as –RCOOH or –R=C=O) can be used to corroborate the oxidative modification (Tyurin

et al. 2008; Tyurina et al. 2008; Tyurin et al. 2009; Tyurina et al. 2010; Maciel et al. 2011; Maciel,

Faria, et al. 2013; Melo, Silva, et al. 2013; Maciel, da Silva, et al. 2013; Melo, Santos, et al. 2013).

Figure 10 shows the MS/MS spectra of a long chain oxidation product of PAPE (PAPE + 4O),

acquired in the negative ion mode using an Orbitrap-higher energy collision-induced dissociation

(HCD) (PAPE + 4O, *m/z* 802.488); the characteristic fragments corresponding to the carboxylate

anions can be seen, along with the characteristic neutral loss of modified saturated *sn*-2 as ketene

(R_2'=C=O). Figure 11 exemplifies the tandem MS of a short chain oxidation product of PE, namely

1-(palmitoyl)-2-(5-oxovaleroyl)-PE, also acquired upon HCD activation in the negative ion mode;

both the native and the shortened fatty acid carboxylate anions, corresponding to the *sn*-1 and the *sn*-

2 fatty acyl chains, respectively, are shown.

606   Besides the characteristic product ions described above for all the oxidized APL, the MS/MS

607 analysis of the PS class in negative ion mode always shows a product ion formed due to the neutral

608 loss of aziridine-2-carboxylic acid from the Ser moiety (identified as neutral loss of 87 Da, Figure

609 12). This abundant neutral loss is typically observed in the negative ion mode MS/MS spectra of

610 native and ox-PS molecular ions (Pulfer and Murphy 2003; Domingues, Reis, and Domingues 2008;

611 Maciel et al. 2011; Maciel, Faria, et al. 2013). Hence, it can be used to further confirm the identity of

612 a long chain or short chain oxidation product of PS, but it is absent in PS modified in the polar head

613 group. PE tandem mass spectra do not display a typical neutral loss in negative ion mode. The identity

614 of long chain and short chain oxidation products of PE can be further verified by MS/MS analysis in

615 positive ion mode through the characteristic neutral loss the polar head (loss of phosphoethanolamine,

616 141 Da) (Pulfer and Murphy 2003; Domingues, Reis, and Domingues 2008; Domingues et al. 2009;

617 Simões et al. 2010). This neutral loss is a common feature of the tandem mass spectra of native and

618 ox-PE $[M+H]^+$ ions, as it can be observed in Figures 13B and 13C. However, this typical neutral loss

619 is also absent in the case of modifications in the polar head group in PE.

620   Our group has published results from several ESI-MS/MS structural characterizations of

621 oxidized APL, either in negative ion mode (Maciel et al. 2011; Maciel, Faria, et al. 2013) or in the

622 positive ion mode (Domingues et al. 2009; Simões et al. 2010; Simões et al. 2013a). Long chain and

623 short chain oxidation products of PE can be characterized by positive ion mode MS/MS. The

624 complete interpretation of the fragmentation patterns should include the observation and

625 interpretation of the following product ions (Domingues et al. 2009; Simões et al. 2010):

626   (I)   Ions arising from the neutral losses of the polar head (141 Da);

627   (II)   Ions arising from the neutral losses of unmodified saturated *sn1* acyl chains (R_1=C=O,

628   ketene, and R_1COOH, carboxylic acid) and modified unsaturated *sn2* acyl chains

629   (R_2'=C=O, ketene, and R_2'COOH, carboxylic acid);

630   (III)   Ions arising from the neutral losses of the fatty acyl chains plus the polar head;

631   (IV)   Ions arising from the neutral loss of the polar head, plus the fragmentation of the C-C bond

632   between a carbon atom bearing an oxygen insertion and the unsaturation in vinylic position.

633   These typical product ions observed in MS/MS spectra in positive ion mode of ox-PE are exemplified

634   in Figures 13B and 13C. These figures compare the positive LC-MS/MS spectra of two ox-PE

635   isomers (PLPE + 3O) (Domingues et al. 2009); ions labelled as A, B and C were formed by the

636   fragmentation occurring between the carbon atom bearing the hydroxyl or hydroperoxyl functional

637   group and the adjacent double bond, thus were used to indicate which carbon atom was modified by

638   the oxygenated moieties (Figures 13B and 13C). Domingues *et al.* (Domingues et al. 2009) also

639   correlated the neutral loss of H_2O_2 (34 Da), that was observed for the ox-PLPE isomer in Figure 13C

640   through the fragment ion at m/z 730.6, with the presence of a hydroperoxy moiety on the *sn-2* fatty

641   acyl chain. The neutral loss of H_2O_2 was also reported for PCs oxidized as hydroperoxy derivatives

642   (Adachi et al. 2004; Adachi et al. 2005; Spickett et al. 2001; Reis et al. 2007). Such a neutral loss

643   would not appear in the MS/MS spectra of hydroxylated species. Differently, multiple losses of H_2O

644   molecules (losses of n x 18 Da) are observed for poly-hydroxy derivatives, as exemplified in Figures

645   13B and 10 (Tyurin et al. 2009).

646

647   *2. Structural characterization of polar head oxidation products*

648

649   The structural characterization of APL bearing an oxidized polar head group is a poorly

650   explored topic that should deserve more attention. These molecules were found to be pro-

651   inflammatory factors in peripheral blood (Silva et al. 2012) and were detected in keratinocytes treated

652   with the oxidant AAPH (Maciel et al. 2014). APL oxidative modifications of the polar head were

653   characterized by negative ion mode MS/MS for ox-PS. The MS/MS spectra are characterized by the

654   following features (Maciel et al. 2011):

655   (I)   Absence of the ions arising from the neutral loss of aziridine-2-carboxylic acid (-87 Da),

656   typical of native PS;

657   (II)   Carboxylate anions of the fatty acids esterified to *sn-1* and *sn-2* positions;

658   (III)   Ions arising from specific neutral losses due to the modification of Ser in the oxidized polar

659   head.

660   Figures 14A and 14 B show two MS/MS spectra of ox-PS bearing a modification in the polar

661   head, acquired in negative ion mode upon collision-induced dissociation (CID) and HCD activation,

662   respectively. In both the MS/MS spectra, the neutral loss of 87 Da from the precursor is not observed,

663   yet it is possible to detect a neutral loss of 58 Da. This fragmentation pattern is characteristic for ox-

664   PS bearing a glycerophosphoacetic acid derivative in the polar head. The structures of this ion are

665   depicted in Figure 14 and Figure 5A (Maciel et al. 2011).

666   A summary of the main product ions that have been characterized by the MS/MS analysis of

667   ox-PE and ox-PS in both positive and negative ion modes is reported in Table 4

668

669   *3. Structural characterization of glycation and glyco-oxidation products*

670

671   The MS/MS-based fingerprinting of glycated and glyco-oxidized APL relies on the

672   interpretation of specific neutral losses, which allow confirming the adduction of a glucose moiety to

673   the polar head. A correct reading of such neutral losses also allows the elucidation of the oxidative

674   modifications that have eventually been introduced on the glycated polar head. A summary of the

675   mass shifts and the characteristic neutral losses that have been observed in the MS/MS spectra of

676   glycated and glyco-oxidized APL acquired in both positive and negative ion modes is reported in

677   Table 5. Importantly, the neutral loss of phosphoethanolamine polar head from PE occurs upon

678   MS/MS in positive ion mode, whereas the neutral loss of Ser from the polar head of PS takes place

679   upon MS/MS in negative ion mode (Pulfer and Murphy 2003). Hence, the fragmentation in positive

680   ion mode is preferred for the analysis of gly-PE and gly-ox-PE, since it allows to observe the neutral

681   loss of the glycated polar head (Simões et al. 2010; Melo, Silva, et al. 2013; Annibal et al. 2016).

682   Conversely, the analysis in negative ion mode is more suitable for gly-PS and gly-ox-PS, because it

allows the observation of the neutral loss of the glycated Ser moiety from the polar head (Maciel, da Silva, et al. 2013). However, MS/MS analysis in negative ion mode is also suitable for gly-PE and gly-ox-PE (Simões et al. 2010; Melo, Silva, et al. 2013). The MS/MS fragmentation of gly-PE in positive ion mode results in typical fragmentation patterns that include the following ions:

(I) Ions arising from the neutral loss of 303 Da, due to the elimination of the phosphoethanolamine polar head (-141 Da) adducted to one glucose molecule (-162 Da) (Simões et al. 2010; Melo, Silva, et al. 2013; Annibal et al. 2016). Figure 15 shows an MS/MS spectrum of gly-PLPE acquired in positive ion mode, in which it is possible to observe a diagnostic neutral loss of polar head adducted to glucose (-303 Da).(Simões et al. 2010);

(II) Ions arising from multiple neutral losses of H_2O and H_2CO, characteristic for the insertion of a glucose moiety (Wang et al. 2008; Simões et al. 2010).

When the glycated polar head of gly-ox-PE is oxidized, different ions arising from neutral losses can be observed in the MS/MS spectra acquired in positive ion mode. These explanatory neutral losses from the parent molecular ion can be classified in two main groups (Table 5) (Simões et al. 2010; Shoji et al. 2010; Melo, Silva, et al. 2013; Annibal et al. 2016):

(I) Ions arising from neutral losses greater than 303 Da, due to the elimination of the phosphoethanolamine polar head adducted to glucose, with additional oxygen insertions (e.g., glucuronic acid, glucose adducted to α-keto-etn) (Simões et al. 2010; Melo, Silva, et al. 2013; Annibal et al. 2016) (Simões, Simões, et al.; Melo, Silva, et al.; Annibal, Riemer, et al.);

(II) Ions arising from neutral losses smaller than 303 Da, due to the elimination of the phosphoethanolamine polar head adducted to end-products of glucose oxidative cleavage (e.g., carboxymethyl, carboxyethyl, formamide, carbamino); Figure 16 shows an MS/MS spectrum of gly-ox-PLPE acquired in positive ion mode. In this

708   case, the new structural feature is characterized by the neutral loss of glyco-oxidized

709   polar head.

710   The common fragmentation pathways observed in the negative ion mode MS/MS spectra of

711 gly-PS and gly-PE are also characterized by specific product ions that are different from those

712 observed in the positive ion mode. The following fragment ions are common to gly-PS and gly-PE,

713 when analyzed in negative ion mode (Table 5) (Simões et al. 2010; Maciel, da Silva, et al. 2013;

714 Maciel, Faria, et al. 2013):

715   (I)   Ions arising from the neutral loss of 162 Da, due to the elimination of the glucose

716   moiety;

717   (II)   Carboxylate anions of the fatty acids, R_1COO^- and R_2COO^-. Nevertheless, it is still

718   possible to observe oxidative modifications that can occur on the fatty acyl chains;

719   (III)   Ions formed by neutral losses of $C_3H_6O_3$, $C_4H_8H_4$, and $C_5H_{10}O_5$ (-90, -120 Da and -

720   150 Da, respectively) due to the cleavage of the glucose moiety that occurs along the

721   glycosidic linkages upon MS/MS (Asam and Glish 1997; Simões et al. 2007).

722   As an illustration of these fragmentation patterns, Figure 17 shows the MS/MS fragmentation

723 of gly-PLPE in negative ion mode, showing the characteristic neutral losses of glucose from the polar

724 head (Simões et al. 2010). The fragmentation of gly-POPS in negative ion mode is shown in Figure

725 18 and is characterized by the typical neutral losses of glycated Ser (Maciel, da Silva, et al. 2013).

726   The MS/MS spectra acquired in negative ion mode of gly-ox-PS also show characteristic

727 neutral losses. If the oxidation occurs on the glycated Ser moiety, the following diagnostic neutral

728 losses can be observed (Table 5) (Maciel, da Silva, et al. 2013; Maciel, Faria, et al. 2013):

729   (I)   Ions arising from neutral losses greater than 249 Da, due to the elimination of the Ser

730   moiety adducted to glucose with additional oxygen insertions; Figure 19B shows the

731   MS/MS spectrum of gly-ox-POPS acquired in negative ion mode, which highlights

732   the oxidation of the glucose moiety adducted to the polar head (Maciel, da Silva, et al.

733   2013);

734   (II)   Ions arising from neutral losses smaller than 249 Da, due to the elimination of the Ser

735   moiety adducted to end-products from glucose oxidative cleavage (AGE of glycated

736   Ser).

737   The MS/MS spectrum of gly-ox-POPS bearing an AGE of glycated Ser acquired in negative

738 ion mode is depicted in Figure 20. This spectrum shows the characteristic fragmentation pattern of a

739 derivative which is oxidatively shortened at C2 of the glucose moiety (Maciel, da Silva, et al. 2013).

740

741   *4. Structural characterization of aldehyde-adduction products*

742

743   Adducts of APL with aldehydes have been highlighted as bioactive molecules, able to promote

744 macrophage viability (Riazy et al. 2011) and monocyte adhesion (Guo et al. 2011). MS/MS allowed

745 the structural elucidation of several adducts of PE produced *in-vitro* using reactive products from

746 lipid peroxidation as hexanoic acid (Tsuji et al. 2003) and iso-LGs (Bernoud-Hubac et al. 2004).

747 Bernoud-Hubac and co-authors (Bernoud-Hubac et al. 2004) performed the structural

748 characterization of the adducts formed by the reaction of PLPE and a mixture of synthetic iso-LGs.

749 MS/MS in negative ion mode elucidated the structures of one AL-PE Schiff-base adduct and one AL-

750 PE pyrrole adduct. Figures 21 and 22 show two MS/MS spectra of AL-PLPE adducts, acquired in

751 negative ion mode. The spectrum in Figure 21 shows the fragmentation pattern of the AL-PLPE

752 pyrrole adduct (*m/z* 1031). The spectrum in Figure 22 shows the fragmentation pattern acquired in

753 negative ion mode MS/MS of the second AL-PLPE (*m/z* 1035), that allowed its characterization as

754 Schiff base adduct and the differentiation from the pyrrole adduct (Bernoud-Hubac et al. 2004).

755 Annibal *et al.* (Annibal et al. 2014) performed an elegant structural characterization of a Schiff adduct

756 formed by the reaction of DPPE and hexanal, based on multistage tandem MS analysis. The MS^2,

757 MS^3 and MS^4 spectra acquired in positive ion mode for the characterization of Schiff base DPPE-

758 hexanal are shown in Figure 23A, 23B, and 23C, respectively.

759   Upon the whole, unbiased LC-MS/MS analyzes of modified PE and PS allow the

760   identification of the modified species by characteristic mass shifts in the MS spectra, and the

761   structural characterization of the modifications by the acquisition of the MS/MS spectra. This

762   knowledge can be further applied to the detection and the quantification of biologically relevant

763   species *in vivo*, for example, by developing targeted MS-based analytical methods. The next section

764   reviews the MS approaches that have so far been employed for the targeted analysis of modified APL.

765

766   **E. Targeted MS approaches for the detection of modified APL in biological samples**

767

768   The detailed knowledge acquired, based on the analysis of the MS/MS spectra of modified

769   APL, allowed the development of MS-based targeted approaches, aimed at their detection and

770   quantification *ex-vivo* or *in-vivo*. The targeted detection in cells or biofluids is fundamental, as it can

771   relate the occurrence of modified APL with the biological mechanisms underpinning the onset of a

772   disease, and validate these molecules as biomarkers of a pathological condition. The applications of

773   the targeted MS approaches such as precursor ion scanning (PIS), neutral loss scanning (NLS) and

774   single/multiple reaction monitoring (SRM/MRM) to detect or quantify modified APL in biological

775   samples will be discussed in detail below.

776

777   *1. Precursor ion scanning (PIS)*

778

779   PIS identifies all the precursor ions that fragment in the collision cell to generate a selected

780   reporter ion. The carboxylate anions of the fatty acyl chains esterified to the glycerol backbone

781   (R_1COO^- and R_2COO^-) are typical reporter ions formed during the fragmentation of APL upon

782   MS/MS in negative ion mode (Pulfer and Murphy 2003). In the case of long-chain oxidation products,

783   the observation of characteristic mass shifts (n x 16 Da, n x 16-2 Da) on the carboxylate reporter ions

784   confirms the insertion of oxygen atoms on the unsaturated acyl chains, as reported above. Several

785   studies used the carboxylate anion of hydroxy-arachidonic acid (hydroxy-eicosatetraenoic acid,

786   HETE) as selected reporter ion for PIS analysis. LC-MS methods based on RP separation and PIS of

787   the precursors of HETE (*m/z* 319) were employed to detect HETE-PE generated by LOXs in activated

788   human platelets (Maskrey et al. 2007; Thomas et al. 2010), neutrophils (Clark et al. 2011) and

789   monocytes/macrophages (Maskrey et al. 2007; Morgan et al. 2009). A similar PIS approach reported

790   by Hammond *et al.* (Hammond et al. 2012) used the selection of the carboxylate anion of arachidonic

791   acid bearing one keto insertion (keto-eicosatetraenoic acid, KETE). The authors employed an LC-

792   MS method based on RP separation and PIS with the selection of KETE as reporter ion (*m/z* 317.2),

793   which detected KETE-containing PE generated by LOX in monocytes and macrophages of patients

794   affected by cystic fibrosis. Morgan *et al.* (Lloyd T. Morgan et al. 2010) used a similar PIS approach

795   in negative ion mode, by selecting the carboxylate anion of docosahexaenoic acid with the insertion

796   one hydroxy group (hydroxy-docosahexaenoic acid, HDOHE) as fragment ion. The LC-MS method

797   was based on the PIS of the HDOHE reporter ion at *m/z* 343 and detected four HDOHE-PE generated

798   by 12-LOX in activated human platelets.

799   Zemski Berry *et al.* (Zemski Berry et al. 2010) proposed a PIS approach based on the

800   derivatization of PE with 4-(dimethylamino)benzoic acid (DMABA) for detecting ox-PE in RAW

801   264.7 cells. In this study, the treatment of lipids extracted from RAW 264.7 cells with AAPH led to

802   a complex mixture of native and ox-PE, which were separated by RP-HPLC, and detected by PIS

803   using a peculiar ion formed during the fragmentation of ox-PE derivatized with D6-DMABA (*m/z*

804   197.1) (Figure 24). The structures of the ox-PE precursor ions identified by PIS were elucidated by

805   MS/MS, allowing the characterization of long chain and short chain oxidation products of PE (Zemski

806   Berry et al. 2010).

807   Maciel *et al.* (Maciel et al. 2014) reported a PIS approach for the detection of ox-PS

808   derivatives in keratinocytes subjected to *in vitro* radical oxidation with AAPH. The authors studied

809   the fragmentation of ox-PS with polar head modified as GPAA (Figures 4A and 14) by MS/MS in

810   negative ion mode, observing the formation of the reporter ion at *m/z* 137.1 ($HOPO_3CH_2COO^-$).

811 Subsequently, the PIS scan detected several oxidation derivatives of PS with polar head oxidized as

812 GPAA in the oxidatively stressed cells (Maciel et al. 2014).

813 *2. Neutral loss scanning (NLS)*

814

815 NLS identifies all the precursor ions that fragment in the collision cell by the loss of a reporter

816 neutral fragment. Both AGE and early glycation products of PE have been detected using this tandem

817 MS approach. Amadori gly-PE in plasma from diabetic patients were detected by scanning of the

818 neutral loss of 303 Da, corresponding to the loss of glycated polar head and formation of a

819 diacylglyceride ion (see also Figure 15 and Table 5) (Nakagawa 2005). In another study, profiling of

820 the PE AGE CM-PE and CE-PE in human diabetic plasma was carried out by NLS of parent ions,

821 yielding neutral losses of 199 Da and 213 Da, respectively, which again correspond to the loss of

822 modified polar heads (Shoji et al. 2010). Also, Maciel *et al.* (Maciel et al. 2014) profiled PS oxidation

823 products with polar head modified as GPAA in keratinocytes subjected to *in vitro* radical oxidation

824 with AAPH, using an NLS of the reporter neutral fragment corresponding to the acetic acid moiety

825 of GPAA (58 Da) as shown in Figure 14A.

826

827 *3. Single and multiple reaction monitoring (SRM/MRM)*

828

829 Reaction monitoring routines are more suitable when the presence of an analyte has been

830 confirmed, and a quantitative assessment is required. In single reaction monitoring (SRM) a single

831 fragmentation step is monitored, and the reporter ion that is selected is usually the most diagnostic

832 and abundant among the ions characterizing the MS/MS pattern. If the fragmentation of the parent

833 ion leads to several reporter ions which are diagnostic and intense, multiple transitions, from one

834 precursor ion to one or more reporter ions, can be monitored. This approach is known as multiple

835 reaction monitoring (MRM).

836 Positive mode reaction monitoring has been used for detecting gly-PE in biological samples,

837 through the formation of the diacylglyceride derivative fragment ions arising from the loss of glucose-

838 adducted polar head (303 Da) (Nakagawa 2005; Sookwong et al. 2011). In these reports, the transition

839 906.5 -> 603.7 was used to quantify Amadori-dioleoyl-PE in plasma from healthy and diabetic

840 humans (Nakagawa 2005). Also, the transition 908.8 -> 605.7 was used to quantify Amadori-1-

841 stearoyl-2-oleoyl-PE in several tissues from healthy and diabetic rats (Sookwong et al. 2011).

842 Similarly, CE-PE and CM-PE were quantified by reaction monitoring in human erythrocytes and

843 blood plasma, using the transition leading to the elimination of modified polar head and formation of

844 diglyceride product ion (Shoji et al. 2010). SRM and MRM were also used in the quantification of

845 different ox-PE from rat tissues. Positive mode MRM was used to quantify 14 different short chain

846 oxidation derivatives of PE in rat retina, by setting one specific parent-product transition for each

847 oxidatively truncated analyte (Gugiu et al. 2006).

848   Different isomers of long-chain oxidation products of PE are generated by LOXs in activated

849 blood cells, including platelets, neutrophils, and monocytes/macrophages. In these cells, negative ion

850 mode MRM based on the modified fatty acid carboxylate product ions as KETE (m/z 317) and HETE

851 (m/z 319) has been used for detection and quantification of HETE-PE (Thomas et al. 2010; Clark et

852 al. 2011; Morgan et al. 2009) and KETE-PE (Hammond et al. 2012) derivatives, respectively.

853

854

855   **IV. Conclusive remarks**

856

857   PE and PS, also named APL, are essential phospholipids that are found in the plasma

858 membrane of mammalian cells, displaying structural and signaling roles. APL can be modified to

859 oxidized, glycated, glyco-oxidized and aldehyde-adducted derivatives. Over the last 20 years, several

860 studies have reported the bioactivities of modified APL and their occurrences in several

861 inflammation-related pathologies, highlighting potential roles as signaling molecules and biomarkers

862 of disease. However, structural complexity and low *in vivo*-concentration have represented the two

main challenges for the analysis of modified APL. MS is a sensible and selective analytical platform that has been fundamental in the identification, structural characterization, detection and quantification of modified APL. Some MS-based strategies have already provided brilliant insights on modified PE, with several studies focusing on its characterization *in vitro* and, to a lesser extent, on its detection in biological samples. Nevertheless, the literature focused on the MS analysis of APL modifications is still scarce, particularly in the case of PS. As a challenge for the future, a more comprehensive knowledge of the modifications that can occur in PE and PS is needed, relying on systematic experimental approaches that merge *in vitro* biomimetic methods to modern MS platforms. Databases of fragment ions of modified APL can be generated from an extensive *in vitro* characterization, and finally translated to MS-based targeted methods, which represent a reliable tool for the detection of these molecules in clinical samples. This bioanalytical knowledge, accompanied by a more detailed investigation of the biological functions of modified PE and PS, will contribute to unveil the implications of modified APL in, for example, inflammatory diseases, and will provide new biomarkers of highly-debilitating pathologies like cancer, diabetes, and atherosclerosis.

V. Abbreviations

AAPH   2,2'-Azobis(2-amidinopropane) dihydrochloride

AD   Alzheimer's disease

AGE   advanced glycation end product(s)

Al-PE   aldehyde-PE

Al-PS   aldehyde-PS

APL   aminophospholipid

CE   carboxyethyl

CID   collision-induced dissociation

CM   carboxymethyl

889	DHPE	1,2-diheptadecanoyl-*sn*-3-glycerophosphoethanolamine
890	DPPE	1,2-dipalmitoyl-*sn*-3-glycerophosphoethanolamine
891	DPPS	1,2-dipalmitoyl-*sn*-3-glycerophosphoserine
892	EI	electronic impact
893	ER	endoplasmic reticulum
894	ESI	electrospray ionization
895	Etn	ethanolamine
896	GC	gas chromatography
897	Gly-ox-PE	glyco-oxidized PE
898	Gly-ox-PS	glyco-oxidized PS
899	Gly-PE	glycated PE
900	Gly-PS	glycated PS
901	GPAA	glycerophosphoacetic acid
902	H_2O_2	hydrogen peroxide
903	HCD	higher energy collision-induced dissociation
904	HDDE	4-hydroxydodeca-(2,6)-dienal
905	HDOHE	hydroxydocosahexaenoic acid
906	HETE	hydroxyeicosatetraenoic acid
907	HHE	4-hydroxy-2-hexenal
908	HNE	4-hydroxy-2-nonenal
909	HUVEC	human umbilical vein endothelial cells
910	Iso-LG	iso-ketal
911	KETE	keto-eicosatetraenoic acid
912	LC	liquid chromatography
913	LDL	low-density lipoprotein
914	LOX	lipoxygenase

915	MALDI	matrix-assisted laser desorption/ionization
916	MDA	malondialdehyde
917	MPO	myeloperoxidase
918	MRM	multiple reaction monitoring
919	MS	mass spectrometry
920	NL	neutral loss
921	NLS	neutral loss scanning
922	NP-HPLC	normal phase high performance liquid chromatography
923	O_2	molecular oxygen
924	$O_2^{-\bullet-}$	superoxide radical
925	$^1O_2$	singlet oxygen
926	$^\bullet OH$	hydroxyl radical
927	ONE	4-oxo-2-nonenal
928	Ox-PE	oxidized PE
929	Ox-PS	oxidized PS
930	PE	phosphatidylethanolamine
931	PLPE	1-palmitoyl-2-linoleoyl-*sn*-3-glycerophosphoethanolamine
932	PLPS	1-palmitoyl-2-linoleoyl-*sn*-3-glycerophosphoserine
933	POPE	1-palmitoyl-2-oleoyl-*sn*-3-glycerophosphoethanolamine
934	PS	phosphatidylserine
935	RA	relative abundance
936	ROS	reactive oxygen species
937	RP-HPLC	reversed phase high performance liquid chromatography
938	Ser	serine
939	SIM	single ion monitoring
940	SRM	single reaction monitoring

941　TFAME　　　trifluoroacetyl-methyl ester

942　TIC　　　　total ion count

943　TLC　　　　thin layer chromatography

944　VEGF　　　vascular endothelial growth factor

945

946

947　**VI. Acknowledgments**

948

956
957
958
959
960　**VII. References**

961

962
963　Adachi, Junko, Naoki Yoshioka, Rika Funae, et al.
964　　2004　Determination of Phosphatidylcholine Monohydroperoxides Using Quadrupole Time-of-Flight Mass
965　Spectrometry. Journal of Chromatography B 806(1): 41–46.

966
967　Adachi, Junko, Naoki Yoshioka, Mariko Sato, et al.
968　　2005　Detection of Phosphatidylcholine Oxidation Products in Rat Heart Using Quadrupole Time-of-Flight
969　Mass Spectrometry. Journal of Chromatography B 823(1): 37–43.

970
971　Afonyushkin, Taras, Olga V. Oskolkova, and Valery N. Bochkov
972　　2012　Permissive Role of miR-663 in Induction of VEGF and Activation of the ATF4 Branch of Unfolded
973　Protein Response in Endothelial Cells by Oxidized Phospholipids. Atherosclerosis 225(1): 50–55.

974

975 Amarnath, Venkataraman, Kapil Amarnath, Kalyani Amarnath, Sean Davies, and L. Jackson Roberts
976   2004   Pyridoxamine: An Extremely Potent Scavenger of 1,4-Dicarbonyls. Chemical Research in
977 Toxicology 17(3): 410–415.
978

979 Annibal, Andrea, Thomas Riemer, Olga Jovanovic, et al.
980   2016   Structural, Biological and Biophysical Properties of Glycated and Glycoxidized
981 Phosphatidylethanolamines. Free Radical Biology and Medicine 95: 293–307.
982

983 Annibal, Andrea, Kristin Schubert, Ulf Wagner, et al.
984   2014   New Covalent Modifications of Phosphatidylethanolamine by Alkanals: Mass Spectrometry Based
985 Structural Characterization and Biological Effects: Phosphatidylethanolamines Modified by Alkanals.
986 Journal of Mass Spectrometry 49(7): 557–569.
987

988 Arroyo, Antonio, Martin Modriansky̍, F. Behice Serinkan, et al.
989   2002   NADPH Oxidase-Dependent Oxidation and Externalization of Phosphatidylserine during Apoptosis
990 in Me2SO-Differentiated HL-60 Cells Role in Phagocytic Clearance. Journal of Biological Chemistry
991 277(51): 49965–49975.
992

993 Asam, Michael R., and Gary L. Glish
994   1997   Tandem Mass Spectrometry of Alkali Cationized Polysaccharides in a Quadrupole Ion Trap. Journal
995 of the American Society for Mass Spectrometry 8(9): 987–995.
996

997 Bacot, S.
998   2003   Covalent Binding of Hydroxy-Alkenals 4-HDDE, 4-HHE, and 4-HNE to Ethanolamine Phospholipid
999 Subclasses. The Journal of Lipid Research 44(5): 917–926.
1000

1001 Bacot, S., N. Bernoud-Hubac, B. Chantegrel, et al.
1002   2007   Evidence for in Situ Ethanolamine Phospholipid Adducts with Hydroxy-Alkenals. The Journal of
1003 Lipid Research 48(4): 816–825.
1004

1005 Balasubramanian, K., B. Mirnikjoo, and A. J. Schroit
1006   2007   Regulated Externalization of Phosphatidylserine at the Cell Surface: IMPLICATIONS FOR
1007 APOPTOSIS. Journal of Biological Chemistry 282(25): 18357–18364.
1008

1009 Benedetti, Angelo, Mario Comporti, and Hermann Esterbauer
1010   1980   Identification of 4-Hydroxynonenal as a Cytotoxic Product Originating from the Peroxidation of
1011 Liver Microsomal Lipids. Biochimica et Biophysica Acta (BBA) - Lipids and Lipid Metabolism 620(2):
1012 281–296.
1013

1014 Bernoud-Hubac, Nathalie, Laurent B. Fay, Venkataraman Armarnath, et al.
1015   2004   Covalent Binding of Isoketals to Ethanolamine Phospholipids. Free Radical Biology and Medicine
1016 37(10): 1604–1611.
1017

1018 Bevers, E. M., P. Comfurius, and R. F. Zwaal
1019   1983   Changes in Membrane Phospholipid Distribution during Platelet Activation. Biochimica Et
1020 Biophysica Acta 736(1): 57–66.
1021

1022 Bhuyan, Kailash C., Ravidatt W.P. Master, Robert S. Coles, and Durga K. Bhuyan
1023   1986   Molecular Mechanisms of Cataractogenesis: IV. Evidence of Phospholipid · Malondialdehyde
1024 Adduct in Human Senile Cataract. Mechanisms of Ageing and Development 34(3): 289–296.
1025

1026 Birukova, A. A., P. Fu, S. Chatchavalvanich, et al.
1027   2006   Polar Head Groups Are Important for Barrier-Protective Effects of Oxidized Phospholipids on
1028 Pulmonary Endothelium. AJP: Lung Cellular and Molecular Physiology 292(4): L924–L935.

1029
1030 Bluml, S., B. Rosc, A. Lorincz, et al.
1031 2008   The Oxidation State of Phospholipids Controls the Oxidative Burst in Neutrophil Granulocytes. The
1032 Journal of Immunology 181(6): 4347–4353.
1033
1034 Breitling-Utzmann, Carmen M., Anke Unger, D.Alexander Friedl, and Markus O. Lederer
1035 2001   Identification and Quantification of Phosphatidylethanolamine- Derived Glucosylamines and
1036 Aminoketoses from Human ErythrocytesĐInfluence of Glycation Products on Lipid Peroxidation. Archives
1037 of Biochemistry and Biophysics 391(2): 245–254.
1038
1039 Carr, Anitra C., Jeroen JM van den Berg, and Christine C. Winterbourn
1040 1998   Differential Reactivities of Hypochlorous and Hypobromous Acids with Purified Escherichia Coli
1041 Phospholipid: Formation of Haloamines and Halohydrins. Biochimica et Biophysica Acta (BBA)-Lipids and
1042 Lipid Metabolism 1392(2): 254–264.
1043
1044 Clark, Stephen R., Christopher J. Guy, Martin J. Scurr, et al.
1045 2011   Esterified Eicosanoids Are Acutely Generated by 5-Lipoxygenase in Primary Human Neutrophils
1046 and in Human and Murine Infection. Blood 117(6): 2033–2043.
1047
1048 Colombo, Simone, Giulia Coliva, Agnieszka Kraj, et al.
1049 2018   Electrochemical Oxidation of Phosphatidylethanolamines Studied by Mass Spectrometry. Journal of
1050 Mass Spectrometry 53(3): 223–233.
1051
1052 Connor, J., C. H. Pak, R. F. Zwaal, and A. J. Schroit
1053 1992   Bidirectional Transbilayer Movement of Phospholipid Analogs in Human Red Blood Cells.
1054 Evidence for an ATP-Dependent and Protein-Mediated Process. The Journal of Biological Chemistry
1055 267(27): 19412–19417.
1056
1057 Connor, J., and A. J. Schroit
1058 1990   Aminophospholipid Translocation in Erythrocytes: Evidence for the Involvement of a Specific
1059 Transporter and an Endofacial Protein. Biochemistry 29(1): 37–43.
1060
1061 Cullis, P. R., and B. De Kruijff
1062 1978   Polymorphic Phase Behaviour of Lipid Mixtures as Detected by 31P NMR. Evidence That
1063 Cholesterol May Destabilize Bilayer Structure in Membrane Systems Containing Phosphatidylethanolamine.
1064 Biochimica Et Biophysica Acta 507(2): 207–218.
1065
1066 Daleke, D. L.
1067 2003   Regulation of Transbilayer Plasma Membrane Phospholipid Asymmetry. The Journal of Lipid
1068 Research 44(2): 233–242.
1069
1070 Daleke, D. L., and J. V. Lyles
1071 2000   Identification and Purification of Aminophospholipid Flippases. Biochimica Et Biophysica Acta
1072 1486(1): 108–127.
1073
1074 Deleault, N. R., J. R. Piro, D. J. Walsh, et al.
1075 2012   Isolation of Phosphatidylethanolamine as a Solitary Cofactor for Prion Formation in the Absence of
1076 Nucleic Acids. Proceedings of the National Academy of Sciences 109(22): 8546–8551.
1077
1078 Domingues, M. Rosário M., Ana Reis, and Pedro Domingues
1079 2008   Mass Spectrometry Analysis of Oxidized Phospholipids. Chemistry and Physics of Lipids 156(1–2):
1080 1–12.
1081
1082 Domingues, M. Rosário M., Cláudia Simões, João Pinto da Costa, Ana Reis, and Pedro Domingues
1083 2009   Identification of 1-Palmitoyl-2-Linoleoyl-Phosphatidylethanolamine Modifications under Oxidative
1084 Stress Conditions by LC-MS/MS. Biomedical Chromatography 23(6): 588–601.

Dröge, Wulf

 2002   Free Radicals in the Physiological Control of Cell Function. Physiological Reviews 82(1): 47–95.

Elliott, James I., Annmarie Surprenant, Federica M. Marelli-Berg, et al.

 2005   Membrane Phosphatidylserine Distribution as a Non-Apoptotic Signalling Mechanism in Lymphocytes. Nature Cell Biology 7(8): 808–816.

Emoto, Kazuo, Toshihide Kobayashi, Akiko Yamaji, et al.

 1996   Redistribution of Phosphatidylethanolamine at the Cleavage Furrow of Dividing Cells during Cytokinesis. Proceedings of the National Academy of Sciences 93(23): 12867–12872.

Emoto, Kazuo, and Masato Umeda

 2000   An Essential Role for a Membrane Lipid in Cytokinesis Regulation of Contractile Ring Disassembly by Redistribution of Phosphatidylethanolamine. The Journal of Cell Biology 149(6): 1215–1224.

Fabisiak, J. P., Y. Y. Tyurina, V. A. Tyurin, J. S. Lazo, and V. E. Kagan

 1998   Random versus Selective Membrane Phospholipid Oxidation in Apoptosis: Role of Phosphatidylserine. Biochemistry 37(39): 13781–13790.

Fabisiak, James P., Yulia Y. Tyurina, Vladimir A. Tyurin, and Valerian E. Kagan

 2005   Quantification of Selective Phosphatidylserine Oxidation during Apoptosis. Methods in Molecular Biology (Clifton, N.J.) 291: 449–456.

Fadok, V. A., A. de Cathelineau, D. L. Daleke, P. M. Henson, and D. L. Bratton

 2001   Loss of Phospholipid Asymmetry and Surface Exposure of Phosphatidylserine Is Required for Phagocytosis of Apoptotic Cells by Macrophages and Fibroblasts. Journal of Biological Chemistry 276(2): 1071–1077.

Fadok, V. A., D. R. Voelker, P. A. Campbell, et al.

 1992   Exposure of Phosphatidylserine on the Surface of Apoptotic Lymphocytes Triggers Specific Recognition and Removal by Macrophages. Journal of Immunology (Baltimore, Md.: 1950) 148(7): 2207–2216.

Fadok, Valerie A., Donna L. Bratton, Anatole Konowal, et al.

 1998   Macrophages That Have Ingested Apoptotic Cells in Vitro Inhibit Proinflammatory Cytokine Production through Autocrine/Paracrine Mechanisms Involving TGF-Beta, PGE2, and PAF. Journal of Clinical Investigation 101(4): 890.

Finkielstein, C. V., M. Overduin, and D. G. S. Capelluto

 2006   Cell Migration and Signaling Specificity Is Determined by the Phosphatidylserine Recognition Motif of Rac1. Journal of Biological Chemistry 281(37): 27317–27326.

Fischer, K., S. Voelkl, J. Berger, et al.

 2006   Antigen Recognition Induces Phosphatidylserine Exposure on the Cell Surface of Human CD8+ T Cells. Blood 108(13): 4094–4101.

Fountain, W. C., J. R. Requena, A. J. Jenkins, et al.

 1999   Quantification of N-(Glucitol)ethanolamine and N-(Carboxymethyl)serine: Two Products of Nonenzymatic Modification of Aminophospholipids Formed in Vivo. Analytical Biochemistry 272(1): 48–55.

Frankel, E. N., W. E. Neff, W. K. Rohwedder, et al.

 1977   Analysis of Autoxidized Fats by Gas Chromatography-Mass Spectrometry: II. Methyl Linoleate. Lipids 12(11): 908–913.

Ghaste, Manoj, Robert Mistrik, and Vladimir Shulaev
 2016   Applications of Fourier Transform Ion Cyclotron Resonance (FT-ICR) and Orbitrap Based High Resolution Mass Spectrometry in Metabolomics and Lipidomics. International Journal of Molecular Sciences 17(6): 816.

Greenberg, Michael E., Mingjiang Sun, Renliang Zhang, et al.
 2006   Oxidized phosphatidylserine–CD36 Interactions Play an Essential Role in Macrophage-Dependent Phagocytosis of Apoptotic Cells. The Journal of Experimental Medicine 203(12): 2613–2625.

Gugiu, Bogdan G., Clementina A. Mesaros, Mingjiang Sun, et al.
 2006   Identification of Oxidatively Truncated Ethanolamine Phospholipids in Retina and Their Generation from Polyunsaturated Phosphatidylethanolamines. Chemical Research in Toxicology 19(2): 262–271.

Guichardant, M., P. Taibi-Tronche, L. B. Fay, and M. Lagarde
 1998   Covalent Modifications of Aminophospholipids by 4-Hydroxynonenal. Free Radical Biology & Medicine 25(9): 1049–1056.

Guo, Lilu, Zhongyi Chen, Brian E. Cox, et al.
 2011   Phosphatidylethanolamines Modified by γ-Ketoaldehyde (γKA) Induce Endoplasmic Reticulum Stress and Endothelial Activation. Journal of Biological Chemistry 286(20): 18170–18180.

Hailey, Dale W., Angelika S. Rambold, Prasanna Satpute-Krishnan, et al.
 2010   Mitochondria Supply Membranes for Autophagosome Biogenesis during Starvation. Cell 141(4): 656–667.

Hammond, V. J., A. H. Morgan, S. Lauder, et al.
 2012   Novel Keto-Phospholipids Are Generated by Monocytes and Macrophages, Detected in Cystic Fibrosis, and Activate Peroxisome Proliferator-Activated Receptor-. Journal of Biological Chemistry 287(50): 41651–41666.

Heller, Jozsef I., Jan R. Crowley, Stanley L. Hazen, et al.
 2000   P-Hydroxyphenylacetaldehyde, an Aldehyde Generated by Myeloperoxidase, Modifies Phospholipid Amino Groups of Low Density Lipoprotein in Human Atherosclerotic Intima. Journal of Biological Chemistry 275(14): 9957–9962.

Higgins, JOAN A., and W. HOWARD Evans
 1978   Transverse Organization of Phospholipids across the Bilayer of Plasma-Membrane Subfractions of Rat Hepatocytes. Biochemical Journal 174(2): 563–567.

Hisaka, Shinsuke, Naomi Yamada, Kentaro Naito, and Toshihiko Osawa
 2010   The Immunological and Chemical Detection of N-(Hexanoyl)phosphatidylethanolamine and N-(Hexanoyl)phosphatidylserine in an Oxidative Model Induced by Carbon Tetrachloride. Biochemical and Biophysical Research Communications 393(4): 631–636.

Hochreiter-Hufford, A., and K. S. Ravichandran
 2013   Clearing the Dead: Apoptotic Cell Sensing, Recognition, Engulfment, and Digestion. Cold Spring Harbor Perspectives in Biology 5(1): a008748–a008748.

Hoffmann, P. R., J. A. Kench, A. Vondracek, et al.
 2005   Interaction between Phosphatidylserine and the Phosphatidylserine Receptor Inhibits Immune Responses In Vivo. The Journal of Immunology 174(3): 1393–1404.

Huang, Bill X., Mohammed Akbar, Karl Kevala, and Hee-Yong Kim
 2011   Phosphatidylserine Is a Critical Modulator for Akt Activation. The Journal of Cell Biology 192(6): 979–992.

Hyötyläinen, Tuulia, and Matej Orešič

  2016   Bioanalytical Techniques in Nontargeted Clinical Lipidomics. Bioanalysis 8(4): 351–364.

Improta-Brears, T., S. Ghosh, and R. M. Bell

  1999   Mutational Analysis of Raf-1 Cysteine Rich Domain: Requirement for a Cluster of Basic Aminoacids for Interaction with Phosphatidylserine. Molecular and Cellular Biochemistry 198(1–2): 171–178.

Kagan, V. E., B. Gleiss, Y. Y. Tyurina, et al.

  2002   A Role for Oxidative Stress in Apoptosis: Oxidation and Externalization of Phosphatidylserine Is Required for Macrophage Clearance of Cells Undergoing Fas-Mediated Apoptosis. The Journal of Immunology 169(1): 487–499.

Kagan, Valerian E., Grigory G. Borisenko, Yulia Y. Tyurina, et al.

  2004   Oxidative Lipidomics of Apoptosis: Redox Catalytic Interactions of Cytochrome c with Cardiolipin and Phosphatidylserine. Free Radical Biology and Medicine 37(12): 1963–1985.

Kagan, Valerian E, Gaowei Mao, Feng Qu, et al.

  2016   Oxidized Arachidonic and Adrenic PEs Navigate Cells to Ferroptosis. Nature Chemical Biology 13(1): 81–90.

Karas, Michael., and Franz. Hillenkamp

  1988   Laser Desorption Ionization of Proteins with Molecular Masses Exceeding 10,000 Daltons. Analytical Chemistry 60(20): 2299–2301.

Khaselev, N., and R. C. Murphy

  1999   Susceptibility of Plasmenyl Glycerophosphoethanolamine Lipids Containing Arachidonate to Oxidative Degradation. Free Radical Biology & Medicine 26(3–4): 275–284.

Kim, Hee-Yong, Bill X. Huang, and Arthur A. Spector

  2014   Phosphatidylserine in the Brain: Metabolism and Function. Progress in Lipid Research 56: 1–18.

Kim, H.-Y.

  2007   Novel Metabolism of Docosahexaenoic Acid in Neural Cells. Journal of Biological Chemistry 282(26): 18661–18665.

Kimani, Stanley Gititu, Ke Geng, Canan Kasikara, et al.

  2014   Contribution of Defective PS Recognition and Efferocytosis to Chronic Inflammation and Autoimmunity. Frontiers in Immunology 5. http://journal.frontiersin.org/article/10.3389/fimmu.2014.00566/abstract, accessed October 4, 2016.

Koivusalo, Mirkka, Perttu Haimi, Liisa Heikinheimo, Risto Kostiainen, and Pentti Somerharju

  2001   Quantitative Determination of Phospholipid Compositions by ESI-MS: Effects of Acyl Chain Length, Unsaturation, and Lipid Concentration on Instrument Response. Journal of Lipid Research 42(4): 663–672.

Koty, Patrick P., Yulia Y. Tyurina, Vladimir A. Tyurin, Shang-Xi Li, and Valerian E. Kagan

  2002   Depletion of Bcl-2 by an Antisense Oligonucleotide Induces Apoptosis Accompanied by Oxidation and Externalization of Phosphatidylserine in NCI-H226 Lung Carcinoma Cells. Molecular and Cellular Biochemistry 234–235(1–2): 125–133.

van Kuijk, F. J., D. W. Thomas, R. J. Stephens, and E. A. Dratz

  1985   Gas Chromatography-Mass Spectrometry Method for Determination of Phospholipid Peroxides; I. Transesterification to Form Methyl Esters. Journal of Free Radicals in Biology & Medicine 1(3): 215–225.

1251
1252   Lee, Seon Hwa, and Ian A. Blair
1253   2000   Characterization of 4-Oxo-2-Nonenal as a Novel Product of Lipid Peroxidation. Chemical Research
1254   in Toxicology 13(8): 698–702.
1255
1256   Lemmon, Mark A.
1257   2008   Membrane Recognition by Phospholipid-Binding Domains. Nature Reviews. Molecular Cell Biology
1258   9(2): 99–111.
1259
1260   Lertsiri, Sittiwat, Mayumi Shiraishi, and Teruo Miyazawa
1261   1998   Identification of Deoxy-Fructosyl Phosphatidylethanolamine as a Non-Enzymic Glycation Product
1262   of Phosphatidylethanolamine and Its Occurrence in Human Blood Plasma and Red Blood Cells. Bioscience,
1263   Biotechnology, and Biochemistry 62(5): 893–901.
1264
1265   Li, Min, Zhigui Zhou, Honggang Nie, Yu Bai, and Huwei Liu
1266   2011   Recent Advances of Chromatography and Mass Spectrometry in Lipidomics. Analytical and
1267   Bioanalytical Chemistry 399(1): 243–249.
1268
1269   Li, Wei, James M. Laird, Liang Lu, et al.
1270   2009   Isolevuglandins Covalently Modify Phosphatidylethanolamines in Vivo: Detection and Quantitative
1271   Analysis of Hydroxylactam Adducts. Free Radical Biology and Medicine 47(11): 1539–1552.
1272
1273   Maciel, Elisabete, Renata Faria, Deolinda Santinha, M. Rosário M. Domingues, and Pedro Domingues
1274   2013   Evaluation of Oxidation and Glyco-Oxidation of 1-Palmitoyl-2-Arachidonoyl-Phosphatidylserine by
1275   LC–MS/MS. Journal of Chromatography B 929: 76–83.
1276
1277   Maciel, Elisabete, Bruno M. Neves, Deolinda Santinha, et al.
1278   2014   Detection of Phosphatidylserine with a Modified Polar Head Group in Human Keratinocytes
1279   Exposed to the Radical Generator AAPH. Archives of Biochemistry and Biophysics 548: 38–45.
1280
1281   Maciel, Elisabete, Raquel Nunes da Silva, Cláudia Simões, et al.
1282   2013   Liquid Chromatography–tandem Mass Spectrometry of Phosphatidylserine Advanced Glycated End
1283   Products. Chemistry and Physics of Lipids 174: 1–7.
1284
1285   Maciel, Elisabete, Raquel Nunes da Silva, Cláudia Simões, Pedro Domingues, and M. Rosário M.
1286   Domingues
1287   2011   Structural Characterization of Oxidized Glycerophosphatidylserine: Evidence of Polar Head
1288   Oxidation. Journal of The American Society for Mass Spectrometry 22(10): 1804–1814.
1289
1290   Maki, R. A., V. A. Tyurin, R. C. Lyon, et al.
1291   2009   Aberrant Expression of Myeloperoxidase in Astrocytes Promotes Phospholipid Oxidation and
1292   Memory Deficits in a Mouse Model of Alzheimer Disease. Journal of Biological Chemistry 284(5): 3158–
1293   3169.
1294
1295   Malleier, Julia M., Olga Oskolkova, Valery Bochkov, et al.
1296   2007   Regulation of Protein C Inhibitor (PCI) Activity by Specific Oxidized and Negatively Charged
1297   Phospholipids. Blood 109(11): 4769–4776.
1298
1299   Maskrey, B. H., A. Bermudez-Fajardo, A. H. Morgan, et al.
1300   2007   Activated Platelets and Monocytes Generate Four Hydroxyphosphatidylethanolamines via
1301   Lipoxygenase. Journal of Biological Chemistry 282(28): 20151–20163.
1302
1303   Matsura, Tatsuya, Masachika Kai, Kazuo Yamada, Anna A. Shvedova, and Valerian E. Kagan
1304   2004   Fine-Tuning Phagocytic Clearance of Apoptotic Cells by Phosphatidylserine Oxidation. Journal of
1305   Clinical Biochemistry and Nutrition 34(1): 11–24.

1306

1307 Matsura, Tatsuya, Behice F Serinkan, Jianfei Jiang, and Valerian E Kagan
1308 2002 Phosphatidylserine Peroxidation/Externalization during Staurosporine-Induced Apoptosis in HL-60
1309 Cells. FEBS Letters 524(1–3): 25–30.
1310

1311 Melo, Tânia, Nuno Santos, Diana Lopes, et al.
1312 2013 Photosensitized Oxidation of Phosphatidylethanolamines Monitored by Electrospray Tandem Mass
1313 Spectrometry: ESI-MS of Photosensitized Phosphatidylethanolamines. Journal of Mass Spectrometry 48(12):
1314 1357–1365.
1315

1316 Melo, Tânia, Eduarda M. P. Silva, Cláudia Simões, Pedro Domingues, and M. Rosário M. Domingues
1317 2013 Photooxidation of Glycated and Non-Glycated Phosphatidylethanolamines Monitored by Mass
1318 Spectrometry: Photooxidation of PE and GlucPE. Journal of Mass Spectrometry 48(1): 68–78.
1319

1320 Menon, A. K., and V. L. Stevens
1321 1992 Phosphatidylethanolamine Is the Donor of the Ethanolamine Residue Linking a
1322 Glycosylphosphatidylinositol Anchor to Protein. The Journal of Biological Chemistry 267(22): 15277–
1323 15280.
1324

1325 Morgan, A. H., V. Dioszeghy, B. H. Maskrey, et al.
1326 2009 Phosphatidylethanolamine-Esterified Eicosanoids in the Mouse: TISSUE LOCALIZATION AND
1327 INFLAMMATION-DEPENDENT FORMATION IN Th-2 DISEASE. Journal of Biological Chemistry
1328 284(32): 21185–21191.
1329

1330 Morgan, Alwena H, Victoria J Hammond, Lloyd Morgan, et al.
1331 2010 Quantitative Assays for Esterified Oxylipins Generated by Immune Cells. Nature Protocols 5(12):
1332 1919–1931.
1333

1334 Morgan, Lloyd T., Christopher P. Thomas, Hartmut Kühn, and Valerie B. O'Donnell
1335 2010 Thrombin-Activated Human Platelets Acutely Generate Oxidized Docosahexaenoic-Acid-
1336 Containing Phospholipids via 12-Lipoxygenase. Biochemical Journal 431(1): 141–148.
1337

1338 Murphy, Michael P.
1339 2009 How Mitochondria Produce Reactive Oxygen Species. Biochemical Journal 417(1): 1–13.
1340

1341 Nakagawa, K.
1342 2005 Ion-Trap Tandem Mass Spectrometric Analysis of Amadori-Glycated Phosphatidylethanolamine in
1343 Human Plasma with or without Diabetes. The Journal of Lipid Research 46(11): 2514–2524.
1344

1345 Ni, Zhixu, Ivana Milic, and Maria Fedorova
1346 2015 Identification of Carbonylated Lipids from Different Phospholipid Classes by Shotgun and LC-MS
1347 Lipidomics. Analytical and Bioanalytical Chemistry 407(17): 5161–5173.
1348

1349 Oak, Jeong-Ho, Kiyotaka Nakagawa, and Teruo Miyazawa
1350 2000 Synthetically Prepared Amadori-Glycated Phosphatidylethanolamine Can Trigger Lipid Peroxidation
1351 via Free Radical Reactions. FEBS Letters 481(1): 26–30.
1352

1353 Pamplona, Reinald, Jesús R. Requena, Manuel Portero-Otín, et al.
1354 1998 Carboxymethylated Phosphatidylethanolamine in Mitochondrial Membranes of Mammals. European
1355 Journal of Biochemistry 255(3): 685–689.
1356

1357 Pécheur, Eve-Isabelle, Isabelle Martin, Olaf Maier, et al.
1358 2002 Phospholipid Species Act as Modulators in p97/p47-Mediated Fusion of Golgi Membranes.
1359 Biochemistry 41(31): 9813–9823.
1360

1361 Post, J. A., J. J. Bijvelt, and A. J. Verkleij

1362   1995   Phosphatidylethanolamine and Sarcolemmal Damage during Ischemia or Metabolic Inhibition of
1363 Heart Myocytes. The American Journal of Physiology 268(2 Pt 2): H773-780.
1364
1365 Powell, Kate A., Valentina A. Valova, Chandra S. Malladi, et al.
1366   2000   Phosphorylation of Dynamin I on Ser-795 by Protein Kinase C Blocks Its Association with
1367 Phospholipids. Journal of Biological Chemistry 275(16): 11610–11617.
1368
1369 Pulfer, Melissa, and Robert C. Murphy
1370   2003   Electrospray Mass Spectrometry of Phospholipids. Mass Spectrometry Reviews 22(5): 332–364.
1371
1372 Ravandi, A., A. Kuksis, L. Marai, et al.
1373   1996   Isolation and Identification of Glycated Aminophospholipids from Red Cells and Plasma of Diabetic
1374 Blood. FEBS Letters 381(1–2): 77–81.
1375
1376 Ravandi, A., A. Kuksis, and J. J. Myher
1377   1995   Preparation and Characterization of Glucosylated Aminoglycerophospholipids. Lipids 30(10): 885–
1378 891.
1379
1380 Ravandi, A., A. Kuksis, and N. A. Shaikh
1381   2000   Glucosylated Glycerophosphoethanolamines Are the Major LDL Glycation Products and Increase
1382 LDL Susceptibility to Oxidation : Evidence of Their Presence in Atherosclerotic Lesions. Arteriosclerosis,
1383 Thrombosis, and Vascular Biology 20(2): 467–477.
1384
1385 Reis, Ana, M. R. M. Domingues, F. M. L. Amado, A. J. Ferrer-Correia, and P. Domingues
1386   2007   Radical Peroxidation of Palmitoyl-Lineloyl-Glycerophosphocholine Liposomes: Identification of
1387 Long-Chain Oxidised Products by Liquid Chromatography-Tandem Mass Spectrometry. Journal of
1388 Chromatography. B, Analytical Technologies in the Biomedical and Life Sciences 855(2): 186–199.
1389
1390 Reis, Ana, and Corinne M. Spickett
1391   2012   Chemistry of Phospholipid Oxidation. Biochimica et Biophysica Acta (BBA) - Biomembranes
1392 1818(10): 2374–2387.
1393
1394 Requena, Jesús R., Mahtab U. Ahmed, C. Wesley Fountain, et al.
1395   1997   Carboxymethylethanolamine, a Biomarker of Phospholipid Modification during the Maillard
1396 Reaction in Vivo. Journal of Biological Chemistry 272(28): 17473–17479.
1397
1398 Riazy, Maziar, Marilee Lougheed, Hans H. Adomat, et al.
1399   2011   Fluorescent Adducts Formed by Reaction of Oxidized Unsaturated Fatty Acids with Amines
1400 Increase Macrophage Viability. Free Radical Biology and Medicine 51(10): 1926–1936.
1401
1402 Richter, Grit, Celestina Schober, Rosmarie Süß, et al.
1403   2008   The Reaction between Phosphatidylethanolamines and HOCl Investigated by TLC: Fading of the
1404 Dye Primuline Is Induced by Dichloramines. Journal of Chromatography B 867(2): 233–237.
1405
1406 Salomon, Robert G.
1407   2005   Distinguishing Levuglandins Produced through the Cyclooxygenase and Isoprostane Pathways.
1408 Chemistry and Physics of Lipids 134(1): 1–20.
1409
1410 Sankhagowit, Shalene, Ernest Y. Lee, Gerard C. L. Wong, and Noah Malmstadt
1411   2016   Oxidation of Membrane Curvature-Regulating Phosphatidylethanolamine Lipid Results in Formation
1412 of Bilayer and Cubic Structures. Langmuir 32(10): 2450–2457.
1413
1414 Schick, P K, K B Kurica, and G K Chacko
1415   1976   Location of Phosphatidylethanolamine and Phosphatidylserine in the Human Platelet Plasma
1416 Membrane. Journal of Clinical Investigation 57(5): 1221–1226.

von Schlieffen, E., O. V. Oskolkova, G. Schabbauer, et al.

2009 Multi-Hit Inhibition of Circulating and Cell-Associated Components of the Toll-Like Receptor 4 Pathway by Oxidized Phospholipids. Arteriosclerosis, Thrombosis, and Vascular Biology 29(3): 356–362.

Schroit, Alan J., and Robert F.A. Zwaal

1991 Transbilayer Movement of Phospholipids in Red Cell and Platelet Membranes. Biochimica et Biophysica Acta (BBA) - Reviews on Biomembranes 1071(3): 313–329.

Segawa, Katsumori, Sachiko Kurata, Yuichi Yanagihashi, et al.

2014 Caspase-Mediated Cleavage of Phospholipid Flippase for Apoptotic Phosphatidylserine Exposure. Science (New York, N.Y.) 344(6188): 1164–1168.

Sethi, Sumit, and Elisa Brietzke

2017 Recent Advances in Lipidomics: Analytical and Clinical Perspectives. Prostaglandins & Other Lipid Mediators 128–129: 8–16.

Seyerl, Maria, Stefan Blüml, Stefanie Kirchberger, et al.

2008 Oxidized Phospholipids Induce Anergy in Human Peripheral Blood T Cells. European Journal of Immunology 38(3): 778–787.

Shiratsuchi, A., M. Ichiki, Y. Okamoto, et al.

2008 Inhibitory Effect of N-Palmitoylphosphatidylethanolamine on Macrophage Phagocytosis through Inhibition of Rac1 and Cdc42. Journal of Biochemistry 145(1): 43–50.

Shoji, N., K. Nakagawa, A. Asai, et al.

2010 LC-MS/MS Analysis of Carboxymethylated and Carboxyethylated Phosphatidylethanolamines in Human Erythrocytes and Blood Plasma. The Journal of Lipid Research 51(8): 2445–2453.

Shvedova, Anna A., Julia Y. Tyurina, Kazuaki Kawai, et al.

2002 Selective Peroxidation and Externalization of Phosphatidylserine in Normal Human Epidermal Keratinocytes during Oxidative Stress Induced by Cumene Hydroperoxide. Journal of Investigative Dermatology 118(6): 1008–1018.

Signorell, A., J. Jelk, M. Rauch, and P. Butikofer

2008 Phosphatidylethanolamine Is the Precursor of the Ethanolamine Phosphoglycerol Moiety Bound to Eukaryotic Elongation Factor 1A. Journal of Biological Chemistry 283(29): 20320–20329.

Silva, Raquel Nunes da, Ana Cristina Silva, Elisabete Maciel, et al.

2012 Evaluation of the Capacity of Oxidized Phosphatidylserines to Induce the Expression of Cytokines in Monocytes and Dendritic Cells. Archives of Biochemistry and Biophysics 525(1): 9–15.

Simões, Cláudia, Ana Cristina Silva, Pedro Domingues, et al.

2013a Phosphatidylethanolamines Glycation, Oxidation, and Glycoxidation: Effects on Monocyte and Dendritic Cell Stimulation. Cell Biochemistry and Biophysics 66(3): 477–487.

2013b Modified Phosphatidylethanolamines Induce Different Levels of Cytokine Expression in Monocytes and Dendritic Cells. Chemistry and Physics of Lipids 175–176: 57–64.

Simões, Cláudia, Vanda Simões, Ana Reis, Pedro Domingues, and M. Rosário M. Domingues

2010 Oxidation of Glycated Phosphatidylethanolamines: Evidence of Oxidation in Glycated Polar Head Identified by LC-MS/MS. Analytical and Bioanalytical Chemistry 397(6): 2417–2427.

Simões, Joana, Pedro Domingues, Ana Reis, et al.

2007 Identification of Anomeric Configuration of Underivatized Reducing Glucopyranosyl-Glucose Disaccharides by Tandem Mass Spectrometry and Multivariate Analysis. Analytical Chemistry 79(15): 5896–5905.

1473
1474 Sookwong, Phumon, Kiyotaka Nakagawa, Ikuko Fujita, Naoki Shoji, and Teruo Miyazawa
1475 2011   Amadori-Glycated Phosphatidylethanolamine, a Potential Marker for Hyperglycemia, in
1476 Streptozotocin-Induced Diabetic Rats. Lipids 46(10): 943–952.
1477
1478 Spickett, Corinne M., Nicola Rennie, Helen Winter, et al.
1479 2001   Detection of Phospholipid Oxidation in Oxidatively Stressed Cells by Reversed-Phase HPLC
1480 Coupled with Positive-Ionization Electroscopy MS. Biochemical Journal 355(2): 449–457.
1481
1482 Spickett, Corinne M., Ingrid Wiswedel, Werner Siems, Kamelija Zarkovic, and Neven Zarkovic
1483 2010   Advances in Methods for the Determination of Biologically Relevant Lipid Peroxidation Products.
1484 Free Radical Research 44(10): 1172–1202.
1485
1486 Stadelmann-Ingrand, Sabrina, Raymond Pontcharraud, and Bernard Fauconneau
1487 2004   Evidence for the Reactivity of Fatty Aldehydes Released from Oxidized Plasmalogens with
1488 Phosphatidylethanolamine to Form Schiff Base Adducts in Rat Brain Homogenates. Chemistry and Physics
1489 of Lipids 131(1): 93–105.
1490
1491 Stafford, Jason H., and Philip E. Thorpe
1492 2011   Increased Exposure of Phosphatidylethanolamine on the Surface of Tumor Vascular Endothelium.
1493 Neoplasia 13(4): 299-IN2.
1494
1495 Suzuki, Satoru, Hideyuki Yamatoya, Masashi Sakai, et al.
1496 2001   Oral Administration of Soybean Lecithin Transphosphatidylated Phosphatidylserine Improves
1497 Memory Impairment in Aged Rats. The Journal of Nutrition 131(11): 2951–2956.
1498
1499 Swairjo, M. A., N. O. Concha, M. A. Kaetzel, J. R. Dedman, and B. A. Seaton
1500 1995   Ca(2+)-Bridging Mechanism and Phospholipid Head Group Recognition in the Membrane-Binding
1501 Protein Annexin V. Nature Structural Biology 2(11): 968–974.
1502
1503 Tadolini, Bruna, Claudia Juliano, Luisella Piu, Flavia Franconi, and Luciana Cabrini
1504 2000   Resveratrol Inhibition of Lipid Peroxidation. Free Radical Research 33(1): 105–114.
1505
1506 Tanaka, Koichi, Hiroaki Waki, Yutaka Ido, et al.
1507 1988   Protein and Polymer Analyses up Tom/Z 100 000 by Laser Ionization Time-of-Flight Mass
1508 Spectrometry. Rapid Communications in Mass Spectrometry 2(8): 151–153.
1509
1510 Thomas, C. P., L. T. Morgan, B. H. Maskrey, et al.
1511 2010   Phospholipid-Esterified Eicosanoids Are Generated in Agonist-Activated Human Platelets and
1512 Enhance Tissue Factor-Dependent Thrombin Generation. Journal of Biological Chemistry 285(10): 6891–
1513 6903.
1514
1515 Tietjen, G. T., Z. Gong, C.-H. Chen, et al.
1516 2014   Molecular Mechanism for Differential Recognition of Membrane Phosphatidylserine by the Immune
1517 Regulatory Receptor Tim4. Proceedings of the National Academy of Sciences 111(15): E1463–E1472.
1518
1519 Tsuji, Kentaro, Yoshichika Kawai, Yoji Kato, and Toshihiko Osawa
1520 2003   Formation of N-(Hexanoyl)ethanolamine, a Novel Phosphatidylethanolamine Adduct, during the
1521 Oxidation of Erythrocyte Membrane and Low-Density Lipoprotein. Biochemical and Biophysical Research
1522 Communications 306(3): 706–711.
1523
1524 Tyurin, Vladimir A., Yulia Y. Tyurina, Weihong Feng, et al.
1525 2008   Mass-Spectrometric Characterization of Phospholipids and Their Primary Peroxidation Products in
1526 Rat Cortical Neurons during Staurosporine-Induced Apoptosis. Journal of Neurochemistry 107(6): 1614–
1527 1633.

Tyurin, Vladimir A., Yulia Y. Tyurina, Mi-Yeon Jung, et al.
  2009   Mass-Spectrometric Analysis of Hydroperoxy- and Hydroxy-Derivatives of Cardiolipin and Phosphatidylserine in Cells and Tissues Induced by pro-Apoptotic and pro-Inflammatory Stimuli. Journal of Chromatography B 877(26): 2863–2872.

Tyurina, Y. Y., V. A. Tyurin, A. M. Kaynar, et al.
  2010   Oxidative Lipidomics of Hyperoxic Acute Lung Injury: Mass Spectrometric Characterization of Cardiolipin and Phosphatidylserine Peroxidation. AJP: Lung Cellular and Molecular Physiology 299(1): L73–L85.

Tyurina, Yulia Y., Elena R. Kisin, Ashley Murray, et al.
  2011   Global Phospholipidomics Analysis Reveals Selective Pulmonary Peroxidation Profiles upon Inhalation of Single-Walled Carbon Nanotubes. ACS Nano 5(9): 7342–7353.

Tyurina, Yulia Y., Vladimir A. Tyurin, Michael W. Epperly, Joel S. Greenberger, and Valerian E. Kagan
  2008   Oxidative Lipidomics of γ-Irradiation-Induced Intestinal Injury. Free Radical Biology and Medicine 44(3): 299–314.

Tyurina, Yulia Y., Vladimir A. Tyurin, Valentyna I. Kapralova, et al.
  2011   Oxidative Lipidomics of γ-Radiation-Induced Lung Injury: Mass Spectrometric Characterization of Cardiolipin and Phosphatidylserine Peroxidation. Radiation Research 175(5): 610–621.

Tyurina, Yulia Y., Vladimir A. Tyurin, Qing Zhao, et al.
  2004   Oxidation of Phosphatidylserine: A Mechanism for Plasma Membrane Phospholipid Scrambling during Apoptosis? Biochemical and Biophysical Research Communications 324(3): 1059–1064.

Uderhardt, Stefan, Martin Herrmann, Olga V. Oskolkova, et al.
  2012   12/15-Lipoxygenase Orchestrates the Clearance of Apoptotic Cells and Maintains Immunologic Tolerance. Immunity 36(5): 834–846.

Üllen, Andreas, Günter Fauler, Harald Köfeler, et al.
  2010   Mouse Brain Plasmalogens Are Targets for Hypochlorous Acid-Mediated Modification in Vitro and in Vivo. Free Radical Biology and Medicine 49(11): 1655–1665.

Vance, J. E.
  2008   Thematic Review Series: Glycerolipids. Phosphatidylserine and Phosphatidylethanolamine in Mammalian Cells: Two Metabolically Related Aminophospholipids. The Journal of Lipid Research 49(7): 1377–1387.

Vance, Jean E., and Guergana Tasseva
  2013   Formation and Function of Phosphatidylserine and Phosphatidylethanolamine in Mammalian Cells. Biochimica et Biophysica Acta (BBA) - Molecular and Cell Biology of Lipids 1831(3): 543–554.

Vay, Daria, Cristina Rigamonti, Matteo Vidali, et al.
  2006   Anti-Phospholipid Antibodies Associated with Alcoholic Liver Disease Target Oxidized Phosphatidylserine on Apoptotic Cell Plasma Membranes. Journal of Hepatology 44(1): 183–189.

Vazdar, Katarina, Danijela Vojta, Davor Margetić, and Mario Vazdar
  2017   Reaction Mechanism of Covalent Modification of Phosphatidylethanolamine Lipids by Reactive Aldehydes 4-Hydroxy-2-Nonenal and 4-Oxo-2-Nonenal. Chemical Research in Toxicology 30(3): 840–850.

Verdaguer, N., S. Corbalan-Garcia, W. F. Ochoa, I. Fita, and J. C. Gómez-Fernández
  1999   Ca(2+) Bridges the C2 Membrane-Binding Domain of Protein Kinase Calpha Directly to Phosphatidylserine. The EMBO Journal 18(22): 6329–6338.

1583
1584 Verkleij, A. J., J. Leunissen-Bijvelt, B. de Kruijff, M. Hope, and P. R. Cullis
1585 1984   Non-Bilayer Structures in Membrane Fusion. Ciba Foundation Symposium 103: 45–59.
1586
1587 Wang, Jun, Yi-Min Lu, Bai-Zhan Liu, and He-Yong He
1588 2008   Electrospray Positive Ionization Tandem Mass Spectrometry of Amadori Compounds. Journal of
1589 Mass Spectrometry 43(2): 262–264.
1590
1591 Wefers, Heribert, and Helmut Sies
1592 1988   The Protection by Ascorbate and Glutathione against Microsomal Lipid Peroxidation Is Dependent
1593 on Vitamin E. European Journal of Biochemistry 174(2): 353–357.
1594
1595 Yamashita, Masamichi, and John B. Fenn
1596 1984   Electrospray Ion Source. Another Variation on the Free-Jet Theme. The Journal of Physical
1597 Chemistry 88(20): 4451–4459.
1598
1599 Yeom, Mijung, Dae-Hyun Hahm, Bong-Jun Sur, et al.
1600 2013   Phosphatidylserine Inhibits Inflammatory Responses in Interleukin-1β–stimulated Fibroblast-like
1601 Synoviocytes and Alleviates Carrageenan-Induced Arthritis in Rat. Nutrition Research 33(3): 242–250.
1602
1603 Zamora, Rosario, and Francisco J. Hidalgo
1604 2003   Phosphatidylethanolamine Modification by Oxidative Stress Product 4,5(*E*)-Epoxy-2(*E*)-Heptenal.
1605 Chemical Research in Toxicology 16(12): 1632–1641.
1606
1607 Zemski Berry, Karin, William Turner, Michael VanNieuwenhze, and Robert Murphy
1608 2010   Characterization of Oxidized Phosphatidylethanolamine Derived from RAW 264.7 Cells Using 4-
1609 (Dimethylamino)benzoic Acid Derivatives. European Journal of Mass Spectrometry 16(1): 463.
1610
1611 Zhao, J., V. B. O'Donnell, S. Balzar, et al.
1612 2011   15-Lipoxygenase 1 Interacts with Phosphatidylethanolamine-Binding Protein to Regulate MAPK
1613 Signaling in Human Airway Epithelial Cells. Proceedings of the National Academy of Sciences 108(34):
1614 14246–14251.
1615
1616 Zieseniss, Susanne, Stefan Zahler, Ingrid Müller, Albin Hermetter, and Bernd Engelmann
1617 2001   Modified Phosphatidylethanolamine as the Active Component of Oxidized Low Density Lipoprotein
1618 Promoting Platelet Prothrombinase Activity. Journal of Biological Chemistry 276(23): 19828–19835.
1619
1620 Zwaal, R. F. A., P. Comfurius, and E. M. Bevers
1621 2005   Surface Exposure of Phosphatidylserine in Pathological Cells. Cellular and Molecular Life Sciences:
1622 CMLS 62(9): 971–988.
1623

1624   Table 1. Main biological activities of phosphatidylserine (PS) and phosphatidylethanolamine (PE)

1625   in mammalian cells.

BIOLOGICAL ACTIVITY	REFERENCES
Phosphatidylserine	
Interaction with PS receptor of macrophages after externalization: apoptosis	(Fadok et al. 2001; Zwaal, Comfurius, and Bevers 2005; Balasubramanian, Mirnikjoo, and Schroit 2007; Segawa et al. 2014; Fadok et al. 1992)
Inhibition of inflammatory response	(Fadok et al. 1998; Kimani et al. 2014)
Inhibition of proinflammatory cytokine production, alleviation of arthritis	(Yeom et al. 2013)
Immune system modulation	(Kimani et al. 2014; Tietjen et al. 2014; Elliott et al. 2005; Fischer et al. 2006; Hoffmann et al. 2005)
Promotion of the blood-clotting cascade in injury-activated platelets	(Schick, Kurica, and Chacko 1976; Schroit and Zwaal 1991; Connor and Schroit 1990; Connor et al. 1992; Bevers, Comfurius, and Zwaal 1983)
Modulation of the activity of membrane-bound proteins (PkC, Annexin V, Rac 1) at the intracellular leaflet	(Powell et al. 2000; Swairjo et al. 1995; Finkielstein, Overduin, and Capelluto 2006; Lemmon 2008)
Intracellular signaling pathway in neuronal cells: neurite growth, neuronal cell survival, and synaptogenesis	(Verdaguer et al. 1999; Huang et al. 2011; Improta-Brears, Ghosh, and Bell 1999; Kim, Huang, and Spector 2014; Kim 2007; Suzuki et al. 2001)
Phosphatidylethanolamine	
Increase in the percentage of cytokine-producing cells (monocytes and mDC)	(Simões et al. 2013b)
Modulation of mammalian cell membrane curvature	(Cullis and De Kruijff 1978; Verkleij et al. 1984)
Biosynthesis of glycosylphosphatidylinositol-ethanolamine anchors	(Menon and Stevens 1992)

Post-translational modification of Eukaryotic Elongation Factor 1A	(Signorell et al. 2008)
Regulation of contractile ring disassembly during cytokinesis of mammalian cells	(Emoto and Umeda 2000; Emoto et al. 1996)
Regulation of Golgi membrane fusion in early-divided mitotic cells	(Pécheur et al. 2002)
Cofactor activity in propagation and infectivity of mammalian brain prions	(Deleault et al. 2012)
Covalent modification and recruitment of common autophagosome markers	(Hailey et al. 2010)
Implication with sarcolemmal damage after ischemia and reperfusion	(Post, Bijvelt, and Verkleij 1995)
Exposure to the outer leaflet in mammalian tumors	(Stafford and Thorpe 2011)

1626

1627

1628　Table 2. Occurrences of modified PS and PE in biological samples and their main biological
1629　activities in mammalian cells.

OXIDIZED PHOSPHATIDYLSERINE	
Occurrence	**References**
Formation and externalization during apoptosis	(Kagan et al. 2002; Fabisiak et al. 1998; Arroyo et al. 2002; Shvedova et al. 2002; Koty et al. 2002; Matsura et al. 2002; Matsura et al. 2004; Kagan et al. 2004)
Formation during oxidative lung injury	(Tyurina, Kisin, et al. 2011; Tyurina et al. 2010; Tyurina, Tyurin, et al. 2011)
Formation in a mouse model of the AD and post-mortem brain samples from AD patients	(Maki et al. 2009)
Formation in rat apoptotic cortical neurons	(Tyurin et al. 2008)
Formation in plasma membranes of apoptotic cells from alcoholic liver disease	(Vay et al. 2006)
Biological activity	**References**
"Eat-me" signal for phagocytes during clearance of apoptotic cells	(Greenberg et al. 2006; Hochreiter-Hufford and Ravichandran 2013; Kagan et al. 2002)
Non-enzymatic scramblase activity	(Tyurina et al. 2004)
Inhibition of peripheral blood T-cells proliferation	(Seyerl et al. 2008)
Upregulation of cytokines production in monocytes and dendritic cells	(Silva et al. 2012)
Inhibition of respiratory burst	(Bluml et al. 2008)
Protection of pulmonary endothelium	(Birukova et al. 2006)
Multi-inhibition of the Toll-like receptor 4 pathway	(von Schlieffen et al. 2009)
Stimulation of the expression of pro-atherogenic genes	(Afonyushkin, Oskolkova, and Bochkov 2012)
Pro-coagulant activity via regulation of PCI	(Malleier et al. 2007)
GLYCATED AND GLYCO-OXIDIZED PHOSPHATIDYLSERINE	
Occurrence	**References**
CMS detected in human red blood cells membranes	(Fountain et al. 1999)
ALDEHYDE-ADDUCTED PHOSPHATIDYLSERINE	
Occurrence	**References**
PS-malondialdehyde (PS-MDA) adducts detected in human senile cataractous tissue	(Bhuyan et al. 1986)
N-hexanoyl-PS detected in red blood cells of carbon tetrachloride-treated rats	(Hisaka et al. 2010)
OXIDIZED PHOSPHATIDYLETHANOLAMINE	
Occurrence	**References**
Direct enzymatic oxidation of membrane PE to 15-hydroxy-eicosatetraenoic acid (15-HETE-PE) in ionophore-activated human platelets and peripheral monocytes	(Maskrey et al. 2007)
Direct enzymatic oxidation of membrane PE to 12-hydroxy-eicosatetraenoic acid (12-HETE-PE) in ovalbumin-treated murine peritoneal macrophages	(Morgan et al. 2009)

Esterification of enzymatically oxidized arachidonic acid and docosahexaenoic acid into the membrane PE pool of thrombin-activated human platelets (12S-HETE-PE) and bacteria-activated human neutrophils (5-hydroxyeicosatetraenoic acid-PE, 5-HETE-PE).	(Lloyd T. Morgan et al. 2010; Thomas et al. 2010; Clark et al. 2011)
Direct enzymatic oxidation of membrane PE to 15-keto-eicosatetraenoic acid (15-KETE-PE) in human monocytes, macrophages; detection of 15-KETE-PE in bronchoalveolar lavage fluid from patients affected by cystic fibrosis	(Hammond et al. 2012)
Spontaneous formation of PE short-chain oxidation products in rat retina	(Gugiu et al. 2006)
Direct oxidation of PE esterified to arachidonic acid and adrenic acid within the ER	(Kagan et al. 2016)
Biological activity	**References**
Enhanced thrombin generation	(Zieseniss et al. 2001; Thomas et al. 2010)
Shift in the mobility of soluble CD14	(von Schlieffen et al. 2009)
Inhibition of cytokines generation in human monocytes	(Morgan et al. 2009)
Increase in the frequency of cytokine-producing cells (monocytes and mDC)	(Simões et al. 2013a)
Activation of PPARγ in mouse macrophages	(Hammond et al. 2012)
Inhibition of extracellular traps and enhanced $O_2^{-\bullet}$ generation in human neutrophils	(Clark et al. 2011)
Pro-coagulant activity via regulation of PCI	(Malleier et al. 2007)
Regulation of MAPK signaling in human airway epithelial cells	(Zhao et al. 2011)
Regulation in the clearance of apoptotic cells and maintenance of immunologic tolerance	(Uderhardt et al. 2012)
Modification in cellular membrane topology	(Sankhagowit et al. 2016)
Mediation of ferroptotic cell death	(Kagan et al. 2016)
GLYCATED AND GLYCO-OXIDIZED PHOSPHATIDYLETHANOLAMINE	
Occurrence	**References**
Formation in red blood cells and plasma of healthy and diabetic subjects	(Ravandi et al. 1996; Requena et al. 1997; Fountain et al. 1999; Breitling-Utzmann et al. 2001; Nakagawa 2005; Shoji et al. 2010; Lertsiri, Shiraishi, and Miyazawa 1998)
Formation in glucose-treated LDL	(Ravandi, Kuksis, and Shaikh 2000)
Formation in diabetic rats	(Sookwong et al. 2011)
CME formation in mitochondrial membranes of different mammalian species	(Pamplona et al. 1998)
Biological activity	**References**
Promotion of lipid peroxidation	(Oak, Nakagawa, and Miyazawa 2000; Nakagawa 2005; Annibal et al. 2016)
Different modulation of the frequency of cytokine-producing cells	(Simões et al. 2013b; Simões et al. 2013a)
Modulation of the expression levels of proteins involved in several metabolic cell pathways	(Annibal et al. 2016)

ALDEHYDE-ADDUCTED PHOSPHATIDYLETHANOLAMINE	
Occurrence	**References**
PE-malondialdehyde (PE-MDA) adducts detected in human senile cataractous tissue	(Bhuyan et al. 1986)
N-hexanoyl-PE detected in red blood cells of carbon tetrachloride-treated rats	(Hisaka et al. 2010)
PE-HNE adducts detected in rats affected by diabetic retinopathy	(Bacot et al. 2007)
IsoLG-PE adducts detected in patients with macular degeneration	(Li et al. 2009)
Para-hydroxyphenylacetaldehyde (pHA-PE) adducts detected in the human atherosclerotic intima	(Heller et al. 2000)
Biological activity	**References**
Increase of the macrophages viability in humans	(Riazy et al. 2011)
Endothelial dysfunction, ER curvature and expression of monocyte adhesion molecules in HUVEC	(Guo et al. 2011)
Increase in platelet aggregation and prothrombinase activity	(Zieseniss et al. 2001)
Inhibition of macrophage phagocytosis	(Shiratsuchi et al. 2008)
Modification in cellular membrane topology	(Annibal et al. 2014)

1630

1631 Table 3. Chemical, physical and enzymatic biomimetic methods that have been used for studying
1632 APL oxidation and that were coupled with mass spectrometry analysis for the identification and
1633 structural characterization of oxidized APL

	System	Species	Matrix	Experimental conditions	References
CHEMICALS	Fe^{2+}/H_2O_2	$^\bullet OH$	Ammonium bicarbonate buffer (5 mM, pH 7.4)	40 µM $FeCl_2$, 50 mM H_2O_2, 72 h and 192 h, 37 °C, dark	(Simões et al. 2010)
				Final volume 50 µL, 144 h, and 192 h, 37 °C dark	(Domingues et al. 2009)
				40 µM $FeCl_2$/EDTA (1:1), 10 mM H_2O_2, 37°C, dark	(Maciel et al. 2011)
				80 mM $FeSO_4$, 50 mM H_2O_2, 2 h, 37 °C	(Annibal et al. 2016)
				40 µM $FeCl_2$, 50 mM H_2O_2, 48 h, 37 °C, dark	(Maciel, da Silva, et al. 2013; Maciel, Faria, et al. 2013)
				500 µM $FeCl_2$, 50 mM H_2O_2, 120 h, 37 °C, dark	(Simões et al. 2013b; Simões et al. 2013a)
	Fe^{2+}/ascorbate	$^\bullet OH$	Rat cerebral cortex homogenates	20 µM $FeCl_2$, 250 µM ascorbate, 6 h, 37 °C	(Stadelmann-Ingrand, Pontcharraud, and Fauconneau 2004)
	Cu^{2+}/H_2O_2	$^\bullet OH$	Phosphate buffer saline (50 mM, pH 7.4)	100 µM $CuCl_2$, 70 mM H_2O_2, up to 3 h, 37 °C	(Khaselev and Murphy 1999; Gugiu et al. 2006)
	AAPH	$ROO^\bullet$	Hank's balanced salt solution	10 mM AAPH, 5 h, 37 °C	(Zemski Berry et al. 2010)
			HaCaT Keratinocytes (15 x 10^6)	30 mM and 50 mM AAPH, 24 h, 37 °C	(Maciel et al. 2014)
	Gly-PE	$O_2^{-\bullet}$	Tris-HCl buffer (10 mM, pH 7.4)	15 mol %, 0.3 mol %, 0.05 mol % Amadori PE, up to 120 h, 37 °C	(Breitling-Utzmann et al. 2001)

			Primary rat cardiomyocytes	1 mM gly-PE or 1 mM gly-ox-PE, 30 min and 16 h	(Annibal et al. 2016)
PHYSICAL	UVA	$^1O_2$	Ammonium bicarbonate buffer (5 mM, pH 7.4)	20 min, 75.4 J/cm^2	(Melo, Silva, et al. 2013)
			Phosphate buffer	28 °C	(Gugiu et al. 2006)
			Rat cerebral cortex homogenates	0-90 min, 0-10.8 J/cm^2	(Stadelmann-Ingrand, Pontcharraud, and Fauconneau 2004)
	White light	$^1O_2$	Ammonium bicarbonate buffer (5 mM, pH 7.4)	Artificial white light irradiation, 30 min, 90 min, 270 min, 7.2 J/cm^2, 21.6 J/cm^2, 64.8 J/cm^2	(Melo, Santos, et al. 2013)
	Electrochemistry	$^{\bullet}OH$	1:1 MeOH:20 mM ammonium formate	20µL/min, 37 °C, 2.5 V or 3 V (depending on the APL species)	(Colombo et al. 2018)
ENZYMES	LOX	-	10 mM dehoxycholate, 0.2 M borate buffer	5.2 KU/mL LOX, 30 min, 95% O_2	(Alwena H Morgan et al. 2010)
	MPO	HOX	Sodium phosphate buffer (50 mM)	5 nM MPO, 100 ng/mL glucose oxidase, 500 µM NaNO$_2$, 100 µg/mL glucose, 200 µM DTPA	(Gugiu et al. 2006)

1634
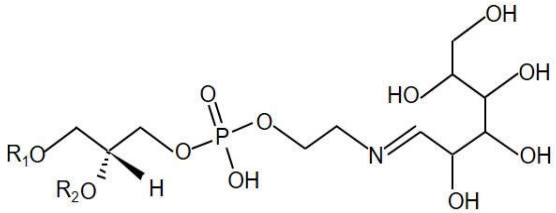
1635
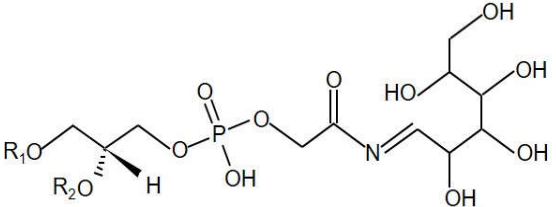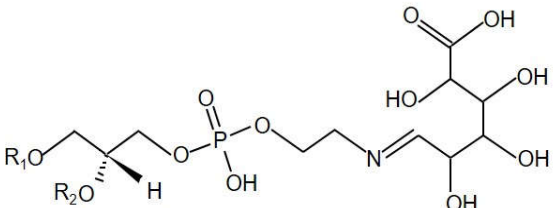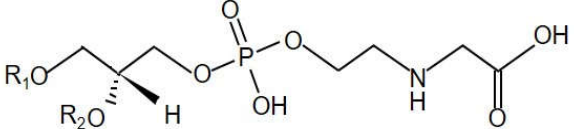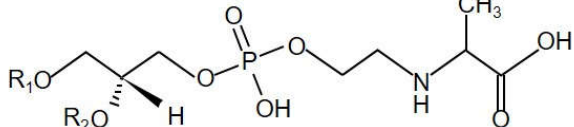
Table 4. Oxidative modifications of APL identified by mass spectrometry either in biomimetic systems and *in vivo*: mass shifts observed in the MS spectra when compared with the respective non modified APL. Characteristic fragmentations (fatty acid carboxylate anions and neutral losses) noticeable in the MS/MS spectra that allow confirming the structural features of the oxidized APL.
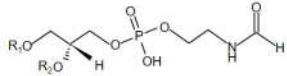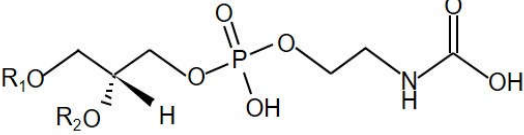
Modification	Modified fatty acid carboxylate anion (*m/z*) [M-H]⁻	Observed neutral loss [M-H]⁻ and [M+H]⁺	References
sn-2 keto (+14 Da)	295 (oleic acid) 293 (linoleic acid) 317 (arachidonic acid) 341 (docosahexaenoic acid)	--	(Melo, Santos, et al. 2013; Hammond et al. 2012; Alwena H Morgan et al. 2010)
sn-2 hydroxy (+16 Da)	297 (oleic acid) 295 (linoleic acid) 319 (arachidonic acid) 343 (docosahexaenoic acid)	$[M+H-18]^+$ $[M-H-18]^-$	(Domingues et al. 2009; Melo, Santos, et al. 2013; Clark et al. 2011; Maskrey et al. 2007; Tyurin et al. 2008; Tyurina et al. 2010; Tyurina et al. 2008; Tyurin et al. 2009; Alwena H Morgan et al. 2010; Lloyd T. Morgan et al. 2010)
sn-2 dihydroxy (+32 Da)	313 (oleic acid) 311 (linoleic acid) 335 (arachidonic acid) 359 (docosahexaenoic acid)	$[M-H-36]^-$ (18 + 18)	(Tyurin et al. 2009)
sn-2 hydroperoxy (+32 Da)	313 (oleic acid) 311 (LA linoleic acid 335 (arachidonic acid) 359 (docosahexaenoic acid)	$[M+H-34]^+$	(Melo, Santos, et al. 2013; Tyurin et al. 2008; Tyurin et al. 2009; Tyurina et al. 2008; Tyurina et al. 2010; Domingues et al. 2009)
sn-2 hydroxy-hydroperoxy (+48 Da)	329 (oleic acid) 327 (linoleic acid) 351 (arachidonic acid) 375 (docosahexaenoic acid)	$[M+H-34]^+$ $[M+H-18]^+$	(Domingues et al. 2009; Melo, Santos, et al. 2013; Tyurin et al. 2008)
sn-2 carboxylic acid terminal C9	187 (linoleic acid)	$[M+H-379]^+$ ($141+R_1=C=O$)	(Maciel et al. 2011; Domingues et al. 2009; Simões et al. 2010)
sn-2 carboxylic acid terminal C5	131 (arachidonic acid)	$[M-H-190]^-$ ($58+R_2'COOH$) $[M+H-141]^+$	(Maciel, Faria, et al. 2013; Gugiu et al. 2006)
Polar head deamination + decarboxylation + oxidation (-29 Da)	--	$[M-H-58]^-$	(Maciel et al. 2011)
Polar head decarboxylation + oxidation (-30 Da)	--	$[M-H-57]^-$	(Maciel et al. 2011)
Polar head deamination (-1 Da)	--	--	(Melo, Santos, et al. 2013)

1641 Table 5. Glycative and glyco-oxidative modifications of APL: Characteristic product ions observed in the MS spectra and corresponding neutral

1642 losses. *This neutral loss was used for the targeted MS detection of modified APL in biological samples.

Modification	Structure (PE is chosen as an example)	Observed neutral loss	References
Glucose (+162 Da)		$[M+H-84]^+$ (18+18+18+30)	(Simões et al. 2010)
		$[M-H-90]^-$	(Maciel, da Silva, et al. 2013; Maciel, Faria, et al. 2013)
		$[M+H-120]^+$	(Simões et al. 2010; Annibal et al. 2016)
		$[M-H-120]^-$ (*)	(Breitling-Utzmann et al. 2001)
		$[M+H-150]^+$	(Simões et al. 2010)
		$[M+H-162]^+$	(Simões et al. 2010)
		$[M-H-162]^-$	(Ravandi, Kuksis, and Shaikh 2000; Maciel, da Silva, et al. 2013; Maciel, Faria, et al. 2013)
		$[M-H-249]^-$ (87+162)	(Maciel, da Silva, et al. 2013; Maciel, Faria, et al. 2013)
		$[M+H-303]^+$ (141+162) (*)	(Simões et al. 2010; Melo, Silva, et al. 2013; Ravandi, Kuksis, and Shaikh 2000; Sookwong et al. 2011; Nakagawa 2005)

59

Glucose adducted to α-keto-etn(+176 Da)		[M+H-317]+ (141+162+14)	(Simões et al. 2010)
Glucuronic acid (+176 Da)		[M-H-263]- (87+162+14)	(Maciel, da Silva, et al. 2013)
		[M+H-317]+ (141+162+14)	(Melo, Silva, et al. 2013; Annibal et al. 2016)
Carboxymethyl (+58 Da)		[M+H-199]+ (141+58) (*)	(Shoji et al. 2010)
		[M-H-58]-	(Maciel, da Silva, et al. 2013; Melo, Silva, et al. 2013)
		--	(Annibal et al. 2016)
Carboxyethyl (+72 Da)		[M+H-213]+ (141+72) (*)	(Shoji et al. 2010)
		--	(Annibal et al. 2016)
Formamide (+28 Da)		[M-H-115]- (87+28)	(Maciel, Faria, et al. 2013; Maciel, da Silva, et al. 2013)

		--	(Simões et al. 2010; Melo, Silva, et al. 2013)
Carbamino acid (+44 Da)		--	1643 (Melo, Silva, et al. 2013)

1645   Table 6. Chromatographic Columns used for LC-MS separation and analysis of modified APL.

Analyte(s)	Stationary phase	Column	ID	Comment	References
4-(dimethylamino)benzoic acid (DMABA)-PE	C_{18}	Gemini®	2.0 mm	-	(Zemski Berry et al. 2010)
HETE-PE KETE-PE	C_{18}	Luna®	2.0 mm	-	(Lloyd T. Morgan et al. 2010; Maskrey et al. 2007; Clark et al. 2011; Hammond et al. 2012; Morgan et al. 2009)
HETE-PE	C_{18}	Luna®	2.0 mm	Separation of the following isobaric species: 18:0a/12-HETE-PE and 16:0a/12-HETE-PC	(Thomas et al. 2010)
HPETE-PE HETE-PE KETE-PE	C_{18}	Luna®	2.0 mm	Separation of positional isomers of 18:0a/HETE-PE	(Alwena H Morgan et al. 2010)
Short chain oxidation products of PE	C_{18}	Prodigy™	2.0 mm	-	(Gugiu et al. 2006)
Oxidized plasmenyl-PE	C_{18}	Ultramex	4.6 mm	-	(Khaselev and Murphy 1999)
Short chain and long chain oxidation products of PE	C_5	Discovery® BIO Wide Pore	0.5 mm	Separation of the following couples of long-chain oxidation products: (i) PLPE-OH-OH and PLPE-OOH (ii) PLPE-OH-OH-OH-OH and PLPE-O-OH-OH-OH	(Domingues et al. 2009)
Long chain oxidation products of PS	Silica	Luna®	2.0 mm	-	(Tyurina et al. 2008; Tyurina et al. 2010)
Gly-PE Gly-PS	Silica	Spherisorb®	4.6 mm	-	(Ravandi, Kuksis, and Myher 1995; Ravandi et al. 1996)
Gly-PE	C_{18}	XTerra™	3 mm	-	(Breitling-Utzmann et al. 2001)
Gly-PE Gly-ox PE	C_5	Discovery® BIO Wide Pore	0.5 mm	Separation of two positional isomers for glyco-oxidized PLPE: (i) Gly-PLPE with ketone modification on the polar head; (ii) Gly-PLPE with ketone modification on the sn-2 fatty acyl chain	(Simões et al. 2010)

Gly-PS	C_5	Discovery® BIO Wide Pore	0.5 mm	Separation of two positional isomers for glyco-oxidized POPS: (i) Gly-POPS with ketone modification on the polar head; (ii) Gly-POPS with ketone modification on the sn-2 fatty acyl chain	(Maciel, da Silva, et al. 2013)
Gly-PS	C_5	Discovery® BIO Wide Pore	0.5 mm	Separation of two isobaric short chain oxidation products of PAPS	(Maciel, Faria, et al. 2013)
CM-PE, CE-PE	C_{18}	XBridge™	2.1 mm	-	(Shoji et al. 2010)
PE adducted to 4,5(E)-Epoxy-2(E)-heptenal	HILIC	LiChrospher®	4 mm	-	(Zamora and Hidalgo 2003)
PE adducted to isoketals	C_{18}	Nucleosil 100-5®	2.1 mm	-	(Bernoud-Hubac et al. 2004)

1646
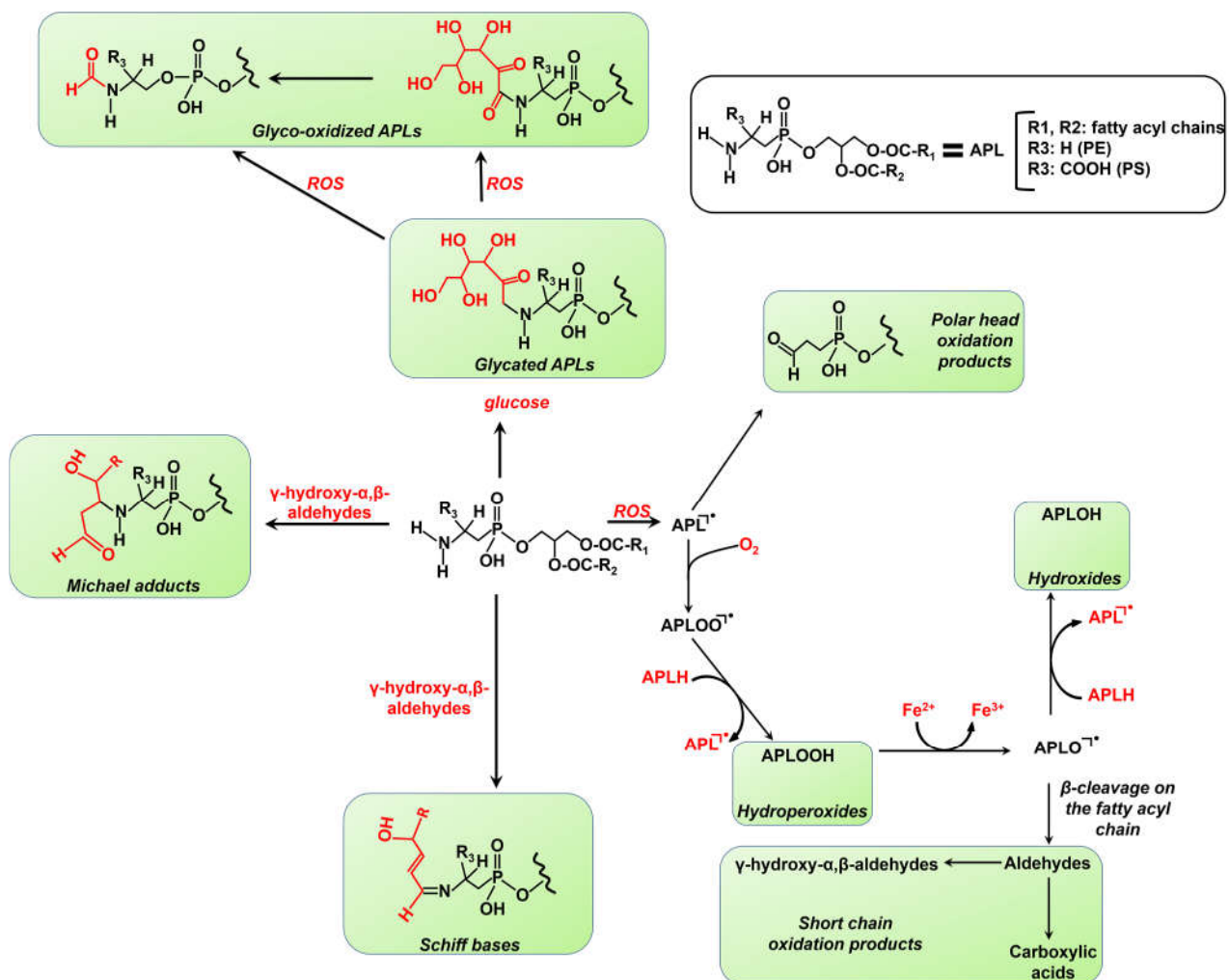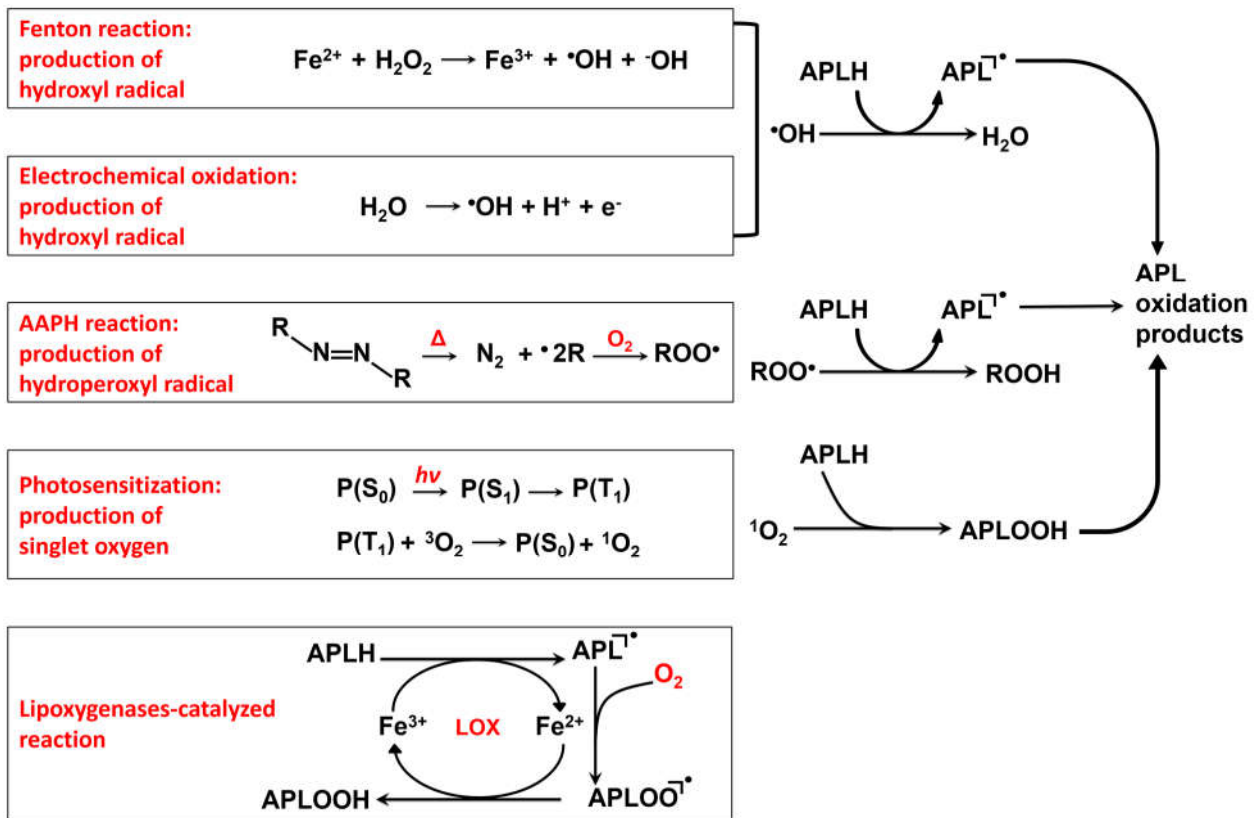
Figure 1

1650 **Figure 2**

1651

1652
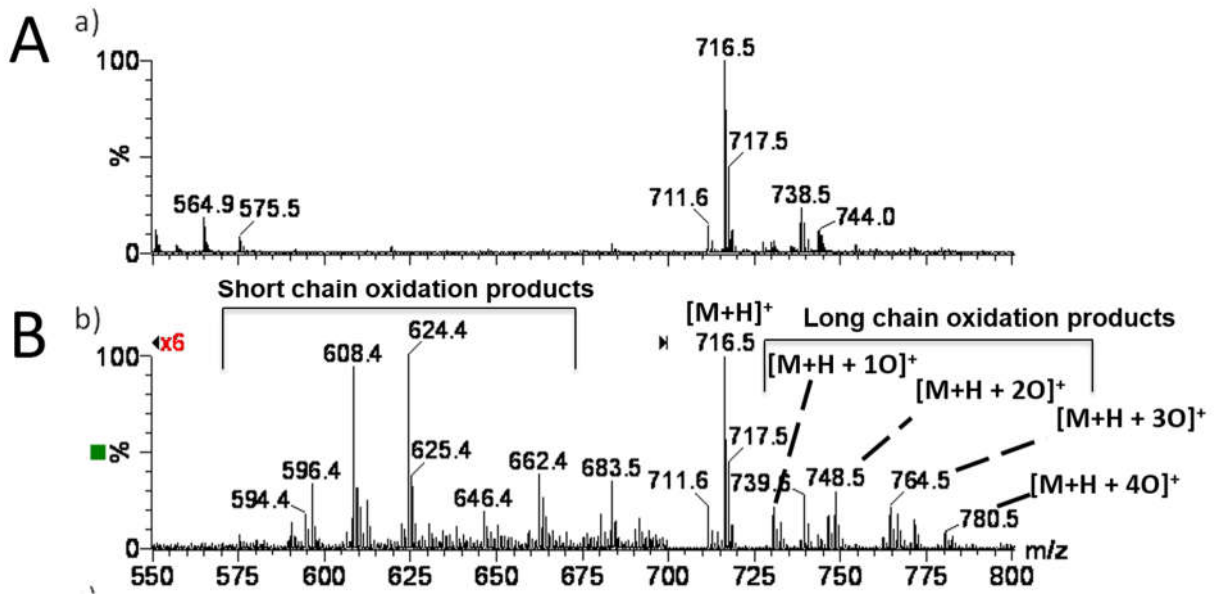
1653   **Figure 3**
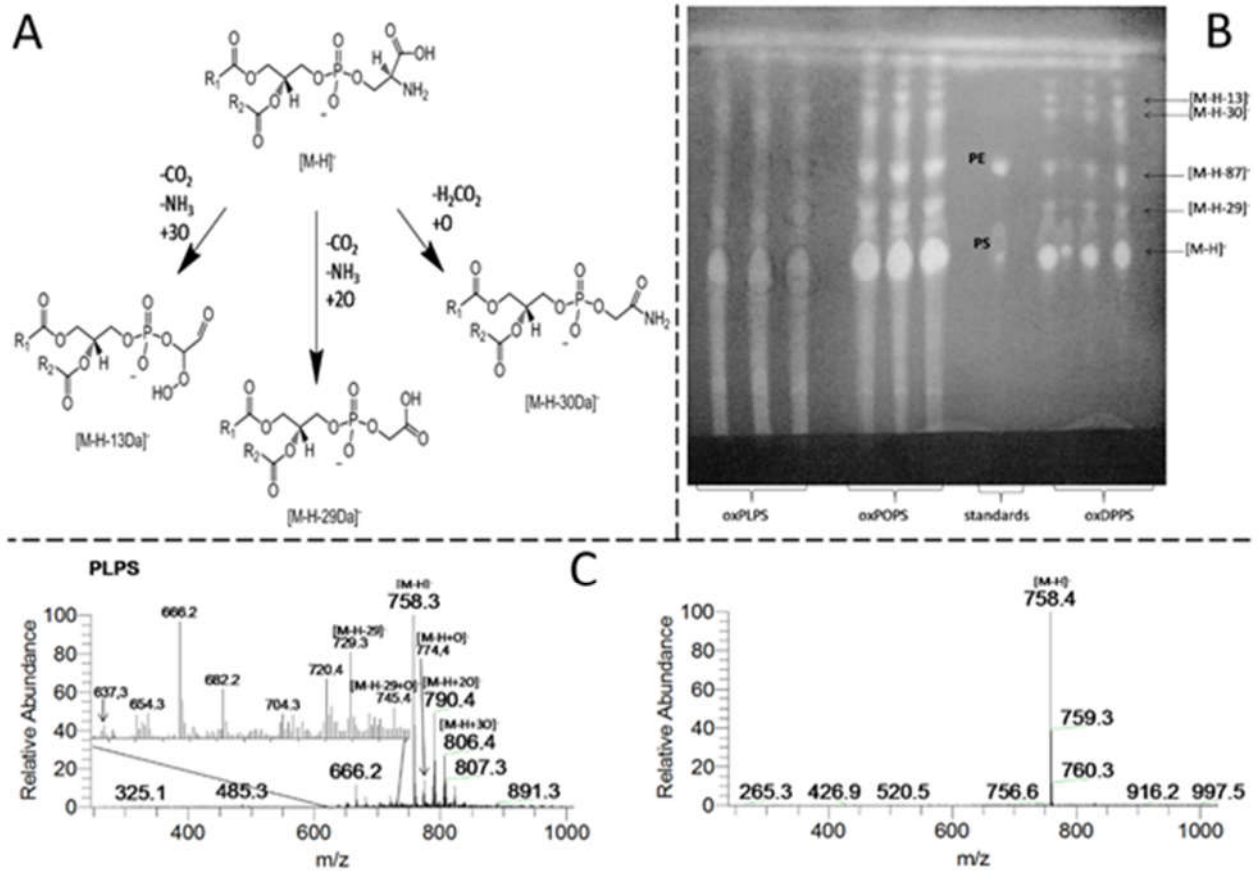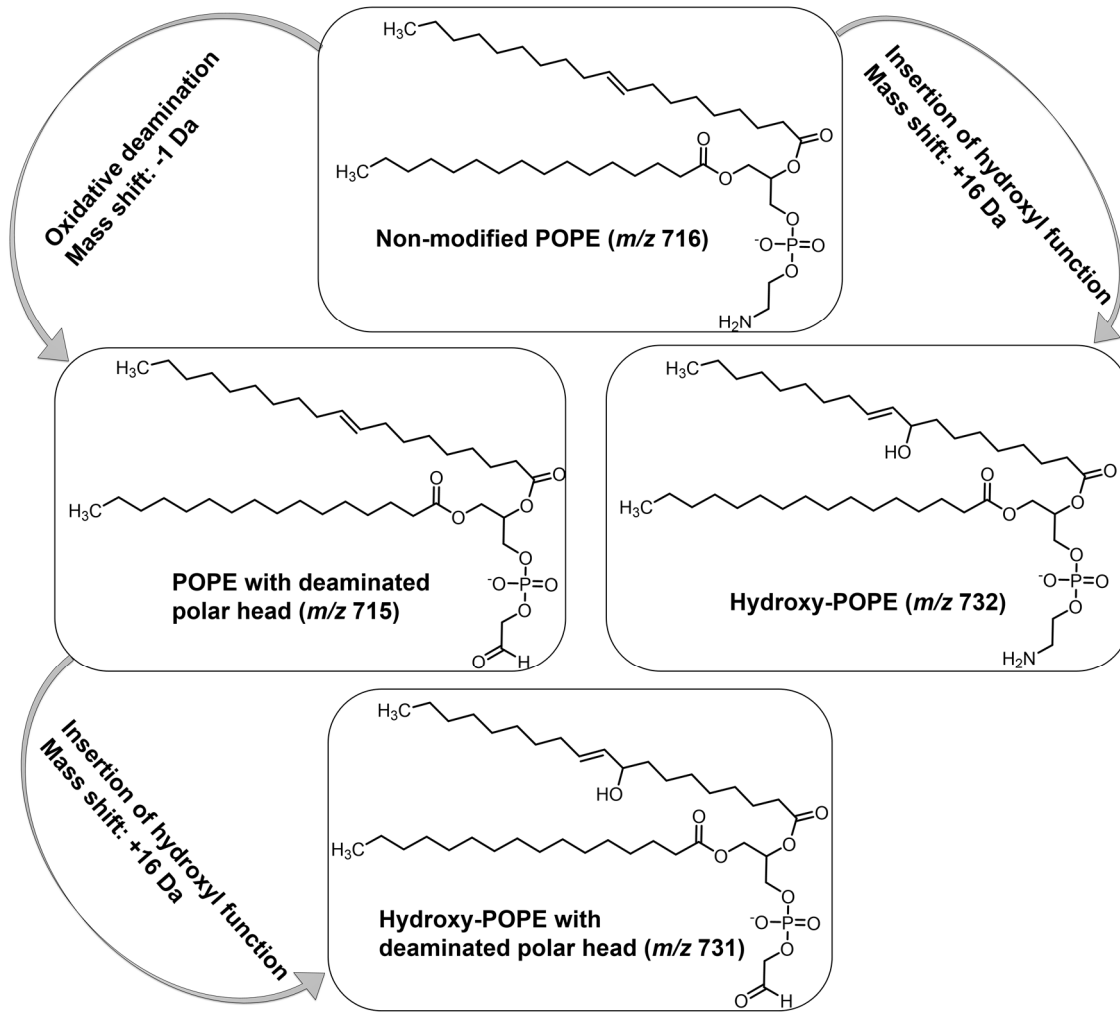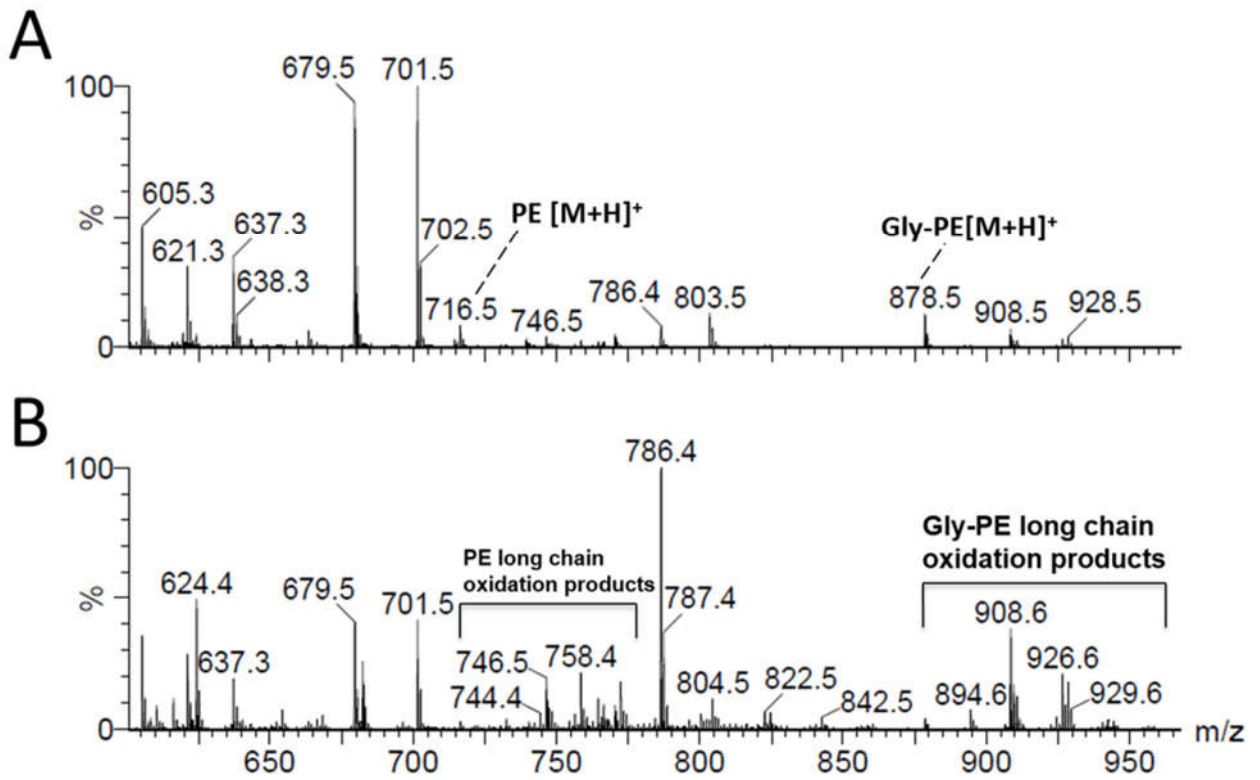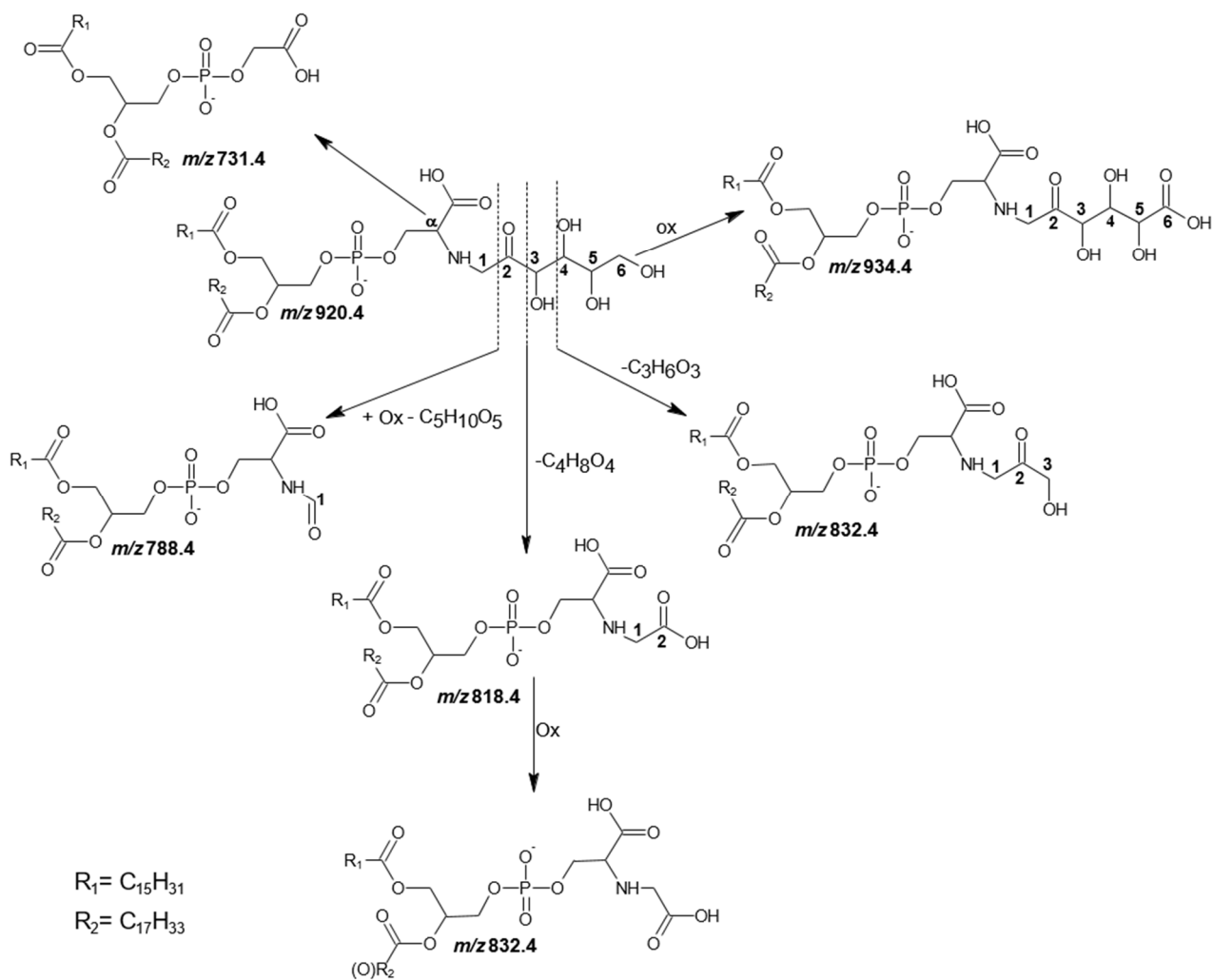
1654

1655

Figure 4

1659 **Figure 5**

Non-modified POPE (*m/z* 716)

Oxidative deamination
Mass shift: -1 Da

Insertion of hydroxyl function
Mass shift: +16 Da

POPE with deaminated
polar head (*m/z* 715)

Hydroxy-POPE (*m/z* 732)

Insertion of hydroxyl function
Mass shift: +16 Da

Hydroxy-POPE with
deaminated polar head (*m/z* 731)

1660
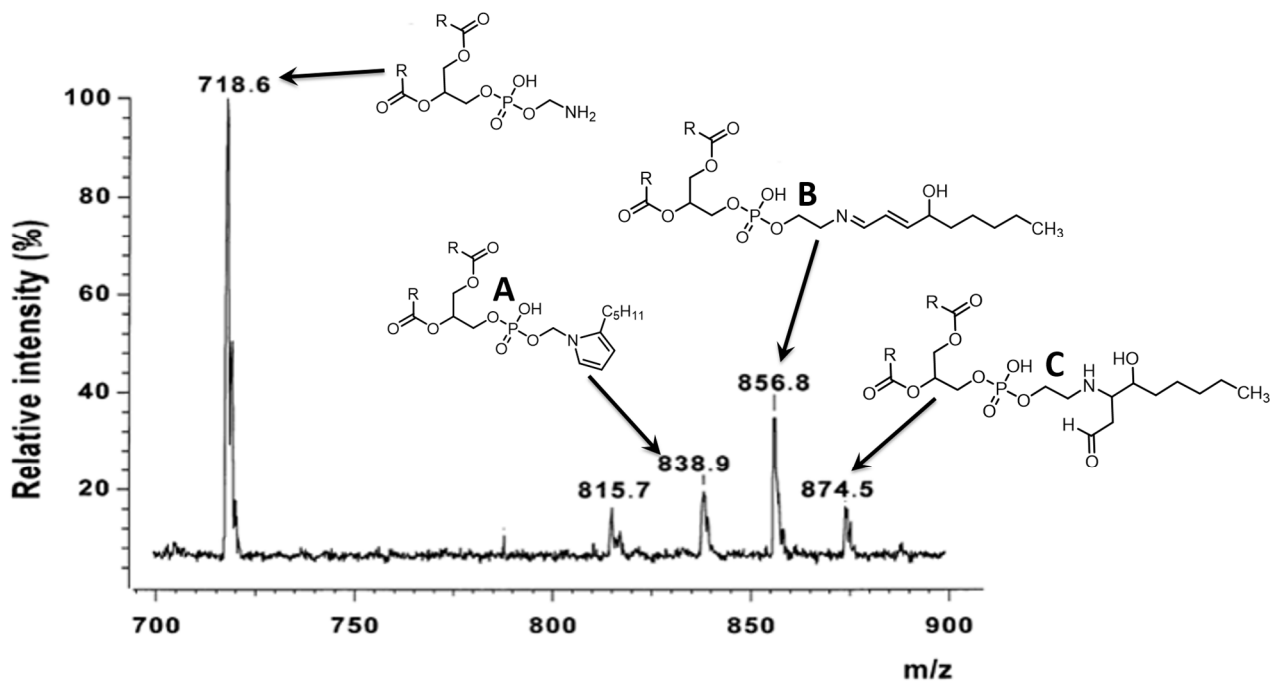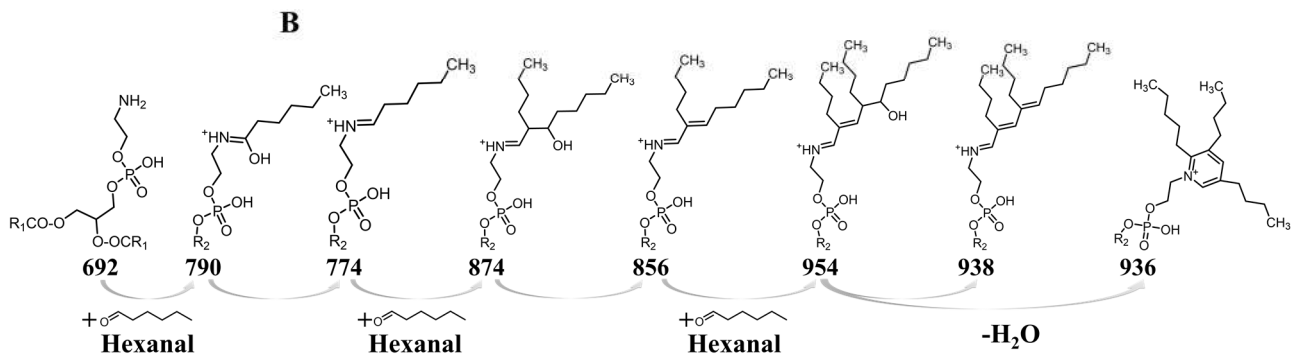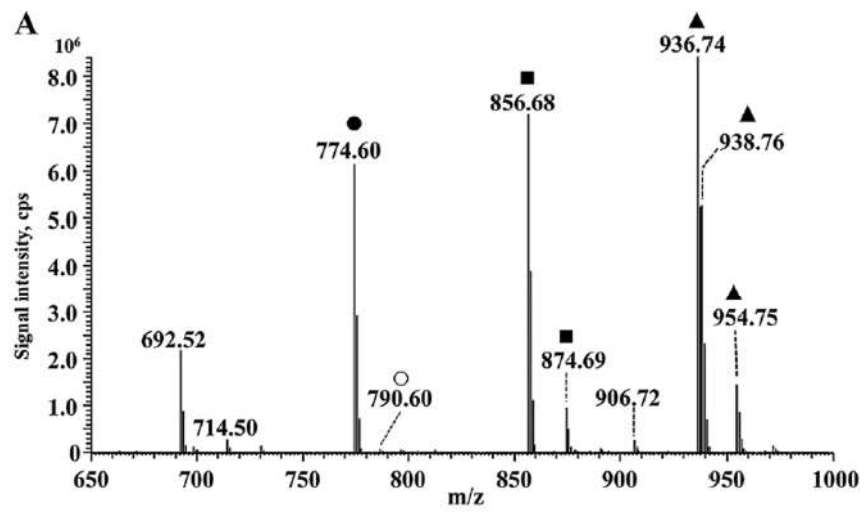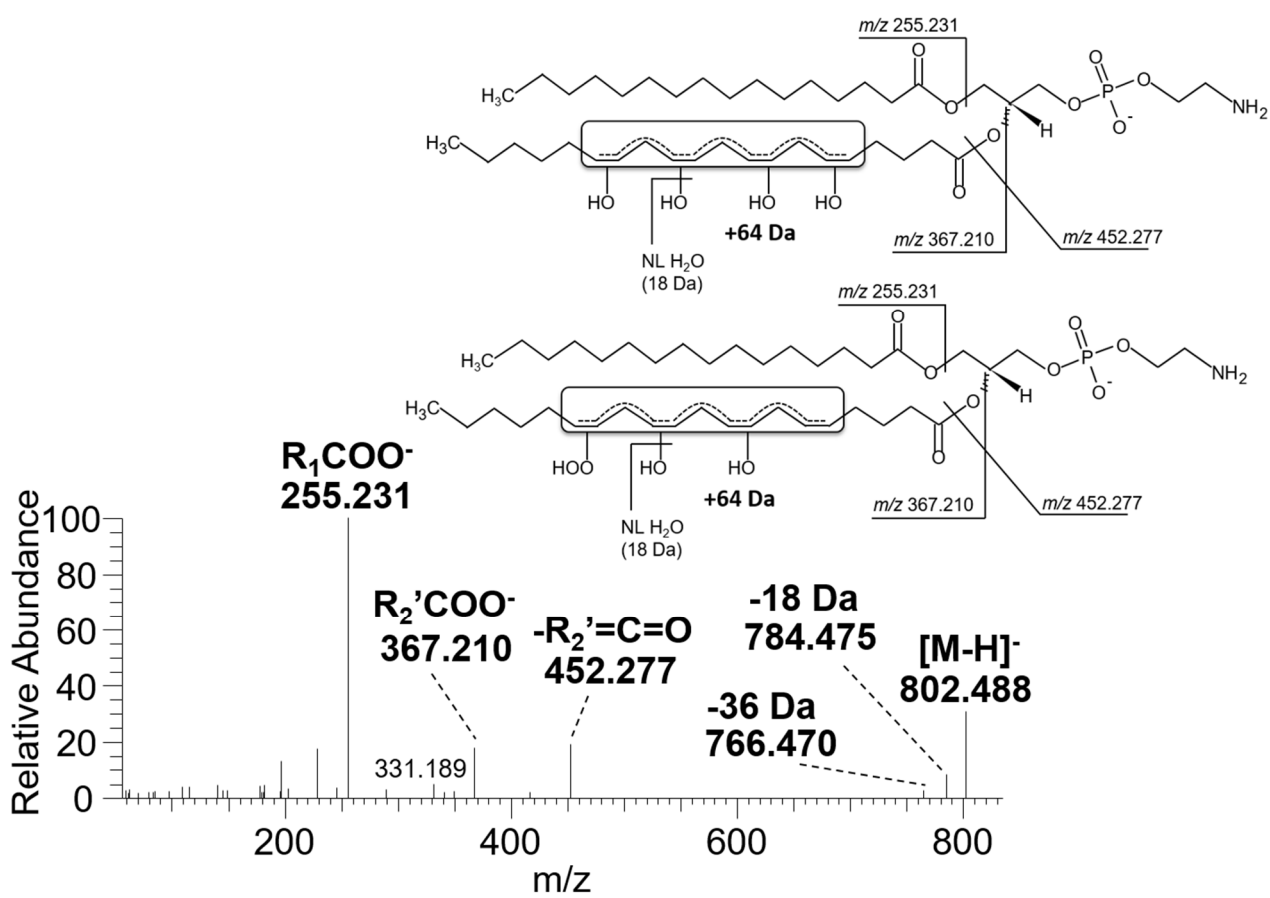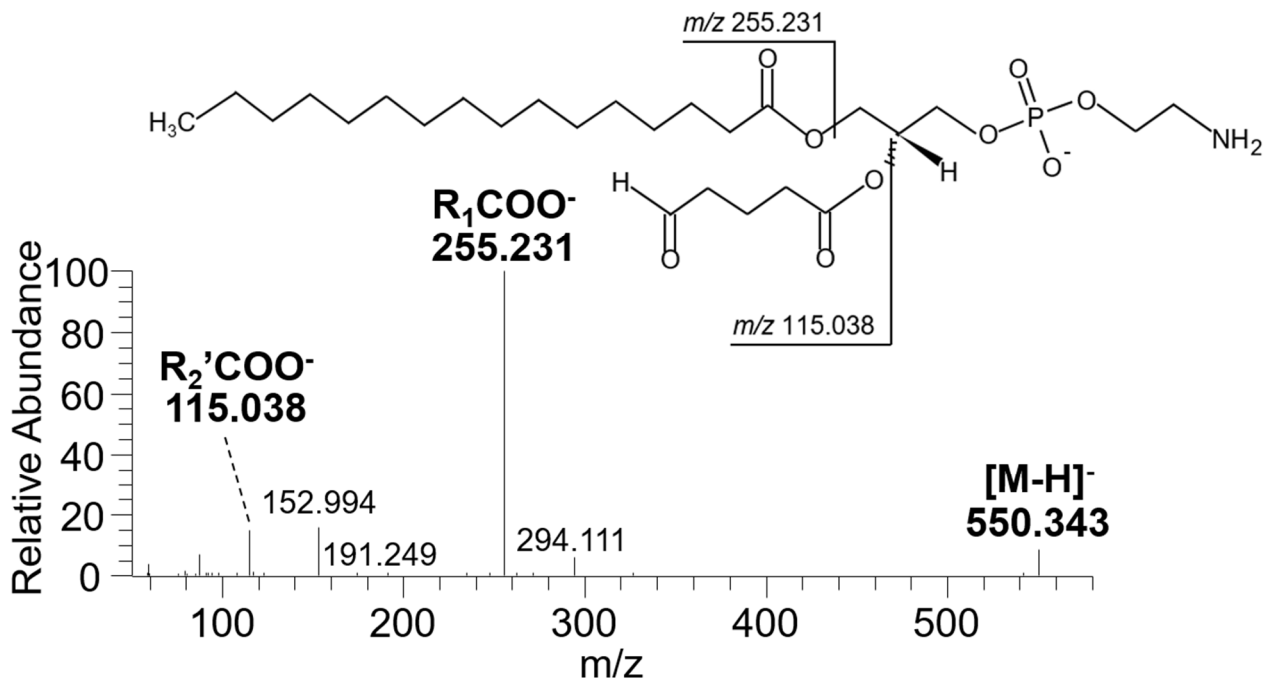
Figure 6

Figure 7

Figure 8

Figure 9

Figure 10

Figure 11

1679   **Figure 12**
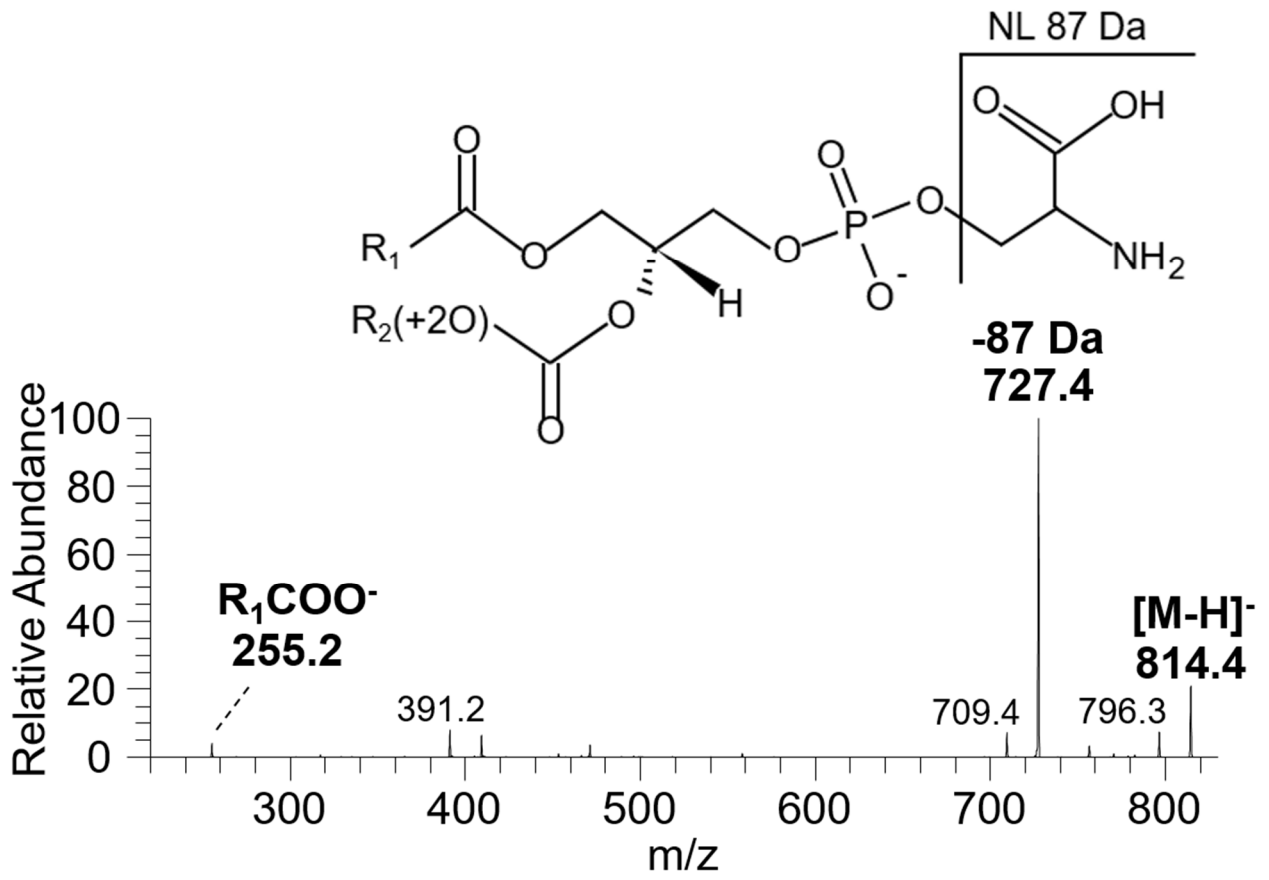
1680

1681
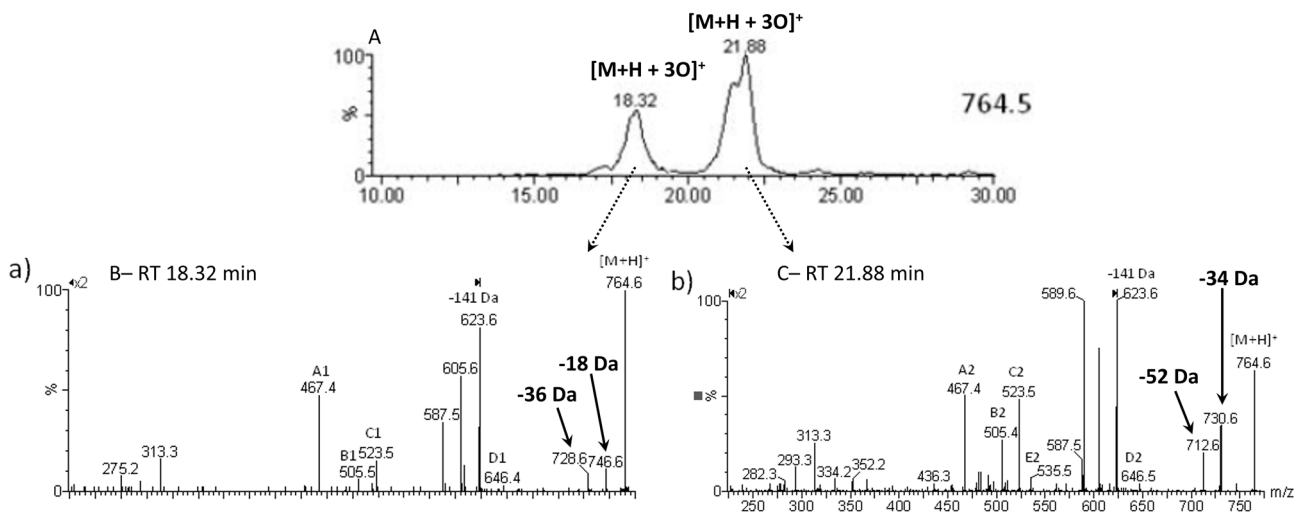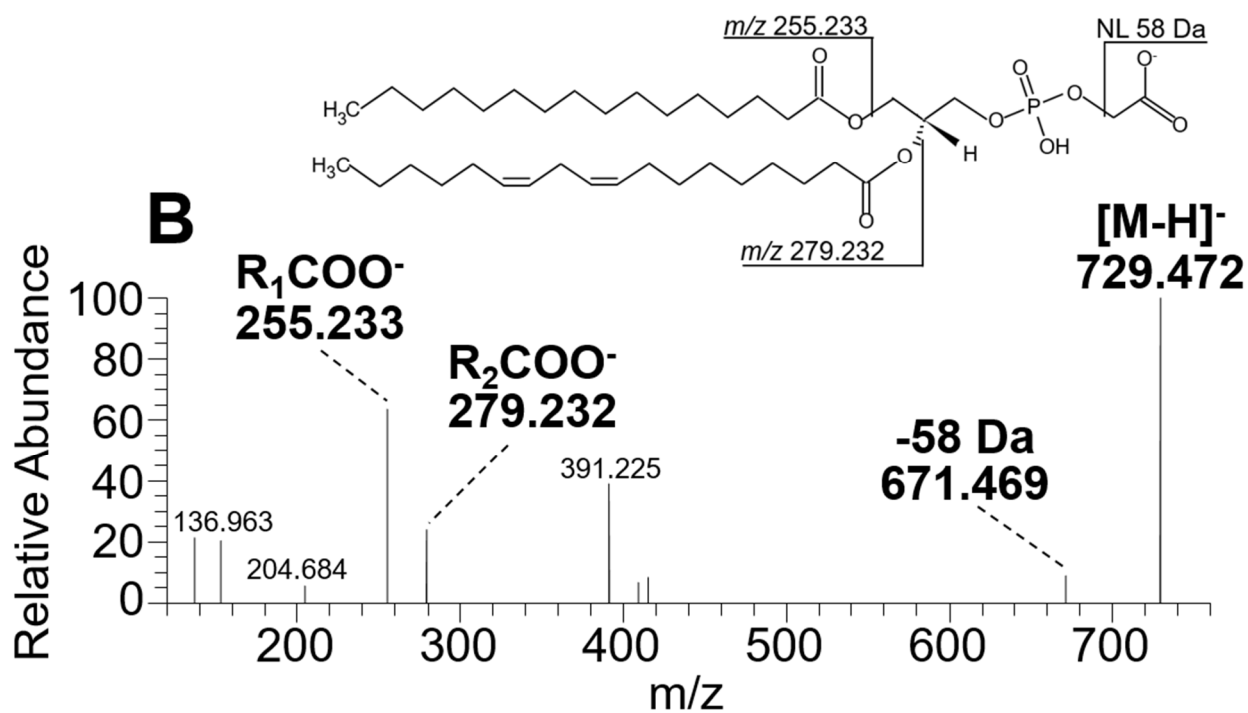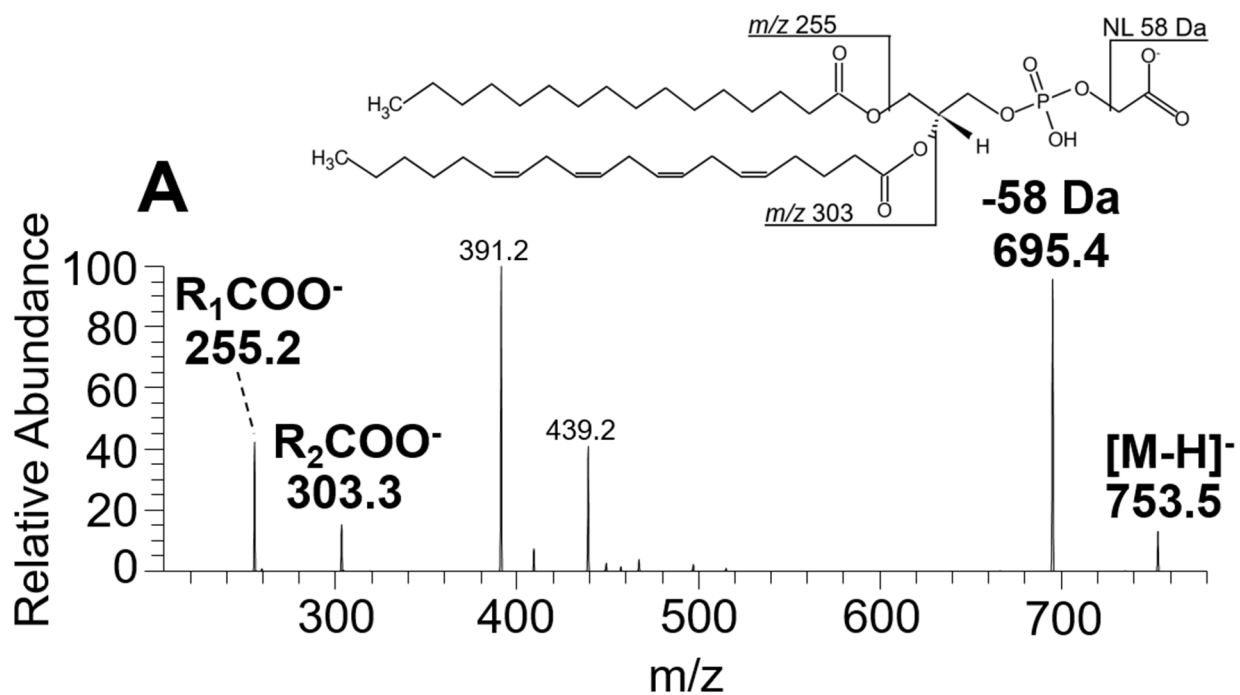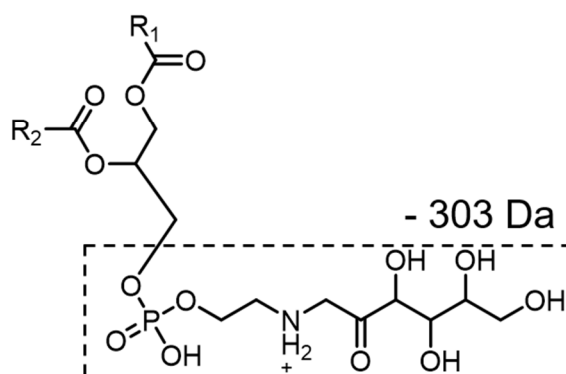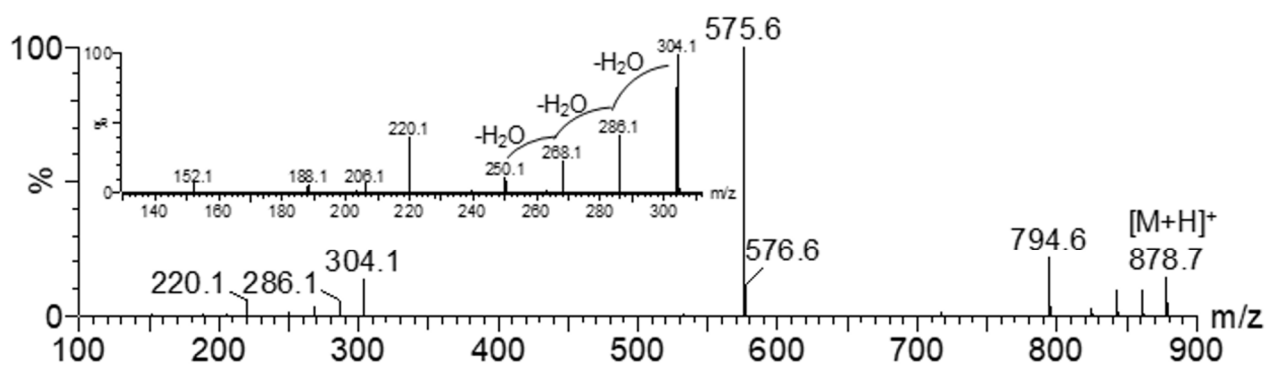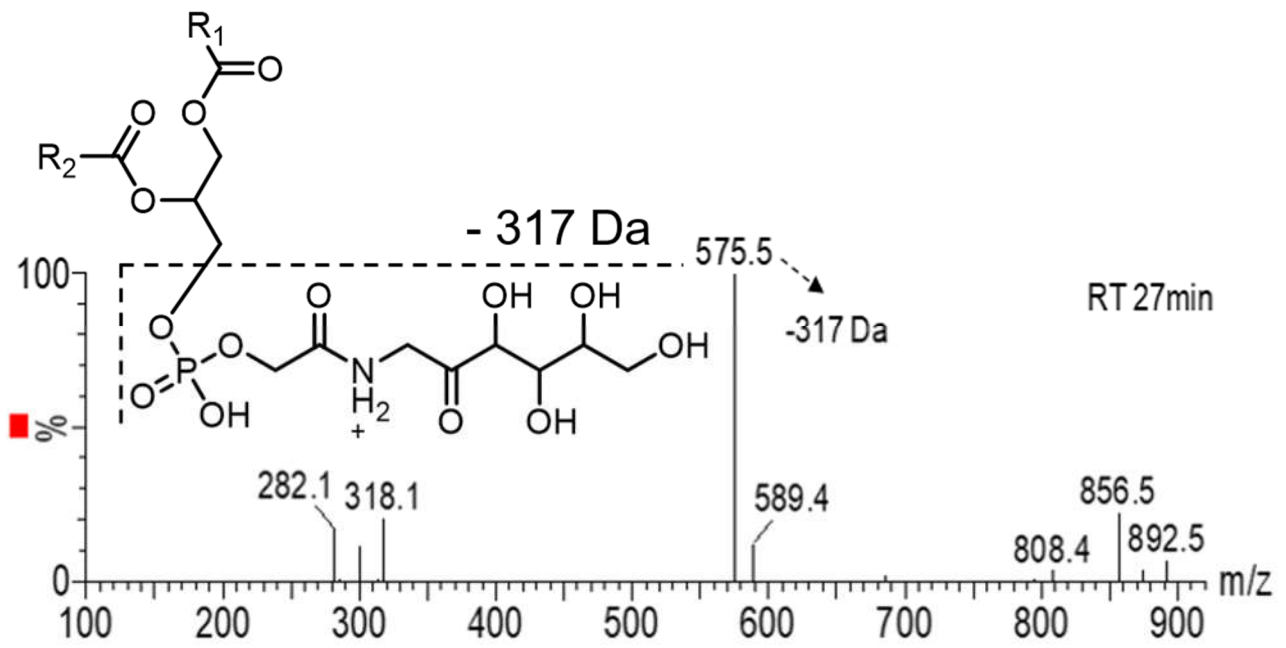
Figure 13
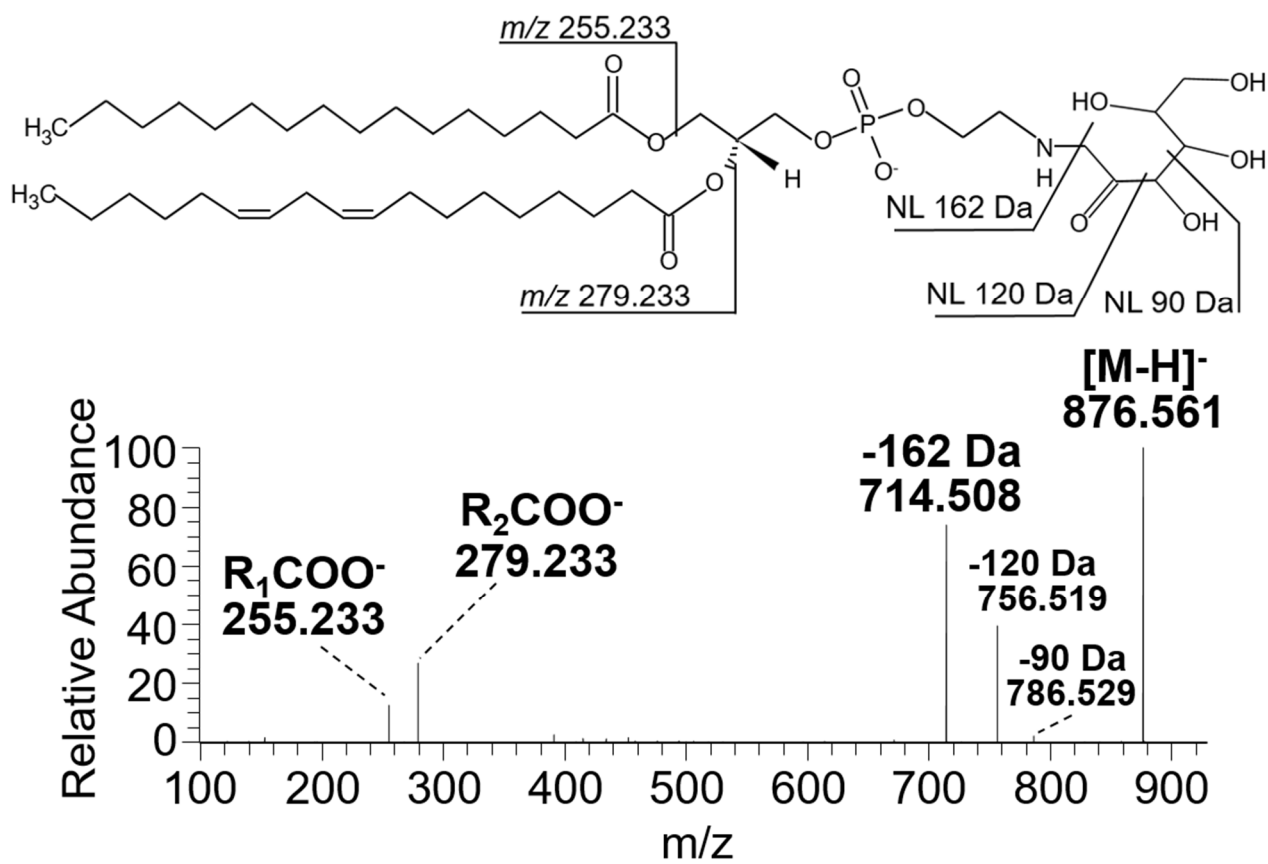
Figure 14

Figure 15
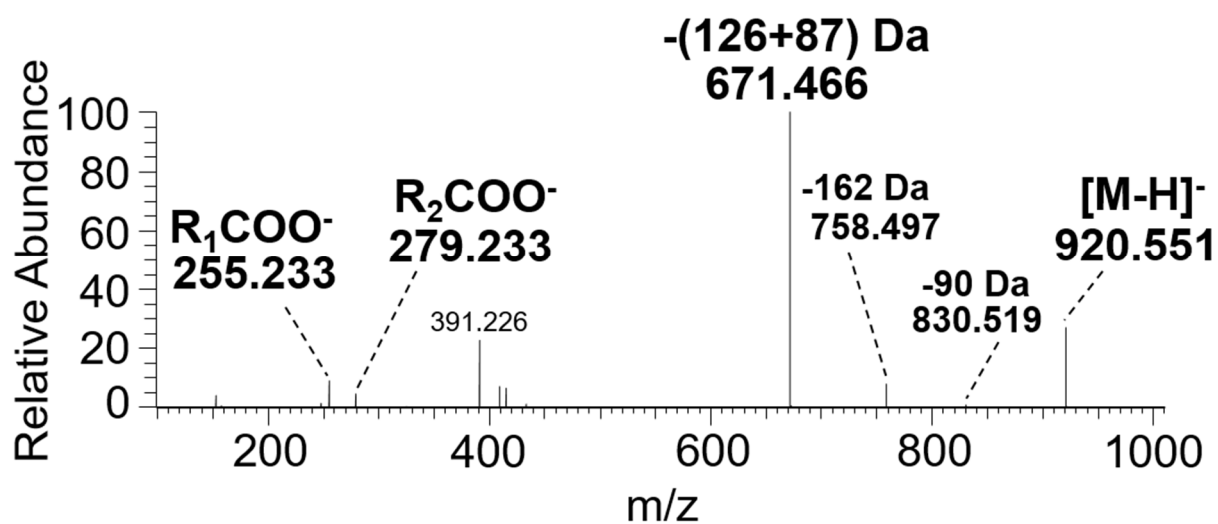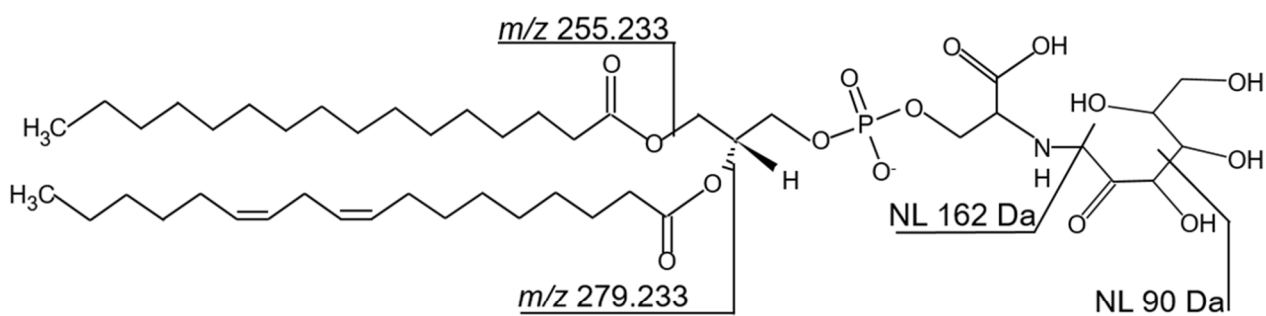
Figure 16
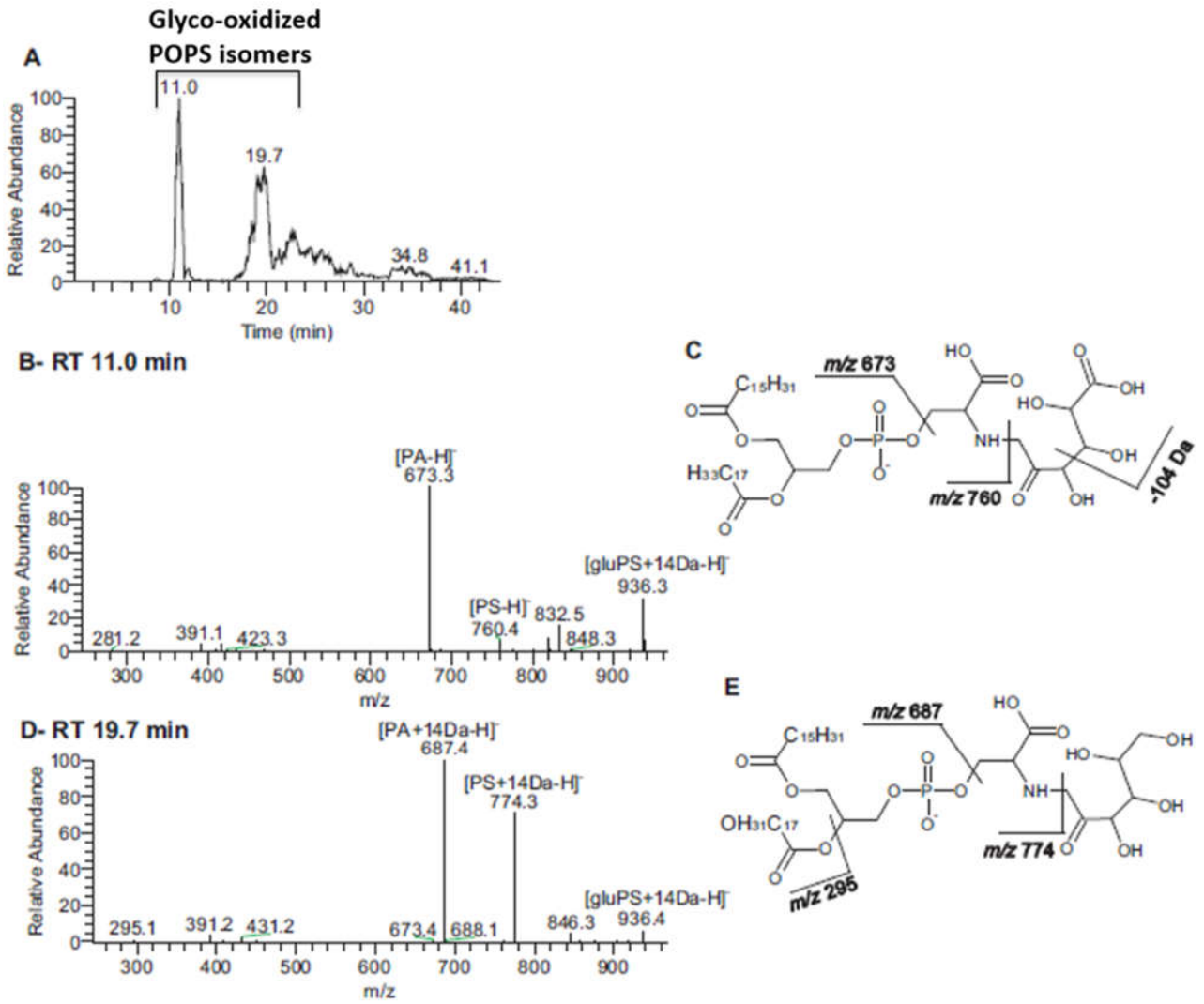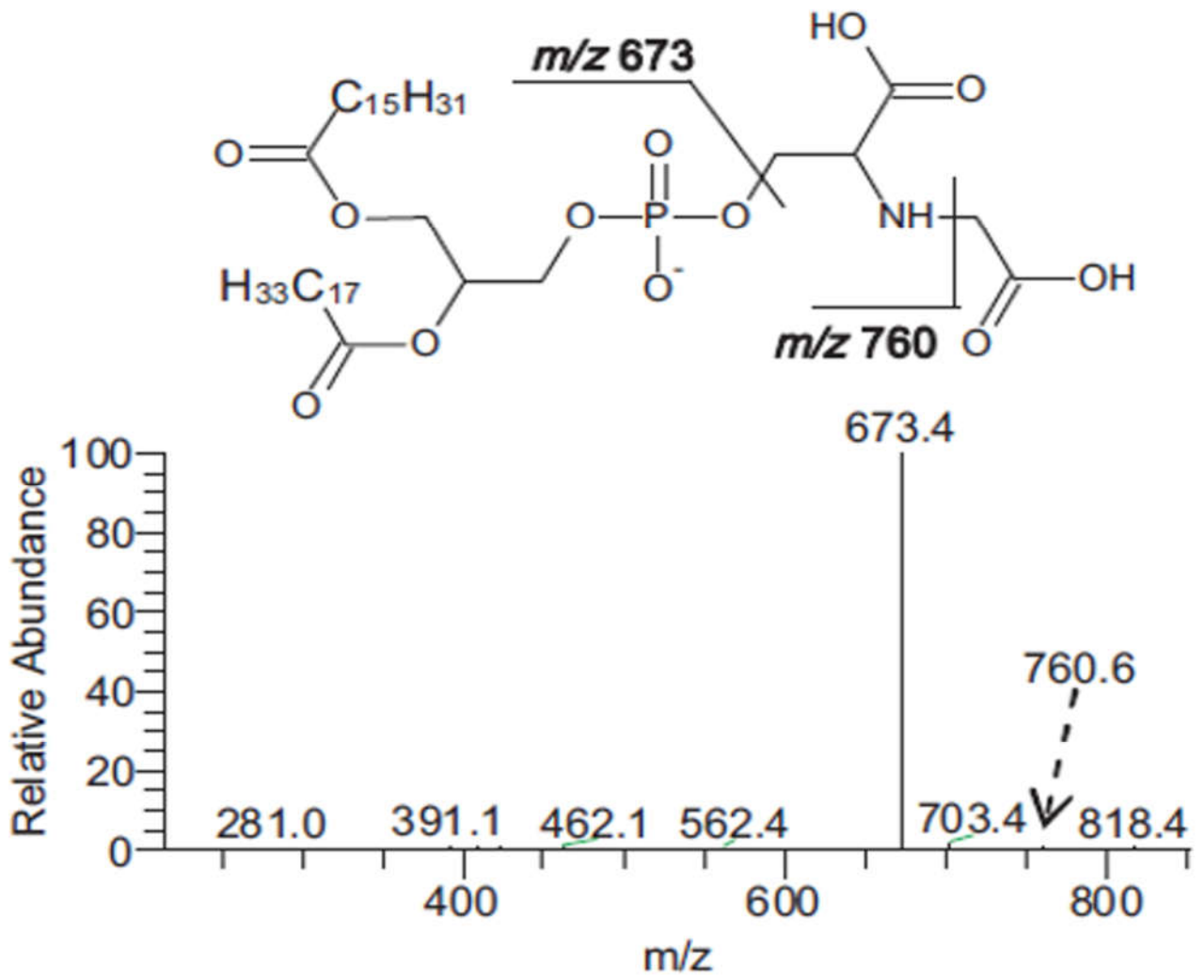
Figure 17

Figure 18

1700   **Figure 19**

1701

1702
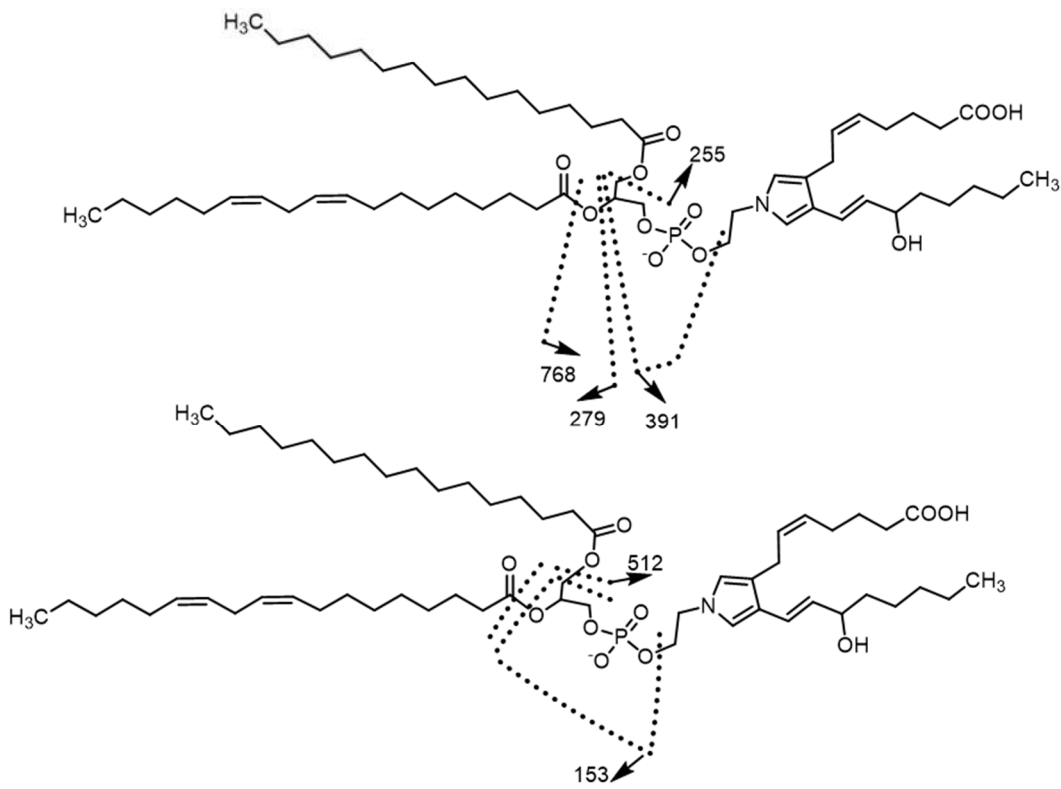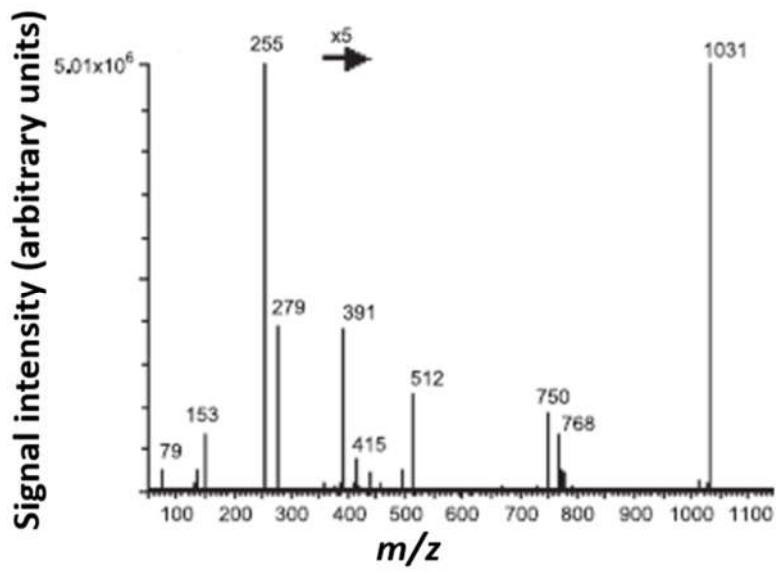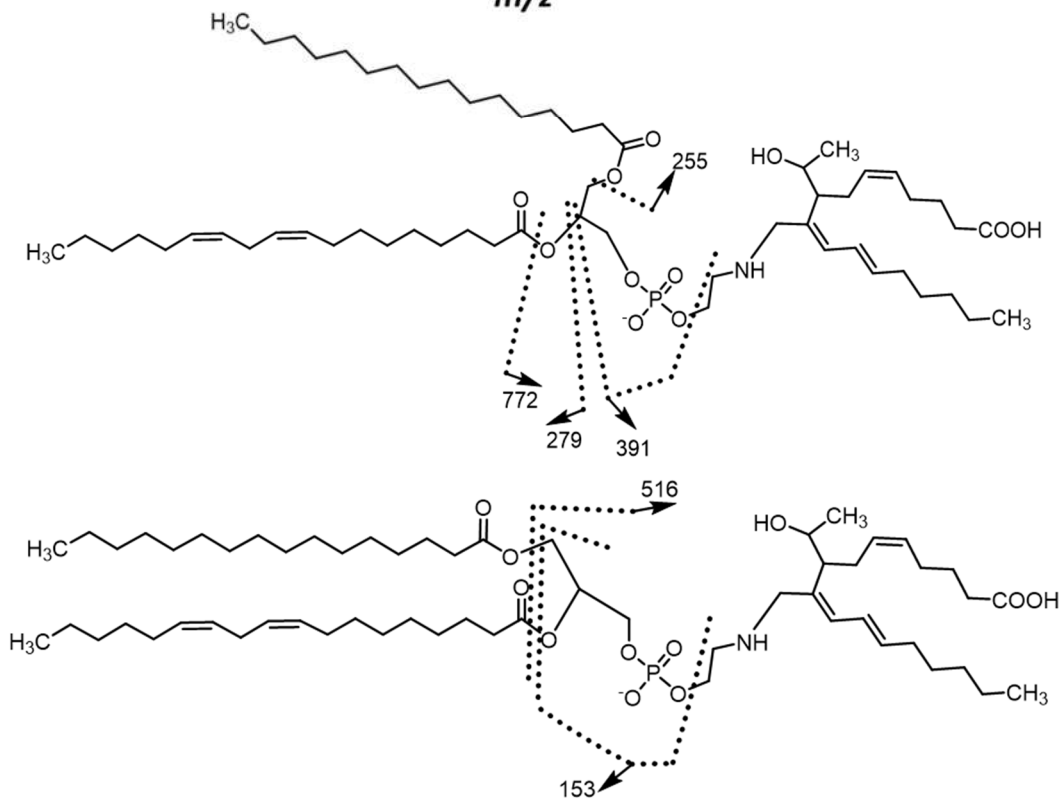
1703   **Figure 20**

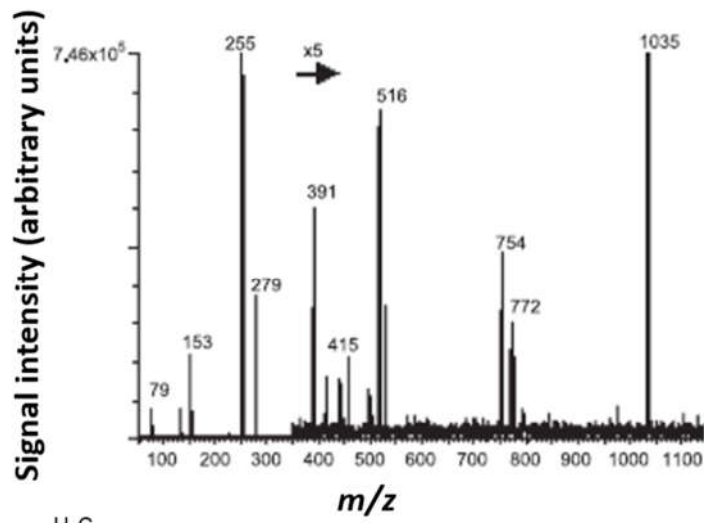1706 **Figure 21**

1707

1708

84
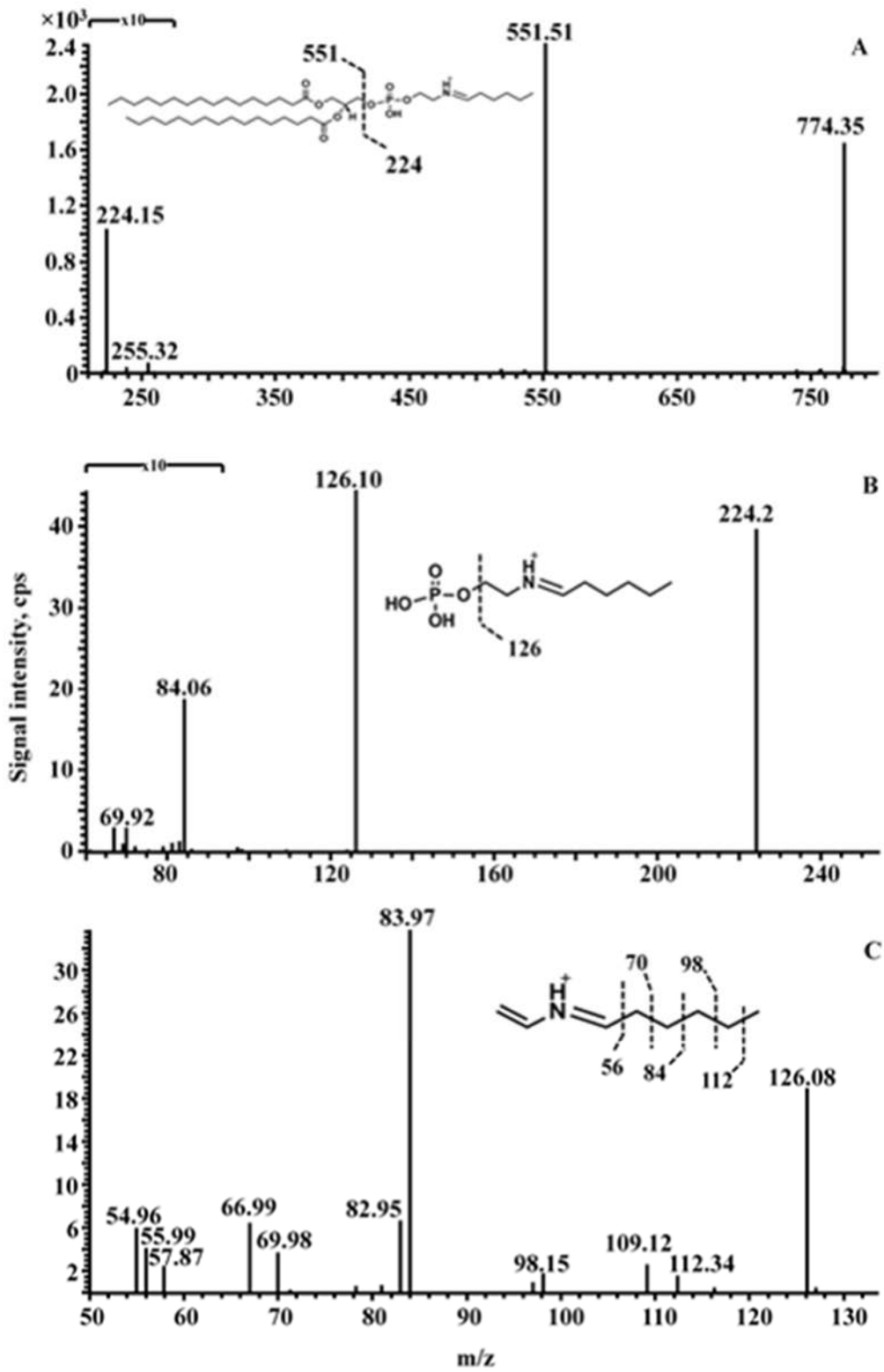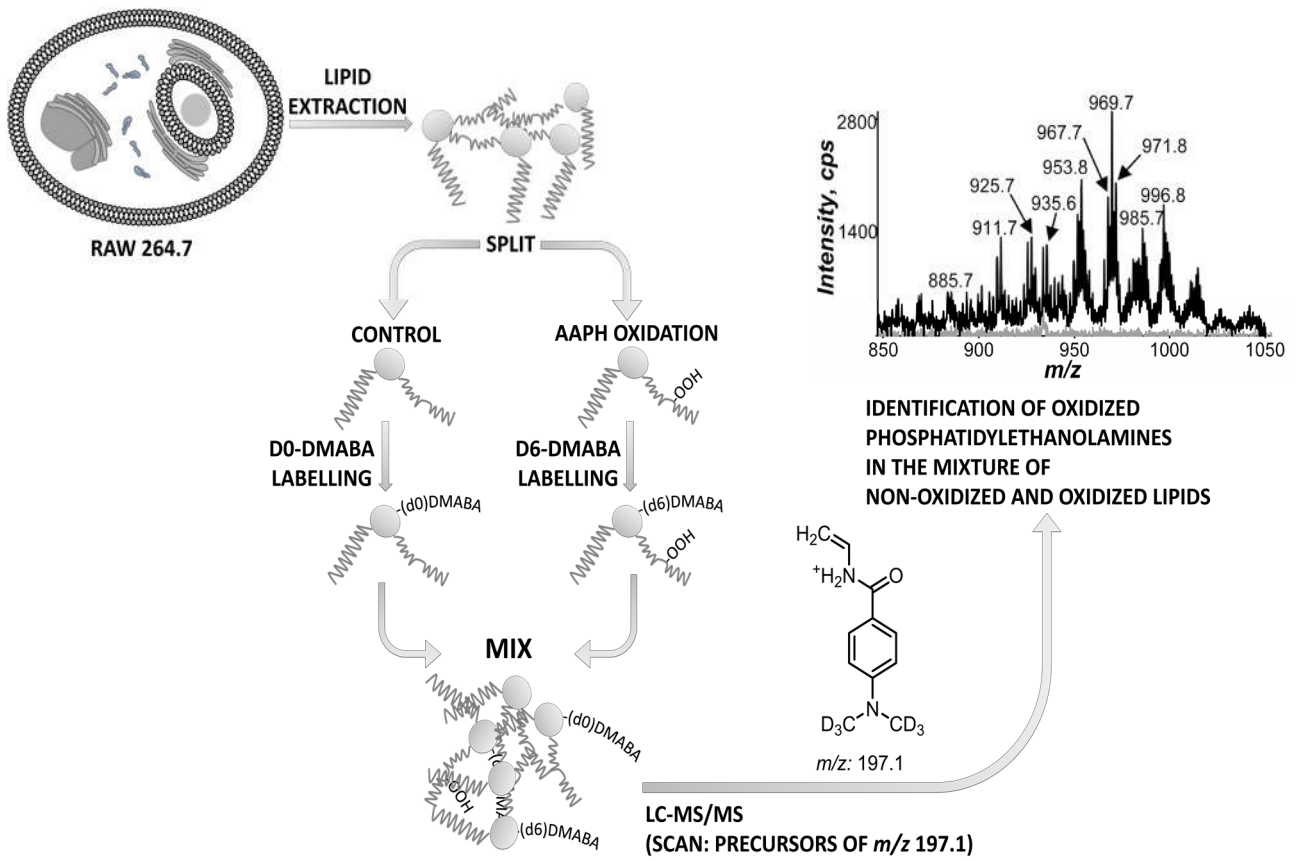
1709   **Figure 22**

1710

1711

1712   **Figure 23**

1713

1714

Figure 24

Figures captions.

Figure 1. Schematic diagram of the chemistry involved in the oxidative and glyco-oxidative

modifications of APL. The shaded green boxes depict the main modified products.

Figure 2. Diagram reporting the main biomimetic methods used in the study of APL oxidation

(Fenton reaction, electrochemical oxidation, AAPH reaction, photosensitization, LOX) and the

radical chemical reactions induced or catalyzed by each method.

Figure 3. MS spectrum of a PLPE before and after the oxidation induced by $^{\bullet}$OH radical formed

during the Fenton reaction (A and B, respectively). The $[M+H]^{+}$ molecular ion of PLPE is depicted

at *m/z* 716.5; the $[M+H]^{+}$ molecular ion at *m/z* 748.5 (Panel B) corresponds to the long-chain

oxidation product of PLPE +2O (PLPE+ 32 Da). PLPE +2O can be assigned as dihydroxy-PLPE

and as hydroperoxy-PLPE. The $[M+H]^{+}$ ion at m/z 764.5 corresponds to the long-chain oxidation

product of PLPE +3O (PLPE+48Da) and can be identified both as hydroxy-hydroperoxy-PLPE and

trihydroxy-PLPE. The $[M+H]^{+}$ ion at *m/z* 608.4 is attributed to the short chain product 1-

(palmitoyl)-2-(9-oxo-nonanoyl)-PE, in which *sn*-2 position is esterified to a nonanoic acid with a

terminal aldehyde in C9. The $[M+H]^{+}$ ion at *m/z* 624.4 corresponds to 1-(palmitoyl)-2-(9-carboxy-

nonanoyl)-PE, which is formed by the oxidation of the terminal aldehydic function of 1-(palmitoyl)-

2-(9-oxo-nonanoyl)-PE. Reprinted with permission from Domingues *et al*. (2009), copyright 2009

[John Wiley & Sons].

Figure 4. (A) Structures of oxidized PS derivatives with modifications in the polar head group

obtained after the oxidation induced by the $^{\bullet}$OH radical generated by Fenton reaction: terminal

hydroperoxyacetaldehyde (−13 Da), terminal acetic acid (−29 Da), and terminal acetamide (−30

Da). (B) Thin Layer Chromatography (TLC) plate under UV light of PS oxidation products with

modifications in the polar head: lines 1, 2, and 3: oxPLPS; lines 4, 5 and 6: oxPOPS; lines 8, 9 and

10: oxidized 1,2-dipalmitoyl-*sn*-3-glycerophosphoserine (DPPS); line 7: PS and PE standards. (C)

ESI-MS spectra of PLPS acquired after and before oxidation induced by the $^\bullet$OH radical (right and left panels, respectively). In Panel C, the ion at *m/z* 758.4 corresponds to the [M-H]$^-$ molecular ion of unoxidized PLPS; The oxidized molecular [M-H]$^-$ ions were observed at: *m/z* 774, PS+O (hydroxy-PLPS) *m/z* 790.4, PLPS +2O, hydroperoxy-PS and/or di-hydroxy-PS (mass shift from native PLPS: M+32 Da); *m/z* 806.4, PLPS +3O hydroxy-hydroperoxy-PS and tri-hydroxy-PS (mass shift from native PLPS: M+48 Da); *m/z* 666.2, 1-(palmitoyl)-2-(9-oxo-nonanoyl)-PS; *m/z* 682.2, 1-(palmitoyl)-2-(9-carboxy-nonanoyl)-PS; *m/z* 728.4; ox-PLPS with Ser polar head modified to terminal acetamide (mass shift from native PLPS: M - 30 Da), *m/z* 745.4, ox-PLPS with Ser polar head modified to terminal hydoperoxy-acetaldehyde (mass shift from native PLPS: M-13 Da); *m/z* 729.4, ox-PLPS with Ser polar head modified to terminal acetic acid (mass shift from native PLPS: M - 29 Da). Reprinted with permission from Maciel *et al*. (2011), copyright 2011 [Springer].

Figure 5. Schematic representation of the oxidative modifications reported for POPE on the unsaturated fatty acyl chains and on the polar head group, along with their characteristic mass shifts.

Figure 6. ESI-MS spectrum of gly-PLPE acquired after and before oxidation induced by the $^\bullet$OH radical (Panels A and B, respectively). In Panel A, the ion at *m/z* 878.5 corresponds to the [M+H]$^+$ molecular ion of glycated PE. In Panel B, the glyco-oxidized [M+H]$^+$ molecular ions were observed at: *m/z* 894.6, gly-PLPE bearing 1 oxygen insertion on the *sn*-2 linoleoyl chain (mass shift from gly-PLPE: M+16 Da); *m/z* 908.6,gly-PLPE bearing 2 oxygen insertions on the *sn*-2 linoleoyl chain (mass shift from gly-PLPE: M+32Da); *m/z* 926.6, gly-PLPE bearing 3 oxygen insertions on the *sn*-2 linoleoyl chain (mass shift from gly-PLPE: M+48 Da); *m/z* 786.4, glycated 1-(palmitoyl)-2-(9-carboxy-nonanoyl)-PE, a short chain product of glycated PE. Reprinted with permission from Simões *et al*. (2010), copyright 2010 [Springer].

Figure 7. AGEs formed during oxidation of glycated POPS induced by the $^\bullet$OH radical (Fenton reaction). The ion at *m/z* 788.4 (POPS + 28 Da) corresponds to the product with a polar head group

1766 bearing a terminal formamide, arising from the oxidative cleavage between C1 and C2 of the

1767 oxidized glucose moiety. The ion at m/z 818.4 (POPS + 58 Da) corresponds to the modified POPS

1768 with terminal carboxymethyl, arising from the oxidative cleavage between C2 and C3 of the

1769 glucose moiety, while the ion at m/z 832.4 (POPS+ 72 Da) corresponds to the modified PS with

1770 terminal carboxyethyl, arising from the oxidative cleavage between C3 and C4 of the glucose

1771 moiety. The ion at m/z 934.4 was formed by the oxidation of the glucose moiety to glucuronic acid,

1772 that resulted in a mass increment of 176 Da from native POPS (162 Da + 14 Da = 176 Da).

1773 Reprinted with permission from Maciel and Silva *et al*. (2013), copyright 2013 [Elsevier].

1774 **Figure 8**. Full ESI-MS of PE after 2 h of treatment with 2 equivalents of HNE. The schematic

1775 representation of native DHPE and its different adducts with HNE is also illustrated. In this spectra,

1776 the ion at m/z 718.6 corresponds to the [M-H]$^-$ molecular ion of the native DHPE, the ion at m/z

1777 874.5 corresponds to the Michael adduct formed by DHPE and HNE (mass shift of 156 Da,

1778 structure C), the ion at m/z 856.8 corresponds to the Schiff base adduct (mass shift of 138 Da,

1779 structure B), the ion at m/z 838.9 was assigned as 2-pentylpyrrole-PE (mass shift of 120 Da,

1780 structure A) arising from the cyclization and dehydration of the Schiff base. Reprinted with

1781 permission from Guichardant *et al*. (1998), copyright 1998 [Elsevier].

1782 **Figure 9.** MS spectrum of DPPE incubated with 400 mM hexanal for 1 h at 37 °C (A). The ion at

1783 m/z 692.52 corresponds to [M+H]$^+$ molecular ion of DPPE; the ion at m/z 774.60 corresponds to the

1784 Schiff base adduct (mass shift of 82 Da); the ion at m/z 856.68 corresponds to the dimeric adduct

1785 due, arising from the covalent adduction of a second molecule of hexanal (mass shift of 164 Da),

1786 the ion at m/z 874.69 was identified as the hydrated form of this dimer; the ion at m/z 936.74

1787 corresponds to the pyridinium ring adduct formed by covalent adduction of a third hexanal

1788 molecule, and followed by cyclization and loss of one H_2O molecule; the ion at at m/z 954.75

1789 corresponds to the hydrated precursor of the pyridinium adduct; the ion at m/z 938.76 corresponds

1790 to the trimeric adduct. The mechanism of the consecutive covalent adductions of hexanal to DPPE

1791   is resumed in Panel B. Reprinted with permission from Annibal *et al*. (2014), copyright 2014 [John

1792   Wiley & Sons].

1793   **Figure 10**. MS/MS spectrum (Orbitrap HCD activation) acquired in negative ion mode of the [M-

1794   H]⁻ molecular ion of the long chain oxidation product of PAPE bearing 4 inserted oxygen atoms

1795   (*m/z* 802.486). The ion at *m/z* 255.231 corresponds to the R_1COO^- of palmitic acid; the ion at *m/z*

1796   367.210 corresponds to the $R_2'COO^-$ of oxidized arachidonic acid (arachidonic acid +4O, 303+64

1797   Da); the ion at *m/z* 452.277, corresponds to the anion of lyso-PAPE, arising from the neutral loss of

1798   oxidized arachidonic acid from *sn*-2 as ketene ($-R_2'=C=O$). The ions at *m/z* 784.475 and *m/z*

1799   766.470 were formed by the neutral losses of 1 and 2 water molecules, respectively (-18 Da and -36

1800   Da). The schematic representation of two possible isomers, along with their fragmentation

1801   mechanisms, is also illustrated.

1802   **Figure 11**. MS/MS spectrum (Orbitrap HCD activation) acquired in negative ion mode showing the

1803   fragmentation of a short chain oxidation product of PAPE (*m/z* 550.343, 1-palmitoyl-2-(5-

1804   oxovaleroyl)-*sn*-3-glycerophosphoethanolamine). The MS/MS spectrum of the [M-H]⁻ molecular

1805   ion shows the fragment ions corresponding to the carboxylate anion of palmitic acid (*m/z* 255.231),

1806   and the carboxylate anion of the shortened arachidonic acid derivative with terminal aldehydic

1807   function (5-oxovalerate) esterified at *sn*-2 (*m/z* 115.038). The schematic representation of the

1808   fragmentation is also illustrated.

1809   **Figure 12**. MS/MS spectrum acquired in the negative mode (Ion Trap CID activation) of the PAPS

1810   bearing 2 inserted oxygens (*m/z* 814). The fragment ion at *m/z* 727.4 arises from the neutral loss of

1811   the Ser moiety from the precursor molecular ion (-87 Da). The schematic representation of the

1812   fragmentation is also illustrated.

1813   **Figure 13**. (A) Reconstructed ion current (RIC) chromatogram of the [M+H]⁺ molecular ion of

1814   PLPE long chain oxidation product, at *m/z* 764.5 (3 inserted oxygen atoms), showing the separation

1815   of two constitutional isomers. (B, C) MS/MS spectra acquired in the positive mode of the isomers

1816   eluted at 18.32 min (identified as the poly-hydroxy derivative) (B) and 21.88 min (identified as the

1817   hydroperoxy derivative) (C). The following ions were observed in both spectra: ion at m/z 623.6

1818   ($[M+H-141]^+$) which arises from the typical neutral loss of the PE polar head; ion at m/z 313.3, is

1819   due to the combined loss of 141 Da and R_2'=C=O; ion at m/z 467.4, arising from the fragmentation

1820   of the C9-C10 bond (C9 with a hydroxyl group and C10 with a double bond), combined with the

1821   loss of polar head ("A1" and "A2" in B and C, respectively); ion at m/z 523.5, arising from the

1822   fragmentation of the C12-C13 bond (C12 with a hydroxyl group and C13 with a double bond),

1823   combined with the loss of polar head (fragments "A1" and "A2" in B and C, respectively); ion at

1824 m/z 646.4, arising from the fragmentation of the C12-C13 bond (C13 with a hydroxyl or

1825   hydroperoxyl group and C12 with a double bond) (fragments "B1" and "B2" in B and C,

1826   respectively); ion at m/z 535.4, arising from the fragmentation of the C13-C14 bond (C13 with a

1827   hydroperoxyl group) combined with the neutral loss of polar head (fragment "C2" in B). In the

1828   MS/MS spectrum at Panel B, it is possible to see the product ions at m/z 746.6 and m/z 728.6,

1829   arising from the loss of one (18 Da) and two H_2O molecules (36 Da), respectively, pinpointing the

1830   presence of a polyhydroxy-derivative. In the MS/MS spectrum at Panel C, it is possible to observe

1831   the product ions at m/z 730.6 and m/z 712.6, formed by the neutral loss of H_2O_2 (34 Da) and the

1832   combined losses of H_2O_2 plus H_2O (52 Da), respectively, pinpointing the presence of a hydroxy-

1833   hydroperoxy derivative. Reprinted with permission from Domingues *et al*. (2009), copyright 2009

1834   [John Wiley & Sons].

1835   **Figure 14**. (A) MS/MS spectrum acquired in the negative mode (Ion Trap CID activation) of the

1836   PAPS oxidized in the polar head (PAPS -29 Da) and (B) MS/MS spectrum acquired in the negative

1837   mode (Orbitrap HCD activation) of PLPS oxidized in the polar head (PLPS -29 Da). Both

1838   derivatives were formed upon oxidation by the •OH radical (Fenton reaction). The MS/MS

1839   spectrum of PAPS -29 Da (A) shows a base peak at m/z 695.4 corresponding to the fragment ion

formed by the neutral loss of acetic acid (-58 Da) from the precursor molecular ion. The fragment

ion at m/z 255.2 corresponds to palmitic acid (R_1COO^-) and the fragment ion at m/z 303.3

corresponds to arachidonic acid (R_2COO^-). In the MS/MS spectrum of PLPS -29 Da (B) the

fragment ion at m/z 671.469 corresponds to the neutral loss of acetic acid (-58 Da) from the

precursor molecular ion. The fragment ion at m/z 255.233 corresponds to palmitic acid (R_1COO^-)

and the fragment ion at m/z 303.232 corresponds to linoleic acid (R_2COO^-). The schematic

representations of the fragmentations are also reported.

Figure 15. MS/MS spectrum acquired in the positive mode of gly-PLPE. The neutral loss of

glycated polar head (-303 Da) is evidenced by the base peak at m/z 575.6; the fragment ion at m/z

794.6 arises from the neutral loss of 84 Da, due to the elimination of three H_2O molecules and one

H_2CO molecule from the precursor molecular ion. The schematic representation of the

fragmentation leading to the neutral loss of the glycated polar head is also illustrated. Reprinted

with permission from Simões *et al*. (2010), copyright 2010 [Springer].

Figure 16. MS/MS spectrum acquired in the positive mode of gly-ox-PLPE. The fragment ion at

m/z 575.5 (base peak) arises from the neutral loss of the oxidized polar head (303+14 Da); the

fragment ion at m/z 318.1 corresponds to the protonated oxidized polar head group. The schematic

representation of the fragmentation leading to the neutral loss of the oxidized glycated polar head is

also illustrated. Reprinted with permission from Simões *et al*. (2010), copyright 2010 [Springer].

Figure 17. MS/MS spectrum acquired in the negative mode (Orbitrap HCD activation) of gly-

PLPE. The fragment ion at m/z 714.508 arises from the neutral loss of glucose (-162 Da). The

fragment ions at m/z 255.233 and m/z 279.233 correspond to the unmodified R_1COO^- and R_2COO^-,

respectively. The fragment ions at m/z 756.519 and m/z 786.529 arise from the neutral losses of 90

Da ($-C_3H_6O_3$), and 120 Da ($- C_4H_8O_4$) from the precursor ion, respectively, and arise from

characteristic fragmentation patterns of the glucose moiety upon negative ion mode MS/MS. The

schematic representation of the fragmentation is also reported.

1865 **Figure 18**. MS/MS spectrum acquired in the negative mode (Orbitrap HCD activation) of gly-

1866 PLPS. The fragment ion at *m/z* 758.497 arises from the neutral loss of glucose (-162 Da). The base

1867 peak at *m/z* 671.466 arises from the combined neutral losses of glucose and aziridine-2-carboxylic

1868 from the precursor ion (162+87 = 249 Da). The fragment ions at *m/z* 255.233 and *m/z* 279.233

1869 correspond to the unmodified R_1COO^- and R_2COO^-, respectively. The ion at *m/z* 830.519 arises

1870 from the neutral loss of 90 Da ($-C_3H_6O_3$). The schematic representation of the fragmentation is also

1871 reported.

1872 **Figure 19**. (A) Reconstructed ion current (RIC) chromatogram of the $[M-H]^-$ molecular ion of gly-

1873 POPS long chain oxidation product, at *m/z* 936.4 (mono-keto-derivative) showing the separation of

1874 two constitutional isomers. (B) MS/MS spectrum and (C) scheme of fragmentation of the isomer

1875 that eluted at 11.0 min; in the MS/MS spectrum at Panel B, the fragment ion at *m/z* 673.3 (base

1876 peak) arises from the neutral loss of 263 Da, which is due to the loss of aziridine-2-carboxylic acid

1877 (87 Da) adducted to the glucuronic acid moiety (162+14 = 176 Da), confirming the insertion of one

1878 oxygen atom on the glycated polar head; the fragment ion at *m/z* 760.4 can be attributed to the

1879 neutral loss of glucuronic acid (176 Da) and further confirms the oxidation of the glucose moiety.

1880 (C) MS/MS spectrum and (D) scheme of fragmentation of the isomer eluted at 19.7min; in the

1881 MS/MS spectrum at Panel B, the fragment ion at *m/z* 687.4 (base peak) arises from the neutral loss

1882 of 249 Da, which corresponds to the aziridine-2-carboxylic acid (87 Da) adducted to the glucose

1883 moiety (162 Da), confirming that the keto insertion (+14 Da) is located on the oleoyl chain of gly-

1884 POPS; the fragment ion at *m/z* 774.3 (neutral loss of glucose, 162 Da) also shows that the glucose

1885 moiety does not bear any oxidative modification. Reprinted with permission from Maciel *et al*.

1886 (2013), copyright 2013 [Elsevier].

1887 **Figure 20**. MS/MS spectrum acquired in the negative mode of the advanced gly-ox-POPS end

1888 product at *m/z* 818.4 (cleavage in the C_2-C_3 bond of the glucose moiety). In this spectrum, the

1889 fragment ion at *m/z* 673.4 (base peak) arises from the neutral loss of 145 Da, that corresponds to the

Ser moiety adducted to a carboxymethyl group, formed by the oxidative cleavage of glucose (87 + 58 Da). This fragmentation pathway confirms that the precursor ion at m/z 818.4 is a PS AGE in which the glucose moiety has been shortened by an oxidative cleavage between C2 and C3. The minor fragment ion at m/z 760.5 arises from the neutral loss of a carboxymethyl moiety from the precursor ion (-58 Da) and further confirms that an oxidative cleavage occurred between C_2 and C_3 of glucose. Reprinted with permission from Maciel et $al.$ (2013), copyright 2013 [Elsevier].

Figure 21. MS/MS spectrum acquired in the negative mode of the IsoLG–PE pyrrole adduct at m/z 1031; the fragment ion at m/z 768 arises from the neutral loss of R_2=C=O; the fragment ion at m/z 512 is due to the combined losses of R_2COOH and R_1COOH; the fragment ion at m/z 415 arises from the neutral losses of the polar head, modified as pyrrole adduct (361 Da), and R_1COOH; the fragment ion at m/z 391 arises from the neutral losses of the polar head modified as pyrrole adduct (361 Da) and R_2COOH.; the fragment ions at m/z 279 and m/z 255 are R_2COO$^-$ and R_1COO$^-$, respectively; the fragment ion at m/z 153 is due to the combined neutral losses of the polar head modified as pyrrole adduct (361 Da) and of R_1COOH and R_2COOH. The schematic representations of the fragmentations are also illustrated. Reprinted with permission from Bernoud-Hubac et $al.$ (2004), copyright 2004 [Elsevier].

Figure 22. MS/MS spectrum acquired in negative ion mode of IsoK–PE Schiff base adduct at m/z 1035; the fragment ion at m/z 772 arises from the neutral loss of R_2=C=O; the combined neutral losses of R_2COOH and R_1COOH led to fragment ion at m/z 516; the fragment ion at m/z 415 is formed by the combined neutral losses of the polar head modified as Schiff base adduct (-365 Da) and R_1COOH; the fragment ion at m/z 391 arises from the combined neutral losses of the polar head modified as Schiff base adduct (-365 Da) and R_2COO-; the fragment ions at m/z 279 and m/z 255 are R_2COO$^-$ and R_1COO$^-$, respectively; the fragment ion at m/z 153 arises from the neutral losses of the polar head modified as Schiff base adduct (-365 Da) and of R_1COOH and R_2COOH. The

1914   schematic representations of the fragmentations are also illustrated. Reprinted with permission from

1915   Bernoud-Hubac *et al*. (2004), copyright 2004 [Elsevier].

1916   **Figure 23**. Positive ion mode multistage tandem MS spectra of a DPPE-hexanal Schiff base adduct.

1917   (A) MS/MS spectrum of the DPPE-hexanal Schiff base adduct; the fragment ion at *m/z* 551.51

1918   corresponds to the diacylglyceride fragment ion, arising from the neutral loss of the

1919   phosphoethanolamine moiety covalently linked to hexanal (-224 Da); the fragment ion

1920   corresponding to the modified polar head group can be seen at *m/z* 224.15 and was selected for

1921   further fragmentation. (B) The MS^3 spectrum of phosphoethanolamine-hexanal Schiff base product

1922   ion; the fragment ion at *m/z* 126.10 corresponds to the of the vinylamine-hexanal Schiff base adduct

1923   due to the neutral loss of phosphoric acid from the precursor ion (-98 Da); this fragment ion at *m/z*

1924   126.10 was further isolated and fragmented. (C) The MS^4 spectrum of the vinylamine-hexanal

1925   Schiff base product ion; several peaks (*m/z* 112.34, 98.15, 83.97, 69.98, 55.99) arise from the

1926   sequential mass losses of 14 Da, which confirm the presence of a hexanal alkyl chain adducted to

1927   the polar head. The schematic representations of the fragmentations are also illustrated. Reprinted

1928   with permission from Annibal *et al*. (2014), copyright 2014 [John Wiley & Sons].

1929   **Figure 24**. Schematic representation of the PIS approach based on D6-DMABA derivatization

1930   proposed for the identification of oxidized PE in lipid extracts from RAW 264.7 cells.